



UNIVERSITÀ  
DEGLI STUDI  
DI PADOVA

UNIVERSITA' DEGLI STUDI DI PADOVA

**Department of Industrial Engineering DII**

Master's degree program in Energy Engineering

DEVELOPMENT, IMPLEMENTATION AND VALIDATION OF A  
HYDROPOWER PLANT MODEL WITH FRANCIS TURBINE

*Supervisor: Prof.ssa Anna Stoppato (UniPD)*

*Co-supervisor: Prof. Pål-Tore Storli (NTNU, Trondheim)*

*Candidate: Asia Ingranata, 2022743*

Academic Year 2021/2022



# Abstract

The main objective of this Master project is the modelling and validation of the hydropower plant present at the *WaterPower Laboratory* of the Norwegian University of Science and technology (NTNU), using the software SIMSEN. The first part is focused on analysing the most important dynamic effects that can happen in hydropower operation, and how some elements of the circuit act to mitigate these problems. In the second, and most relevant part, the model is implemented in the SIMSEN simulation software, considering the whole hydraulic circuit and the governor for the control of the turbine. Then the validation must be carried out, verifying that the simulation is able to correctly represent the real behaviour of the plant. This is important for the development of digital twins and for further digitalization, giving the possibility to use a model to predict problems in the plant, to help the decision making and to improve the performance in hydropower operation.

**Keywords:** Francis turbine, transient simulations, governor, digital twins, hydropower.

# Riassunto in lingua italiana

Con l'aumento dell'uso delle fonti di energia rinnovabile, risulta sempre più importante la partecipazione degli impianti idroelettrici in tutti quei servizi ausiliari legati alla connessione dell'impianto alla rete, come la regolazione di frequenza. Questo richiede sempre maggiore flessibilità e, di conseguenza, aumenta la presenza di problemi dinamici legati alle oscillazioni di pressione ad alta frequenza che possono avvenire in caso di regolazione e riduzione di carico.

Qui entra in gioco l'utilità dei così detti “*digital twins*”, riproduzioni digitali di impianti reali che possano fornire supporto nell'analisi, nella determinazione di possibili miglioramenti e nella manutenzione. Generalmente quando si vogliono realizzare modelli di questo tipo, specialmente per le turbine, sono necessari elevati costi computazionali, si pensi alle simulazioni CFD; questo lavoro di tesi è invece rivolto allo sviluppo di un modello che possa ridurre questi costi.

In particolare, l'obiettivo di questo progetto è la realizzazione di un modello monodimensionale, usando il software SIMSEN, dell'impianto idroelettrico pilota presente al *WaterPower Laboratory* dell'università norvegese NTNU (a Trondheim). Il lavoro si inserisce all'interno di una collaborazione tra l'NTNU e l'università Svizzera EPFL di Losanna, in cui il software in analisi è stato sviluppato. Questo documento parte con la descrizione dei fenomeni dinamici, legati a situazioni di riduzione di carico e all'azione del sistema di controllo della turbina, che possono avvenire durante l'operazione degli impianti idroelettrici. Dopo questa introduzione, i capitoli successivi si rivolgono alla descrizione del modello e di come è stato costruito e infine alla sua validazione utilizzando risultati sperimentali provenienti direttamente dalla piattaforma del laboratorio. Il modello è stato verificato sia in condizioni stazionarie sia in transitorio, attivando la chiusura dei canali di ingresso alla turbina in modo da ridurre la portata entrante.

Nella seconda parte del report, è stato inserito anche il sistema di controllo della turbina; durante il semestre primaverile del 2022 era, infatti, in atto una campagna sperimentale per l'implementazione di un nuovo sistema di controllo e per la dimostrazione che l'impianto potesse funzionare in condizioni di rete isolata provvedendo alla regolazione di frequenza primaria. L'inserimento di questa ulteriore parte nel modello è utile per rendere il modello quanto più fedele possibile alla realtà e in modo da considerare non solo gli effetti idraulici sul sistema, ma anche quelli introdotti dall'azione del sistema di controllo, che provocando variazioni di carico introdurrà importanti oscillazioni di pressione. Grazie a ulteriori risultati

sperimentali, è stato possibile verificare anche il comportamento del modello dopo queste aggiunte, fornendo alla fine un *tool* che potrà essere utilizzato in futuro all'interno del laboratorio.

A causa della limitata conoscenza attualmente disponibile su una specifica parte dell'impianto, non è stato possibile rendere perfetto il modello: una discrepanza risulta ancora presente ed è relativa all'andamento della pressione all'uscita del condotto cono-diffusore, in quanto non è stato possibile modellare quella parte dell'impianto in maniera totalmente fedele alla realtà. Analisi future saranno necessarie, prima per comprendere il fenomeno fisico alla base dell'andamento della pressione nell'impianto e poi per poter incrementare l'accuratezza del modello in SIMSEN. Per il momento i risultati sono stati considerati soddisfacenti, considerando le attuali conoscenze e mettendo in evidenza che il modello è comunque in grado di predire possibili picchi di pressione nei vari punti del sistema di tubature e di riprodurre l'azione di regolazione del sistema di controllo.

# Acknowledgments

The development of this thesis work would not have been possible without the help and supervision of the following persons, whom I would like to extend my most sincere thanks.

- **Prof. Pål-Tore Storli** for agreeing to follow me on the project thanks to the Erasmus+ program, for his supervision and guidance throughout my whole stay at the *WaterPower Laboratory* of NTNU. Finally, for giving me the possibility to work on a very interesting project in collaboration with many different people and in such an international environment.
- **Prof.ssa Anna Stoppato** for agreeing to be my official supervisor in Italy at the University of Padua and for her availability and interest on my research at NTNU during the whole six months spent abroad.
- **Dr. Ing. Elena Vagnoni** and **Ing. Martin Seydoux** for their availability and knowledge about the SIMSEN software, which I used for developing my whole project. Without them my learning path and project development would have been much more complicated. Their presence at the WaterPower laboratory allowed me to go more deeply inside the software and understand better the results of the simulations I was working on.
- **Ing. Truls Edvardsen Aarønes** for his knowledge and availability specially in the last part of my thesis work about the implementation of the governor system into the model. His guidance allowed me to learn more about governors and he played a fundamental role in the realization of the final SIMSEN model.
- Finally, I want to thank all the team of the *WaterPower Laboratory* for making me feel welcomed and integrated, for their knowledge and for all the good times and parties realized at university; I couldn't have hoped for a better place to spend my semester abroad.

# Summary

Abstract .....	I
Riassunto in lingua italiana .....	II
Acknowledgments .....	IV
List of Tables.....	VII
List of figures .....	VIII
Introduction .....	1
Chapter 1 .....	3
Dynamics of hydropower plants .....	3
1.1  Governing equations and dynamic effects.....	3
1.1.1  Water hammer .....	4
1.1.2  Mass oscillations .....	8
1.2  Components.....	12
1.2.1  Conduit.....	12
1.2.2  Surge shaft.....	14
1.2.3  Turbine .....	14
1.3  Governor.....	16
Chapter 2 .....	21
SIMSEN implementation of hydraulic components .....	21
2.1  Modelling of hydraulic components.....	22
2.1.1  Pipe.....	22
2.1.2  Valve .....	24
2.1.3  Surge Tank .....	25
2.1.4  Surge Shaft .....	27
2.1.5  Air Vessel.....	28
2.1.6  Cavitating flow .....	29
2.1.7  Reservoir .....	30

2.1.8	Turbine .....	31
2.2	Initial conditions determination.....	33
Chapter 3	.....	35
Numerical benchmarking: pressure oscillations .....		35
3.1	Propagation of pressure waves .....	35
3.1.1	Verification in the model.....	36
Chapter 4	.....	41
Numerical validation of the model.....		41
4.1	Steady state comparison .....	41
4.2	Load Reduction simulation.....	45
Chapter 5	.....	53
Governor implementation .....		53
5.1	Implementation in SIMSEN .....	53
5.2	Verification of the P-Y function.....	58
5.3	Frequency drop.....	60
Chapter 6	.....	65
Final SIMSEN model.....		65
6.1	Isolated grid operation of the SIMSEN model .....	65
6.2	Isolated grid operation with backlash implementation.....	70
Conclusions .....		77
Bibliography.....		79
APPENDIX A	: Detailed construction of the SIMSEN model .....	81
APPENDIX B	: Computation of the plant's head losses .....	101
APPENDIX C	: Mechanical backlash.....	105



# List of Tables

Table 1 Summary of the main pipe parameters with loss coefficients..... 42

Table 2 Summary of the local loss coefficients for the elbows ..... 42

Table 3 Comparison between SIMSEN results and experimental data in steady state conditions ..... 44

Table 4 Length and cross section of the 2 portions of the cone ..... 94

Table 5 Length and cross section of the 3 portions of the diffuser ..... 94

Table 6 Parameters that must be fixed for the computation of the losses..... 101

Table 7 Characteristic parameters for the piping system of the SIMSEN model ..... 101

Table 8 Summary of the loss coefficients for the elbow’s losses ..... 103

# List of figures

Figure 1.1 Pipe representation and main parameters of interest in studying a flow in a piping system [2] ..... 4

Figure 1.2 Pressure fluctuations in case of water hammer at the end of a pipe, without losses [2] ..... 5

Figure 1.3 Pressure oscillations in case of valve closure over a certain time [2]..... 6

Figure 1.4 Pressure oscillations in the case the valve is closing slower than the reflection time in the pipe [2] ..... 7

Figure 1.5 Simple scheme of a hydropower plant with surge tanks, turbine, and reservoir [2] 8

Figure 1.6 U-tube oscillations for the two surge shafts of the plant in the case of load rejection [2] ..... 9

Figure 1.7 U-tube oscillations for the two surge shafts of the plant at start up [2] ..... 10

Figure 1.8 Scheme of the system with the characteristic parameters for every portion [2].... 11

Figure 1.9 Quasi-steady state frictional loss [2]..... 13

Figure 1.10 Surge shaft representation [2] ..... 14

Figure 1.11 Scheme of the turbine with indication of power and torque [2] ..... 15

Figure 1.12 Block diagram that represents the process addressed by the governor [2] ..... 18

Figure 1.13 Block diagram for a feedback system [2] ..... 19

Figure 2.1 Model of the pipe as an electric circuit [6] ..... 22

Figure 2.2 Stress as a function of the deformation [6] ..... 23

Figure 2.3 Rheologic and equivalent models of a viscoelastic pipe [6]..... 23

Figure 2.4 Resulting model of the pipe [6] ..... 24

Figure 2.5 Electrical representation of a valve as a variable resistance [6] ..... 25

Figure 2.6 Scheme of a surge tank in electrical terms [6]..... 26

Figure 2.7 Resulting equivalent scheme of the surge shaft [6] ..... 27

Figure 2.8 Electrical representation of the air vessel [6]..... 29

Figure 2.9 Electrical representation of a cavitating flow [6]..... 30

Figure 2.10 Reservoir scheme with main parameters [8]..... 30

Figure 2.11 Turbine element in SIMSEN [8]..... 31

Figure 2.12 Representation of the turbine in the software [8] ..... 31

Figure 2.13 Hydraulic load flow procedure for generating mode on the left and for pumping mode on the right [6]..... 33

Figure 3.1 Model realized in SIMSEN with the addition of a valve to simulate water hammer pressure waves propagation .....	37
Figure 3.2 Pressure behaviour at the outlet of the pipe before the valve .....	37
Figure 3.3 Pressure behaviour at the inlet of the turbine after water hammer simulation .....	38
Figure 3.4 Pressure oscillations at the exit of the pipe upstream the tank and zoom with a comparison in the oscillation frequency of the U-tube oscillations for the pipes before the tank and before the turbine, where there are also water hammer waves.....	39
Figure 3.5 Oscillation of the water level in the air vessel .....	39
Figure 4.1 Scheme of the plant with pipe's names as in the previous table.....	42
Figure 4.2 CAD of the plant present at NTNU with various lengths.....	43
Figure 4.3 Model of the plant realized in SIMSEN .....	43
Figure 4.4 Scheme of the plant in SIMSEN for the load reduction simulation .....	45
Figure 4.5 Comparison with experimental results for the generator speed and the guide vane opening.....	46
Figure 4.6 Comparison between the model and the experimental results for the discharge through the turbine .....	46
Figure 4.7 Comparison between the model and the experimental results for the head across the turbine.....	46
Figure 4.8 User interface of the acquiring program in the lab with pressure values .....	47
Figure 4.9 Pressure head at the outlet of the draft tube in the real plant.....	48
Figure 4.10 New head behaviour considering a change in the water level of the lower reservoir in the simulation.....	50
Figure 4.11 Comparison with experimental results for torque and power.....	51
Figure 5.1 Example of governor logic block diagram from the IEC standard [12] .....	53
Figure 5.2 Block diagram used for the implementation of the governor in the laboratory.....	54
Figure 5.3 SIMSEN implementation of the governor .....	55
Figure 5.4 Old function that gives the relation between the power and the guide vane opening .....	56
Figure 5.5 Sigmoid function that gives the new relation between the power and the guide vane opening.....	56
Figure 5.6 User interface for the regulator element .....	57
Figure 5.7 Governor modification to add the Power Set Point change.....	58
Figure 5.8 Comparison between experimental results and SIMSEN simulation for change in Power Set Point .....	59
Figure 5.9 Speed drop applied to the generator to study the response of the governor .....	61

Figure 5.10 Guide Vane Opening applied to the turbine and discharge during the speed drop simulation.....	61
Figure 5.11 Increase in power production due to the frequency drop.....	62
Figure 5.12 Comparison for the head across the turbine.....	62
Figure 5.13 Pressure head at the outlet of the draft tube in the plant.....	63
Figure 5.14 Pressure head at the inlet of the turbine in the plant.....	63
Figure 6.1 Effect of the mechanical slack on the difference between the stroke and the real opening degree of the guide vanes .....	67
Figure 6.2 Reduction on power load inserted and torque plot for governor and turbine .....	68
Figure 6.3 Guide vane opening and flow rate through the turbine with load reduction .....	69
Figure 6.4 Rotational speed behaviour during the simulation .....	69
Figure 6.5 New governor model with implementation of the mechanical backlash.....	71
Figure 6.6 Comparison between the governor signal and the guide vane opening degree really applied to the turbine.....	71
Figure 6.7 Rotational speed behaviour along the simulation .....	72
Figure 6.8 Rotational speed behaviour with an increase in power load.....	73
Figure 6.9 Comparison between the signal given by the governor and real guide vane opening applied to the turbine.....	73
Figure 6.10 Rotational speed behaviour during the simulation .....	74
Figure 6.11 Comparison between the signal given by the governor and the guide vane opening applied to the turbine.....	75
Figure 6.12 Rotational speed during the simulation .....	75
Figure A. 1 Hydropower plant present at the WaterPower laboratory of NTNU .....	81
Figure A. 2 2D view of the Francis turbine model [1].....	82
Figure A. 3 SIMSEN model of the power plant present at NTNU .....	83
Figure A. 4 User interface for the reservoir element.....	84
Figure A. 5 User interface of the Penstock element.....	85
Figure A. 6 User interface for the DLOSS element .....	87
Figure A. 7 User interface for the first horizontal pipe of the model.....	88
Figure A. 8 User interface for the second pipe of the model, the one just before the first air vessel.....	89
Figure A. 9 User interface for the Air Vessel element that model the first surge tank of the plant .....	90
Figure A. 10 User interface of the turbine element.....	92

Figure A. 11	User interface for the second surge tank.....	96
Figure A. 12	User interface for the FPoint element that sets the cross section of the horizontal surge tank .....	97
Figure A. 13	User interface for the reservoir that simulates the pool of the powerplant.....	98
Figure A. 14	New model realized in the software, modifying the tailrace part of the plant...	99
Figure B. 1	Smooth and sharp elbows with related parameters [10] .....	102
Figure C. 1	Linear two-mass system for connection between a motor and load [15].....	105
Figure C. 2	Two mass system with backlash [13].....	106
Figure C. 3	Logic of the backlash implemented into the SIMSEN model.....	107
Figure C. 4	Example of the effect of a mechanical backlash .....	108



# Introduction

Simulations of system hydraulics are an important part of planning, design, and operation of hydropower plants, and also allow the investigation of transient and dynamic phenomena. Such simulations require a model of the turbine that is accurate, simple enough and not too expensive in respect to computational effort and time.

The cost of computational power and time of a highly resolved CFD simulation of a hydraulic turbine is too high, especially if the purpose is to analyse dynamic effects in hydropower operation. This represents a problem for the digitalization of real systems and further development of applications, such as digital twins. Specifically, a digital twin is a virtual model designed to accurately reflect a physical object and can be used as a digital counterpart for real processes and machines. Going in more detail, the virtual model of a system is useful to run simulations, in order to study performance issues, help the decision-making and generate possible improvements; there are also a lot of advantages in the realization of a digital representation of a system: it helps a more effective research and design of products, digital twins can also help monitoring processes and estimating the end of life of a product. So, there is also a very high industrial interest in this topic.

The problem related to the cost of 3D simulations can be solved in two ways: or speeding up the highly resolved CFD simulations or trying to improve the quality and the truthfulness of simpler representations of the components in the system. This work is oriented towards the latter.

The aim of this work is to demonstrate the possibility of using a simulation software to represent the real operation of a hydropower plant, in particular the case study is the plant present at the *WaterPower* laboratory of the *Norwegian University of Science and Technology* (NTNU). During the spring semester 2022 some tests on the Francis99 runner were taken (for information regarding the test rig see [1]), to study the behaviour of the plant and analyse possible improvements; also, a new governor system was implemented following an experimental campaign. In parallel, this work is aimed at realising a digital model of the plant using the software SIMSEN. This software allows the realization of dynamic simulations of hydropower plants in a 1D environment, reducing in this way the computational effort and time. After the creation of the model, simulations must be carried out and the results of such simulations compared with experimental results available from tests taken in the laboratory.

Therefore, in this work no 3D and CFD simulations are done, the purpose is validating a 1D model, simpler than a CFD simulation to solve; the aim is to verify the possibility to create a digital representation of a hydropower plant without a high computational cost. This should help in the development of digital twin concepts and in the possibility of industrial applications. Also, no experimental tests were carried out personally, but the experimental results from the laboratory of NTNU were used to validate and verify the applicability of the model realized with the software.

### **Scope and limitation**

Summarizing, this work is focused on the development of a 1-dimensional model of the hydropower plant present at the *WaterPower Laboratory* of NTNU, using a simulation software called SIMSEN. The main objective is to be able to study transients and the related phenomena, like pressure oscillations, validating the model against experimental results.

The work is not looking into CFD simulations and 3-dimensional representation of a hydro system, therefore no detailed analysis on the flow and fluid structure interaction will be carried out.



# Chapter 1

## Dynamics of hydropower plants

Before starting the development of the model in the software it is necessary to create a theoretical background about dynamic dimensioning of hydropower plants, and it is necessary to understand how to deal with the most important dynamic problems. [2]

The dynamics in a waterpower plant are related to two conditions: first it is necessary to control the hydraulic power that has to be in balance with the demand of the electric grid in all the instants. In Francis turbines this is done regulating the wicket gate, to regulate the flow, keeping constant the speed of rotation at the synchronous speed. The second problem is related to high load variation at start-up and close-down; for example, when there is load rejection, there will be an increase in the speed of rotation, and it is needed to close immediately the wicket gate. Therefore, this will give pressure fluctuations caused by the retardation of water masses, causing the, so called, water hammer phenomenon [2]. To further investigate these phenomena, it is necessary to start by setting the general equations that govern a hydro power plant.

### 1.1 Governing equations and dynamic effects

The governing equations for flow in a hydropower plant are the continuity and momentum equations for closed conduit flow, a derivation of these equations can be studied from [3]. The results are

$$vH_x + H_t - v\sin\alpha + \frac{\xi^2}{g}v_x = 0, \quad \text{Eq. 1.1}$$

$$gH_x + vv_x + v_t + \frac{fv|vv|}{2D} = 0. \quad \text{Eq. 1.2}$$

In the equations  $g$  ( $\text{m/s}^2$ ) is the gravity acceleration,  $H$  (m) is the piezometric head,  $v$  (m/s) is the average velocity in the conduit associating a velocity to the centre line of the pipe,  $D$  (m) is the diameter of the pipe,  $f$  is the Darcy-Weisbach friction factor,  $\xi$  is a constant that collects properties of the fluid and  $\alpha$  (deg) represents the inclination of the pipe. Combined they constitute the 1D wave equation, a second order partial derivative equation where two key dynamic properties are “embedded”; harmonic and complex behaviour. The harmonic behaviour in a hydropower plant is given by mass oscillations, sometimes called U-tube

oscillations. The complex behaviour is related to very fast pressure propagation due to elastic properties of the system known as *the water hammer*. These two will be explained separately in the following.

### 1.1.1 Water hammer

There are dynamic pressure variations in front of the turbine every time there is a change in the flow, this because of the retardation of water masses in the pressure shaft that brings the water to the turbine. The worst case is when there is load rejection, the rotational speed increases and it is necessary to close the wicket gate as fast as possible, this gives the highest pressure rise for the maximum retardation of the flow. To study this phenomenon, it is needed to solve the equation of motion and the continuity equation, expressed previously, in a pipe.

To study this effect let's suppose that the valve at the end of a pipeline closes immediately, referring to the pipe in Figure 1.1.

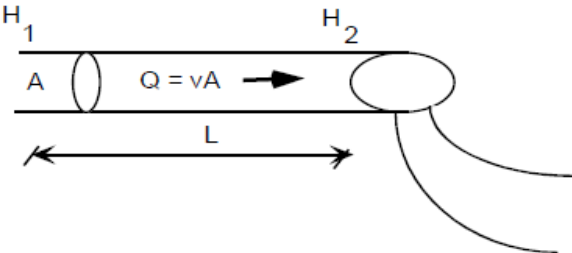


Figure 1.1 Pipe representation and main parameters of interest in studying a flow in a piping system [2]

The velocity will go from a value  $v_0$ , that can be expressed with the Torricelli theorem

$$v_0 = \sqrt{2gH} , \tag{Eq. 1.3}$$

to zero and there will be an immediate pressure rise upstream the valve. However, for the elasticity of water, there will be a pressure wave travelling upstream with a speed equal to the pressure propagation speed. Considering the front of the pressure wave, the velocity downstream will be equal zero, instead the velocity upstream will still be  $v_0$ . Only when the pressure front reaches the reservoir the velocity in the pipeline became zero, but the pressure in the pipeline has increased and this creates an unstable situation, so water will start flowing from the pipeline back to the reservoir. This means that the velocity in the pipeline became negative ( $-v_0$ ) and a new pressure front will travel down to the valve; when the pressure front has reached the valve the velocity is  $-v_0$  in all the pipeline. However, the valve is closed, so there will be a negative pressure or a suction near the valve, and velocity equal zero. A negative pressure wave will travel towards the reservoir giving again zero velocity in the pipeline, but this is an unstable situation and water starts flowing into the pipeline as before; so, the velocity become again  $v_0$

and the whole process is repeated. Only thanks to the losses the pressure waves are dampen out. Pressure fluctuation, without losses, can be represented as in Figure 1.2.

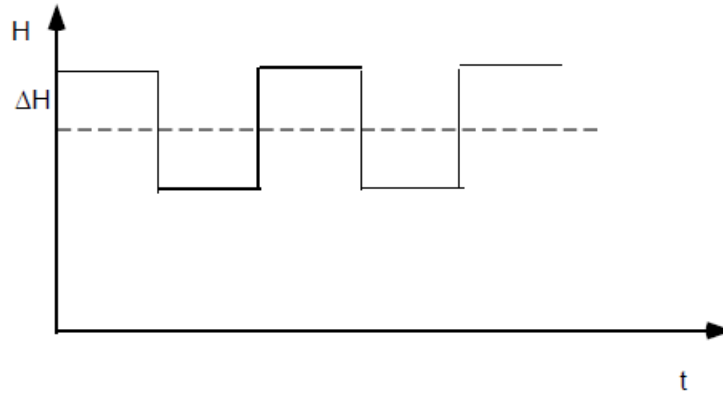


Figure 1.2 Pressure fluctuations in case of water hammer at the end of a pipe, without losses [2]

Considering that the pressure wave travels with velocity equal to  $a$  (m/s) and the pipe length is  $L$  (m), the period of the fluctuations  $T$  (s) is

$$T = \frac{4L}{a} . \quad \text{Eq. 1.4}$$

From Newton's second law and Hook's law it is possible to find the maximum pressure  $p_{max}$  when there is immediate closing of the valve downstream the pipe (referring to [2])

$$p_{max} = \rho a \Delta v , \quad \text{Eq. 1.5}$$

where  $\rho$  ( $\text{kg/m}^3$ ) is the density of the fluid. In meter of water column, the same equation is

$$\Delta H = - \frac{a \Delta v}{g} , \quad \text{Eq. 1.6}$$

where  $\Delta v$  is the variation of velocity in the pipe.

Till this point, it was considered to have immediate valve closure, if it is assumed to have valve closure over a certain time, the behaviour of the pressure will be different, as shown in Figure 1.3.

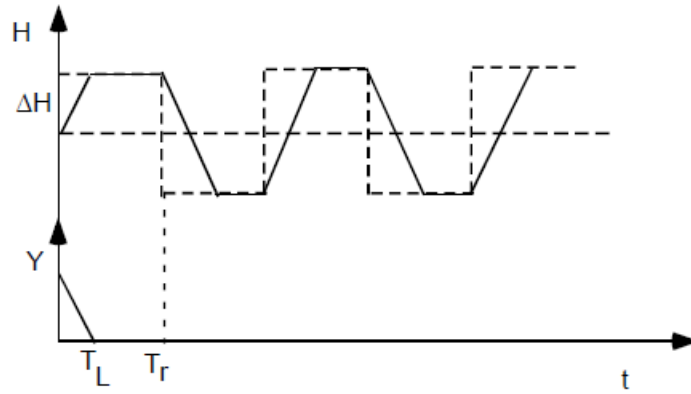


Figure 1.3 Pressure oscillations in case of valve closure over a certain time [2]

The pressure wave is reflected and goes back to the valve in a certain time  $T_r$

$$T_r = \frac{2L}{a} . \quad \text{Eq. 1.7}$$

Where  $a$  is the wave speed as usual and  $L$  is the length of the pipe.

When the propagation of a pressure wave in a pipe is considered, it is necessary to take into account that the pressure propagation speed  $a$  is a function of both compressibility and density of the fluid, but also of the flexibility of the pipeline; this according to the following expression

$$a = \sqrt{\frac{K_{eq}}{\rho}} , \quad \text{Eq. 1.8}$$

where

$$\frac{1}{K_{eq}} = \frac{1}{K} + \frac{d}{tE} . \quad \text{Eq. 1.9}$$

In this last equation  $K_{eq}$  is an equivalent compressibility modulus,  $d$  (m) is the pipeline diameter,  $t$  (m) is the thickness of the wall of the pipe,  $K$  (Pa) is the compressibility modulus and  $E$  (Pa) is the elasticity of the material of the pipe.

It is needed to also note that, if the valve is closed slower than the reflection time  $T_r$ , the maximum pressure described before will not be achieved because the valve will still be open when the pressure wave returns to the valve; so, there will be a different oscillation of pressure, as shown in Figure 1.4.

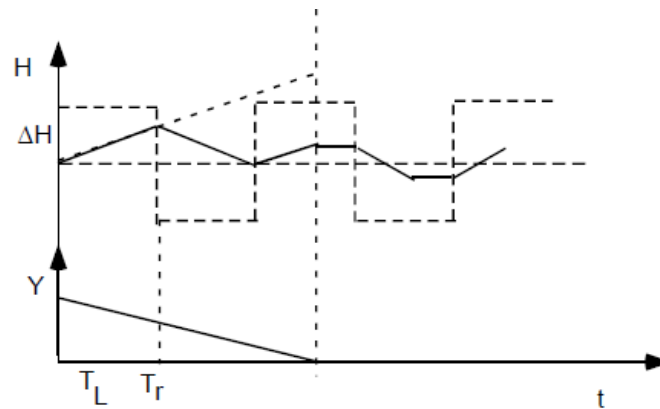


Figure 1.4 Pressure oscillations in the case the valve is closing slower than the reflection time in the pipe [2]

In conclusion, when it is said “immediate valve closure” simply means that there is closure at a closing time less than the reflection time  $T_r$ .

The conclusion of this paragraph is that to calculate the pressure rise during a valve closure it is necessary to consider the elastic properties of water and conduits, also it is needed to solve the continuity equation and the equation of motion, a method to solve is the Method of Characteristics. This is a numerical method for solving the hyperbolic differential equations, to use this, it is necessary to set up a system with the equation of motion and the continuity equation for all the pipes or conduits. Also, boundary conditions are needed.

Now it is possible to study how to reduce the transient pressure during turbine closure; in general, there are two ways of doing this:

- It is possible to increase the closing time to reduce the retardation of water.
- Or it is possible to decrease the hydraulic masses involved.

In the case of full turbines, like the Francis one, the closing time cannot be chosen freely, because in this kind of turbine it is necessary to limit the increasing speed of rotation. In some turbines there can be a by-pass valve; when the wicket gate closes the by-pass valve opens and let the water to pass, so the turbine will not be exposed to hydraulic energy. [2]

Even if increasing the closing time reduces the magnitude of the water hammer pressure, the system is excited and mass oscillations will be induced by the closing (or even opening) manoeuvre, the presence of these oscillations is also due to the introduction of surge shafts into the hydraulic system, an element used to limit the pressure rise (reducing the masses involved). The mass oscillations, sometimes called U-tube oscillations or even pressure surges, are described in the following.

### 1.1.2 Mass oscillations

The water masses participating in retardation phenomena in piping systems are equivalent with the ratio  $L/A$  (length-area ratio of the pipe). To limit pressure rise during closing of a valve, a possibility is to reduce these water masses increasing the areas of the conduits. But the solution that it is generally preferred is the introduction of the *surge shaft*, basically its effect is to move the free water surface nearer to the turbine, reducing in this way the length of the conduits participating in the retardation. However, the surge shaft is another dynamic element that is introduced in the system, and it is involved in U-tube oscillations that must be considered. Studying the effect of surge shafts, it is also possible to study the frequency and the amplitude of U-tube oscillations. In particular, the surge shaft is used to limit the retardation pressure during transients and to improve the quality of the frequency governing. The retardation pressure, as just said, is related to the closure of the turbine wicket gate when there is load rejection; the participating hydraulic mass in the process is the water between the nearest free water surface up-stream in respect to the turbine, to the nearest free water surface down-stream the turbine. It is possible to study the effect of the surge shaft considering the scheme in Figure 1.5.

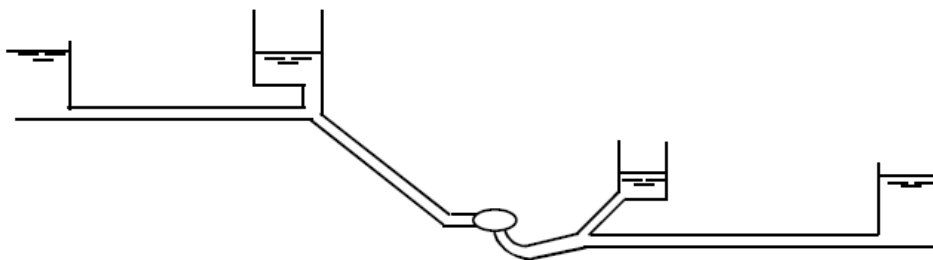


Figure 1.5 Simple scheme of a hydropower plant with surge tanks, turbine, and reservoir [2]

Before the turbine starts the level in the head water surge chamber is equal to the level in the upper reservoir, and the level in the surge chamber in the tail water is equal to the level in the lower reservoir. When the turbine arrives at the steady state operation the reservoir levels will be defined by the hydraulic pressure line in the system.

In the head water surge chamber the level  $z$  (m) is

$$z = H_{ur} - \frac{v^2}{2g} - \text{head losses} . \quad \text{Eq. 1.10}$$

Where  $H_{ur}$  is the level in the upper reservoir. Instead in the tail water surge chamber the level is

$$z = H_{lr} + \frac{v^2}{2g} + \text{head losses} . \quad \text{Eq. 1.11}$$

Where  $H_{lr}$  is the level in the lower reservoir.

Now what happens if there is load rejection?

The wicket gate closes, and this causes a retardation of the water in the pressure shaft, so the water will flow into the surge shaft and the level of the surge chamber increases until the flow in the tunnel stops. However, because of the inertia of water in the head race tunnel, the level in the surge chamber will be higher than the reservoir level, so the water will start flowing back into the reservoir. The level in the surge shaft decreases until the flow in the tunnel became zero; again, because of the inertia, the level in the surge chamber becomes lower than the reservoir level and there will be a flow from the reservoir to the surge shaft. Then the whole process is repeated.

In the tail water, when the wicket gate closes, the water supply to the turbine stops, but for the inertia of water the flow continues taking water from the surge shaft. So, the surge shaft level decreases until the flow in the tail race tunnel stops, the level will be lower in respect to the reservoir level and the water will start flowing from the reservoir into the surge chamber. At this point the surge shaft level will increase until the flow stops, then water will flow in the reservoir again and the process is repeated.

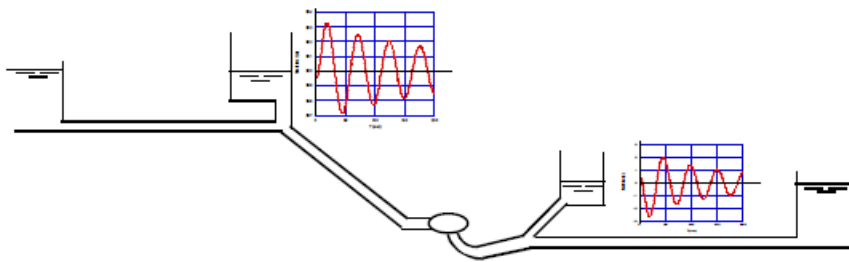


Figure 1.6 U-tube oscillations for the two surge shafts of the plant in the case of load rejection [2]

In Figure 1.6 there are the oscillations for the surge shaft up-stream the turbine and the surge shaft down-stream.

A similar process happens when the turbine starts up, the turbine wicket gate opens, and water will start flowing through the turbine. At the beginning the water is supplied from the surge shaft, because for inertia it takes more time to accelerate the water in the tunnel, therefore the level in the surge shaft will decrease and the pressure difference accelerates the water in the head race tunnel. Because of inertia the flow will exceed the turbine flow and so the surplus must go into the surge chamber, so the level in the shaft increases and will be higher than the

reservoir level, this results in a flow out of the surge shaft. This process continues and then dampen out until the tunnel flow equals the turbine discharge.

In the tail water, when the wicket gate opens the water that is discharged from the turbine will flow into the surge chamber at the beginning, and its level will increase. The difference between the level in the surge chamber and the reservoir level causes an acceleration of water in the tail race tunnel; for the inertia force the level in the surge chamber will go below the reservoir level and give a retardation of the water in the tunnel. So, the level in the surge shaft increases, then the surging process is repeated and then dampen out until the flow discharged by the turbine becomes equal to the flow in the tunnel.

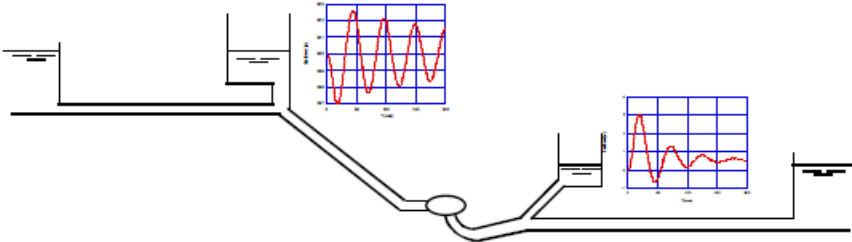


Figure 1.7 U-tube oscillations for the two surge shafts of the plant at start up [2]

In the figure it is possible to see the oscillations of water in the two surge chambers. When it is needed to dimension the surge shafts, the maximum and minimum of the surge chamber levels must be calculated. The maximum level in the head water can be found simulating the turbine closure, instead the minimum simulating the turbine start up. For the surge level in the tail water, the maximum can be found simulating the turbine start up, instead the minimum simulating the turbine closure.

To calculate surging, it is needed to write and study the differential equations of the system, it is not necessary to consider the elasticity of water and of conduits since the oscillation frequency is much smaller in respect to the one of water hammer waves. Introducing the continuity equation without the term of elasticity (equation derived in [2])

$$\frac{L}{gA} * \frac{dQ}{dt} = H_1 - H_2 - kQ|Q| . \tag{Eq. 1.12}$$

Where  $Q$  (m<sup>3</sup>/s) is the volumetric flow rate and  $A$  (m<sup>2</sup>) is the cross section of the pipe. The last term gives the head loss, which is proportional to the square of the flow;  $k$  is the loss coefficient and can be written as

$$k = \lambda * \frac{L}{2gA^2D_h} . \tag{Eq. 1.13}$$



Where  $\lambda$  is the Darcy-Weisbach loss coefficient and  $D_h$  is the hydraulic diameter of the pipe.

The continuity equation in the simple form instead is

$$\sum Q_{in} = \sum Q_{out} . \quad \text{Eq. 1.14}$$

In most cases it is sufficient to represent the turbine by the valve equation (taken from [2])

$$K = \frac{Q}{Q_R} * \frac{\sqrt{2gH_{eR}}}{\sqrt{2gH_e}} . \quad \text{Eq. 1.15}$$

Where  $Q_R$  and  $H_{eR}$  are the rated flow and the rated effective head. Instead  $H_e$  is the effective head and represents the pressure difference over the turbine, it is possible to write

$$H_e = H_{eR} * \left(\frac{Q}{Q_R}\right)^2 . \quad \text{Eq. 1.16}$$

Applying these equations, the system can be modelled, referring to Figure 1.8.

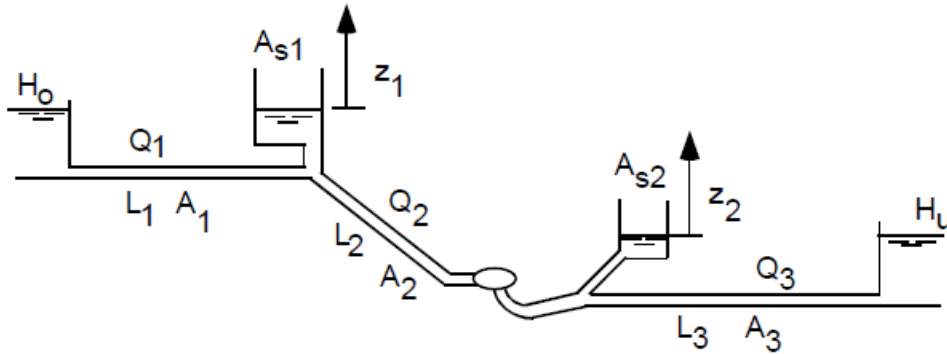


Figure 1.8 Scheme of the system with the characteristic parameters for every portion [2]

It is possible to write the equation of motion for the three conduits as

$$\frac{L_1}{gA_1} * \frac{dQ_1}{dt} = H_0 - z_1 - k_1 Q_1 |Q_1| , \quad \text{Eq. 1.17}$$

$$\frac{L_2}{gA_2} * \frac{dQ_2}{dt} = z_1 - z_2 - H_{eR} \left(\frac{Q_2}{KQ_R}\right)^2 - k_2 Q_2 |Q_2| , \quad \text{Eq. 1.18}$$

$$\frac{L_3}{gA_3} * \frac{dQ_3}{dt} = z_2 - H_u - k_3 Q_3 |Q_3| . \quad \text{Eq. 1.19}$$

Considering the continuity equation, it is possible to also write the differential equations for the shaft's levels.

$$\frac{dz_1}{dt} = \frac{1}{A_{s1}}(Q_1 - Q_2) , \quad \text{Eq. 1.20}$$

$$\frac{dz_2}{dt} = \frac{1}{A_{s2}}(Q_2 - Q_3) . \quad \text{Eq. 1.21}$$

So, there are 5 equations and 5 unknown variables.

The criteria to dimension the surge chambers is to design the shaft considering avoiding flooding during up-surging and avoiding air entrance into the conduits during down-surging. Generally, the highest up and down surge are present during shut-down or start-up of the turbine.

After the analysis on pressure oscillations, an overview of the main components of a hydropower plant is presented. Before talking about the model in the software it is necessary to have in mind which are the elements that must be inserted and how to study them. Subsequently, a sub-chapter will also be dedicated to the governor operation.

## 1.2 Components

When studying a hydraulic system from a dynamic point of view the following components must be considered:

- Conduits
- Surge shaft
- Turbine with generator

It is needed to describe these elements with their characteristic equations, in the following section each component is analysed individually introducing the equations that characterize it, then they must be connected to consider the whole hydropower system.

### 1.2.1 Conduit

The governing equations for a conduit are reported here again, referring to the form developed in the document [2]

$$\dot{m}_{in} - \dot{m}_{out} = \frac{dm_{cv}}{dt} , \quad \text{Eq. 1.22}$$

$$\frac{L}{gA} * \frac{dQ}{dt} = H_1 - H_2 - kQ|Q| . \quad \text{Eq. 1.23}$$

Where  $\dot{m}$  (kg/s) is the mass flow rate, the mass flow rate at the inlet minus the one at the outlet is equal to the variation in the control volume. It is possible to define the pressure with the piezometric head, which is the hydraulic pressure  $h$  plus the geostatic head  $z$  (all in m)

$$H = h + z . \quad \text{Eq. 1.24}$$

In the equation of motion, it can be possible to also identify the frictional loss as

$$\Delta h = k * Q|Q| . \quad \text{Eq. 1.25}$$

Where the absolute sign is used to have reverse pressure gradient when the flow changes direction.

In Figure 1.9 there is the representation of the quasi-steady state frictional loss according to the equation above.

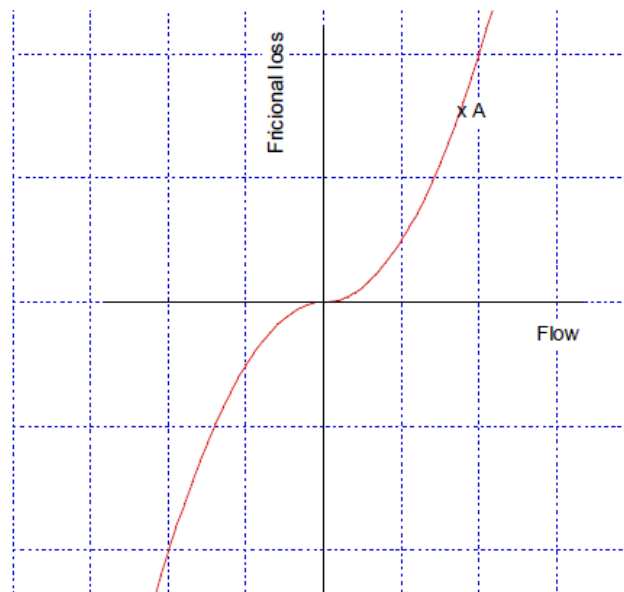


Figure 1.9 Quasi-steady state frictional loss [2]

This model for the losses is not perfect, in fact assumes that the velocity maintains a turbulent profile also when it turns, but experiments shows that the loss is also dependent on the surging frequency, the higher the frequency the higher are the losses. In general, using a steady state formulation for the losses there is an underestimation of the dampening.

Now it is possible to move to the analysis of another important element of a hydraulic system, which is the surge shaft.

### 1.2.2 Surge shaft

The surge shaft can be represented by the following figure.

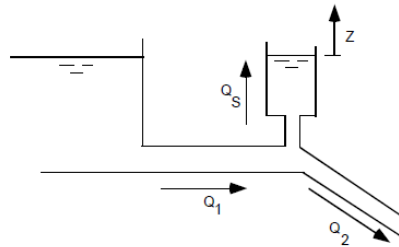


Figure 1.10 Surge shaft representation [2]

It is possible to define the continuity equation for the connection between tunnel and shaft

$$Q_1 = Q_2 + Q_s . \quad \text{Eq. 1.26}$$

Where  $Q_1$  is the flow in the tunnel up-stream,  $Q_2$  is the flow in the tunnel down-stream in respect to the shaft and then  $Q_s$  is the flow going up into the shaft. The flow in the surge shaft can be expressed as the shaft cross section  $A_s$  multiplied by the velocity (that is the variation of the level  $z$ )

$$Q_s = A_s * \frac{dz}{dt} . \quad \text{Eq. 1.27}$$

Combining the previous two equations it is possible to find the differential equation describing the shaft surging.

$$\frac{dz}{dt} = \frac{1}{A_s} * (Q_1 - Q_2) . \quad \text{Eq. 1.28}$$

This last equation gives how the level of water in the surge shaft changes over the time, in respect to the volumetric flow rates before and after the element.

Now it is needed to describe the fundamental element of a hydropower plant, which is the turbine.

### 1.2.3 Turbine

The turbine is the most important element of a hydraulic system, used to convert the hydraulic power into mechanical power. To study the behaviour of the turbine it is possible to express the Newton's law for a rotating system as

$$T = J * \frac{d\omega}{dt} . \quad \text{Eq. 1.29}$$

Where  $T$ (Nm) is the torque,  $J$  ( $\text{kgm}^2$ ) is the polar moment of inertia and  $\omega$  (rad/s) is the angular speed.

Considering the hydraulic power  $P_h$  (W), the electric power demand of the grid  $P_N$  (W), the acceleration of the rotational masses and the losses, it is possible to express a balance as

$$P_h = J\omega * \frac{d\omega}{dt} + P_N + \text{losses} . \quad \text{Eq. 1.30}$$

Where the hydraulic power  $P_h$  can be written as

$$P_h = \rho g Q * (H_1 - H_2) . \quad \text{Eq. 1.31}$$

With  $H_1$  and  $H_2$  heads at the inlet and outlet of the turbine respectively, and  $\rho$  the density of the fluid as usual. This is illustrated in the figure below.

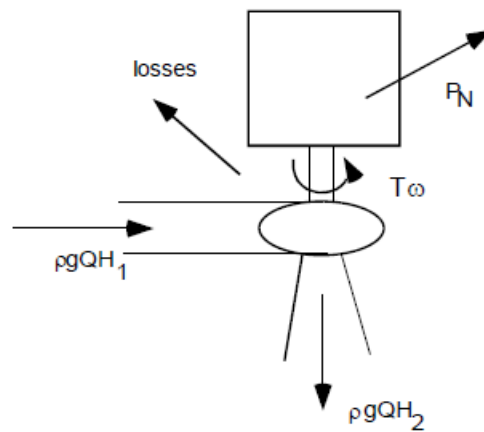


Figure 1.11 Scheme of the turbine with indication of power and torque [2]

Also, the turbine performance diagram is important to study the behaviour and the operating range of the machine; experiments or simulations must be performed to find the turbine characteristics and the efficiency curves of a generic turbine. Regarding the Francis99 runner object of the studies, the paper [4] gives a reference on the studies made at the NTNU *WaterPower laboratory*; also, it describes the equations that are needed for representing the behaviour of a hydraulic machine. The performance diagram of a turbine is generally called “Hill Chart”, and it is convenient to express the parameters in per unit terms, considering a reduced flow and a reduced angular speed. These properties are defined as follow

$$\underline{Q} = \frac{Q}{\sqrt{2gH}} , \quad \text{Eq. 1.32}$$

$$\underline{\omega} = \frac{\omega}{\sqrt{2gH}} . \quad \text{Eq. 1.33}$$

Where  $\underline{Q}$  is the reduced unit flow and  $\underline{\omega}$  is the reduced unit angular speed. For a high head Francis turbine, typically there is a falling flow characteristic: the flow decreases when the speed of rotation increases; instead, for a low head Francis turbine happens the opposite: the flow increases when the speed of rotation increases. [1]

When studying dynamic phenomena in hydropower plant, it is also important to study the influence of the governor, that acts on the guide vane opening changing the power produced by the turbine. The governor action brings the system to work in transient conditions, in the following chapter this important part of a hydropower system will be introduced.

### 1.3 Governor

The governor is a very important part of the hydraulic system, its task is to balance the hydraulic power adjusting the wicket gate opening, keeping the speed of rotation constant at the synchronous speed, and following the variation of the demand.

The governor can be developed in different ways, the most used one is the PI governor (Proportional-Integral), that allows to achieve stabile governing and a zero-speed deviation. The equation that represents the PI governor is

$$\Delta Y = - \left( K_p \Delta n + \frac{K_p}{T_d} \int \Delta n * dt \right) . \quad \text{Eq. 1.34}$$

Or in the differential form

$$\frac{dY}{dt} = -K_p * \frac{dn}{dt} + \frac{K_p}{T_d} * (n_{ref} - n) . \quad \text{Eq. 1.35}$$

Where  $Y$  is the wicket gate opening,  $n$  (rpm) is the speed of rotation and  $K_p$  is the constant related to the proportional term. The second term allows to be sure that the wicket gate will change until the speed deviation ( $n_{ref} - n$ ) is zero and so the speed of rotation is equal to the reference one ( $n_{ref}$ ). The time constant  $T_d$  (s) is also called integration time or dashpot time constant since the integration term in mechanical-hydraulic governors was made possible by a dashpot. The advantage of a PI governor is that does not require an exact knowledge of the behaviour of the process, in respect to a P governor for example. [2]

For some systems it is necessary to use a PID-governor, with a derivative term that will improve the stability of the process; the equation for a PID-governor can be reported

$$\Delta Y = - \left( K_p \Delta n + \frac{K_p}{T_d} \int \Delta n * dt + K_p T_N * \frac{dn}{dt} \right). \quad \text{Eq. 1.36}$$

Calculating the derivative

$$\frac{dY}{dt} = -K_p * \frac{dn}{dt} + \frac{K_p}{T_d} * (n_{ref} - n) - K_p T_N * \frac{d^2n}{dt^2}. \quad \text{Eq. 1.37}$$

Where  $T_N$  is the derivative time constant. It is needed to limit the derivative term with a filter time constant  $T_f$ ; in a commercial governor the dash pot time constant  $T_d$ , the derivative time constant  $T_N$ , the proportional constant  $K_p$  and the filter time constant  $T_f$  can be adjusted depending on the process that has to be governed. [2]

When studying the governor, it is also important to investigate the dynamic effects that the action of the governor introduce. The hydropower plant is usually connected to the grid and has to deliver electricity covering the consumers demand, also the plant has to contribute on keeping the frequency at 50 Hz (nominal value of the grid in Europe). When talking about rotating machines, keeping the frequency constant means keeping constant the rotational speed at the synchronous value.

The synchronous speed can be calculated as

$$n_0 = \frac{60f}{P}. \quad \text{Eq. 1.38}$$

With  $f$  (Hz) nominal frequency of the grid and  $P$  number of pole pairs in the generator.

In hydraulic turbines the hydro power is transformed first into rotating power and then in electrical power thanks to the generator. Considering having at the beginning balance between the power at the outlet of the turbine and the demand of the grid, if at a certain instant the request of the grid decreases, there will be an excess of hydraulic power and a too low resistance torque, so the turbine will accelerate. The speed of rotation increases and there will be a change in the frequency that cannot be accepted. The governor is needed to balance these problems and to keep the frequency at the nominal value, basically the governor measures the rotational speed and its deviation from the nominal value, then gives the message to the servo motors to change the wicket gate opening.

The process addressed by the governor can be described by the following block diagram.

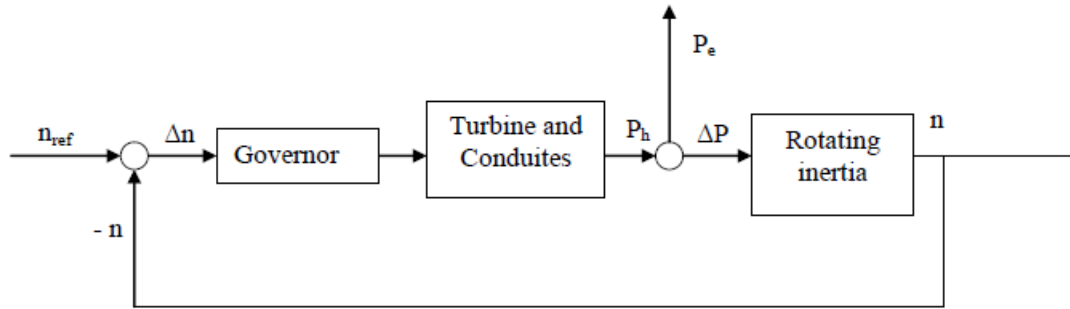


Figure 1.12 Block diagram that represents the process addressed by the governor [2]

If, for example, the demand of power increases, the speed will vary according to the Newton's second law

$$\omega J \frac{d\omega}{dt} = \Delta T \omega = \Delta P . \quad \text{Eq. 1.39}$$

The governor measures the real speed of rotation and compares it with the reference value, if there is a negative speed deviation gives the command to move the wicket gate in closing direction. But, closing the wicket gate, cause a retardation force in the pressure shaft and so the head will go up. This increase of head tends to increase the power output, which is the opposite in respect to the effect that we want, so the correct action of the governor depends on the characteristics of the system.

It is now necessary to go in more detail regarding oscillations and stability. The large part of dynamic processes can be modelled by ordinary differential equations of the type

$$\dot{\bar{x}} = A\bar{x} + B\bar{u} . \quad \text{Eq. 1.40}$$

Where  $\bar{x}$  is the state vector and  $\bar{u}$  is the control vector. The eigenvalues of the matrix A give the dynamic properties of the system, they can be calculated by

$$\text{Det}(A - \lambda I) = 0 . \quad \text{Eq. 1.41}$$

Where  $I$  is the unit matrix and  $\lambda$  the eigenvalues. It is possible to find the characteristic equation, and the eigenvalues are the complex root of this equation. If in the system there are oscillations means that the eigenvalues must have an imaginary term, also if the real value is negative means that the oscillation is damped and stable; instead, if the real value is positive the oscillation is undamped and unstable; in the end if the real value is zero, the oscillation will be steady.



The speed of oscillation is given by the imaginary term, or by the time constant (inverse of the frequency), the real value instead defines where the oscillation dies out; for each eigen value there is associated an eigen vector or eigen frequency given by the following equation

$$A\bar{x} = \lambda\bar{x} . \tag{Eq. 1.42}$$

Where  $\bar{x}$  that satisfies this equation is the eigen vector.

With a time domain analysis, it is possible to determine if a system is stable or not, but if it is needed to determine the resonance frequencies it is necessary to move to the frequency domain; this can be done with the Laplace transform. By the Laplace transform it is possible to determine the transfer function between the control variable  $u$  and the response  $x$ , at the numerator of the transfer function there are the so called “zeros”, at the denominator the so called “poles”, these are critical characteristics of the system.

To model a process in a dynamic way, it is needed to set up a system of differential equations; then thanks to the Laplace transform it is possible to linearize and describe the process by block diagrams, where the output of one transfer function becomes the input of the next, and so on.

A hydro-power system with governor is a feedback system, which can be modelled by a block diagram like the one represented below.

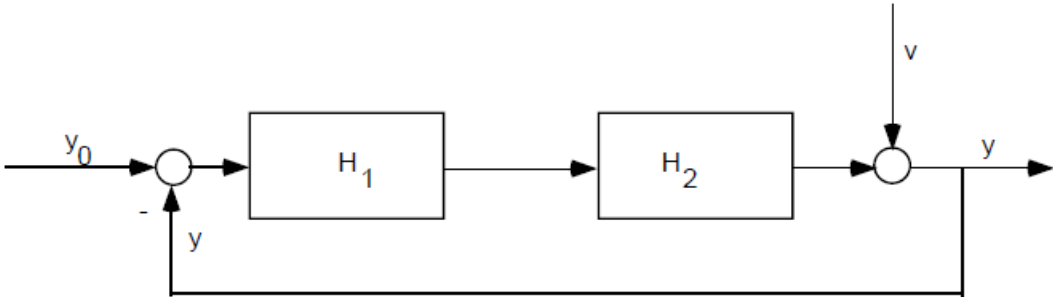


Figure 1.13 Block diagram for a feedback system [2]

Where the transfer function  $H_1$  represents the governor and  $H_2$  instead is the system. The idea is to keep constant  $y$ : it is possible to do this measuring the signal  $y$  and comparing it with the reference  $y_0$ , if there is a difference the control device of the governor acts to correct this.  $v$  is a disturbance that causes a change in the wicket gate opening inflicted by the governor, the issue present here is to choose a transfer function for the governor, to have that the response  $y$  to the disturbance  $v$  is minimized.

All the theory presented in this chapter is taken from [2].

After the analysis of the most important dynamic effects in a hydropower plant and the description of the main components of a plant it is possible to move to the analysis of the software used for the simulations. The next chapter has the purpose of giving an overview about the software SIMSEN, and describes how it works, to allow the reader to better understand the subsequent modelling and simulations.

# Chapter 2

## **SIMSEN implementation of hydraulic components**

After the analysis of the dynamic effects that can happen in hydropower plants, it is necessary to introduce the basis of the software chosen for the simulations, SIMSEN. This software was developed starting from 1992 by the *EPFL Laboratory for Electrical Machines (LME)*, so it is a quite new tool that, in the beginning, was introduced to have a modular system able to perform simulations of electrical power systems. Only in 2001 the hydraulic component's part was introduced (SIMSEN-hydro), with a collaboration between *LME* and the *EPFL Laboratory for Hydraulic Machines*; this to be able to study the dynamic behaviour of a complete hydroelectric power plant, as described in [5]. Today the software is used in many countries by industries, but also for research purposes; it helps the digitalization of hydropower systems, helping in the prevision making and in understanding phenomena of hydropower operation. Specifically, SIMSEN considers complex hydraulic machines and waterways, but also electrical machines, power electronics and the control system. Another reference for learning about SIMSEN is given by [6].

The software is based on a modular structure and allows to create numerical simulations in transient or steady-state mode. It is possible to represent the hydropower plant with blocks, where each one gives a specific element in the network: there are the electrical machine, the mechanical system with the mechanical masses connected with damping and springs, the transformer, the voltage supply, transmission lines, load, static converter, and regulator. In each unit there is a set of differential equations, which are based on the modelling of the various elements; the hydraulic elements are modelled as an assembly of RLC electrical components, the variables are: the piezometric head  $H$  at the nodes and the discharge flow rate  $Q$  through each component, these variables are associated respectively with voltage  $U$  and current  $i$ . In the software the differential equations can be generated with Kirchhoff's law, and they are solved simultaneously. [7] [6]

In the next sub-chapters, it will be analysed how the most important hydraulic components are implemented into the software, and how SIMSEN calculates the initial conditions of the circuit;

the initial condition determination is fundamental before starting any kind of simulation, so it is also important to understand how the software is able to find them.

### 2.1 Modelling of hydraulic components

Before going into detail on the plant implemented, it is necessary to introduce how to model hydraulic components in the SIMSEN software. It is known that a hydraulic circuit is made of several elements that have to be inserted in the software, the modelling is described well in the User Guide of the software ([8]) and in [6], in particular the software is an advanced numerical tool that allows to consider distributed head losses, the geometry, elasticity of water and pipes, and the wave speed in the piping system.

The algorithm of SIMSEN solves simultaneously the electrical, hydraulic and regulation equations, considering the interaction between these three parts of the system; also, the conference paper [7] gives a good reference for starting with this software and understanding the capability of it.

Follows the description of the modelling carried out by the software for each element of a hydropower network, every component will be analysed singularly, to understand the logic used by the software. Everything is taken from [6] and [7].

#### 2.1.1 Pipe

A first important element is the pipe, always present in every hydropower system. Pipes must be analysed carefully to understand phenomena that involve the propagation of pressure waves.

Generally, pipes are made of metallic materials with an elastic behaviour, but recently also polymer materials began to be used for hydraulic applications; many of these polymers present a viscoelastic behaviour, which introduces an additional damping in the system that must be taken into consideration for stability analysis.

The model of the pipe, derived from the momentum and mass equations, gives a representation of a pipe of length  $dx$  as an electrical circuit made of 2 resistances, 2 inductances and 1 capacitance. If there is a pipe with full length, it is possible to model it with  $n$  equivalent elements in series, as shown in Figure 2.1.

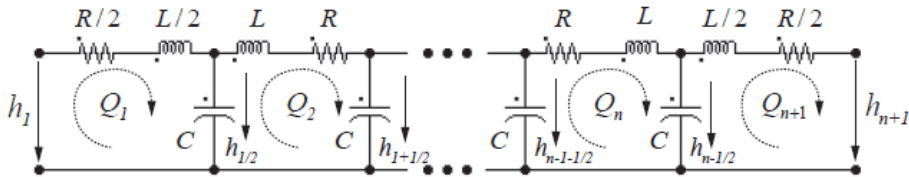


Figure 2.1 Model of the pipe as an electric circuit [6]

If a viscoelastic material is used, there is also a dynamic behaviour represented by a stress  $\sigma$  proportional to the deformation and to the rate of deformation; the next figure shows a typical time evolution of the stress as a function of the deformation.

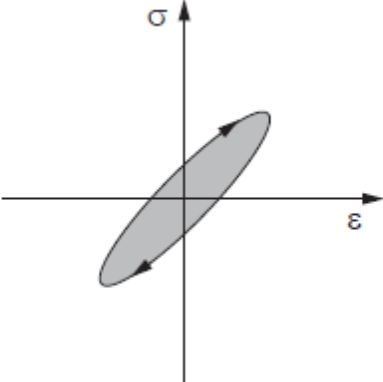


Figure 2.2 Stress as a function of the deformation [6]

To represent this viscoelastic behaviour, it is possible to use rheologic models, like Maxwell's, Kelvin-Voigt's or Standard models. Here the modelling will not be described in detail, the derivation of the most important equations can be read from [6].

In the following figure it is possible to see the rheologic and equivalent models of a viscoelastic pipe considering the contribution of both water and pipe material viscoelastic behaviour.

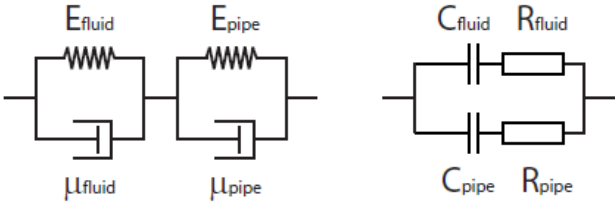


Figure 2.3 Rheologic and equivalent models of a viscoelastic pipe [6]

Referring to Figure 2.3, it is interesting to report here directly the expression of the resistance  $R_{pipe}$  (Ohm) and the capacitance  $C_{pipe}$  (F) of the pipe as

$$R_{pipe} = \frac{\mu_{pipe} e}{AD\rho g dx} , \tag{Eq. 2.1}$$

$$C_{pipe} = \frac{AD\rho g dx}{K_{pipe} e} . \tag{Eq. 2.2}$$

Where  $D$  is the diameter of the pipe,  $A$  is the cross section,  $\mu_{pipe}$  (Pa s) is the viscosity,  $K_{pipe}$  is the compressibility.

Then, also considering the fluid compressibility and viscosity ( $K_{fluid}, \mu_{fluid}$ ), it is possible to find

$$R_{fluid} = \frac{\mu_{fluid}}{A\rho g dx} , \quad Eq. 2.3$$

$$C_{fluid} = \frac{A\rho g dx}{K_{fluid}} . \quad Eq. 2.4$$

Combined the two resistances and capacitances, an equivalent resistance and capacitance can be defined as

$$C_{eq} = C_{pipe} + C_{fluid} = A\rho g dx \left( \frac{D}{K_{pipe}e} + \frac{1}{K_{fluid}} \right) = \frac{gA dx}{a^2} , \quad Eq. 2.5$$

$$R_{eq} = \frac{1}{\frac{1}{R_{pipe}} + \frac{1}{R_{fluid}}} = \frac{1}{A\rho g dx} * \frac{1}{\frac{D}{\mu_{pipe}e} + \frac{1}{\mu_{fluid}}} = \frac{\mu_{eq}}{A\rho g dx} . \quad Eq. 2.6$$

The resulting model is represented in Figure 2.4.

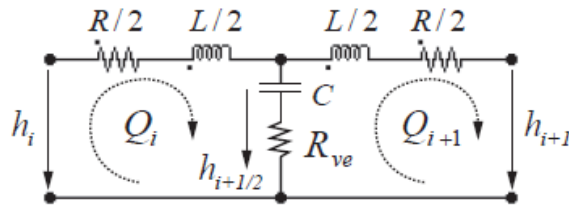


Figure 2.4 Resulting model of the pipe [6]

Where  $R_{ve}$  is the viscoelastic resistance equal to the equivalent resistance calculated previously.

Now it is possible to move to the second important component of a hydropower system, the valve.

### 2.1.2 Valve

The valve induces head losses in hydraulic systems that are function of the valve obturator position, it is possible to calculate the head loss as

$$H_v = \frac{K_v(s)}{2gA_{ref}^2} * Q_i^2 . \quad Eq. 2.7$$

Where  $K_v(s)$  is the valve head loss coefficient,  $A_{ref}$  is the reference cross section of the open valve and  $Q_i$  is the volumetric flow rate through the valve. According to this equation it is possible to represent the valve as a variable resistance defined as

$$R_v(s) = \frac{K_v(s)}{2gA_{ref}^2} * |Q_i| . \quad \text{Eq. 2.8}$$

The equivalent scheme is very simple and can be represented as follow.

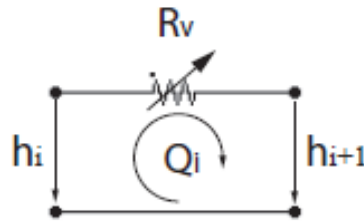


Figure 2.5 Electrical representation of a valve as a variable resistance [6]

### 2.1.3 Surge Tank

To solve dynamic problems, like water hammer effects, an important component is introduced both before and after the turbine in the plant, this element is the surge tank (as presented in the previous chapter of this thesis work). It has the purpose of decreasing the length of the path between the turbine and the first free water surface, to reduce the pressure oscillations, which are also dampen out thanks to this vessel. So now it is needed to analyse this element and how it is modelled by the SIMSEN software.

The surge tank is a device used for protection from water hammer effect, the tank in fact behaves as a free surface for wave reflection and the water level is function of the discharge time. Sometimes the cross section of the surge tank is a function of the elevation  $z$ , so the volume can be expressed as the integral of the cross section

$$V_{ST} = \int A(z)dz . \quad \text{Eq. 2.9}$$

Calculating the derivative

$$\frac{dV_{ST}}{dt} = A(z) * \frac{dz}{dt} . \quad \text{Eq. 2.10}$$

Considering that the volume variation of the water in the surge tank is proportional to the stored discharge  $Q_c = dV_{ST}/dt$ , and introducing also the piezometric head  $h_c$ , it is possible to find

$$A(z) * \frac{dh_c}{dt} = Q_c . \quad \text{Eq. 2.11}$$

From this last equation it is possible to see the capacitive behaviour of the surge tank, where the capacitance can be expressed exactly as the cross section

$$C_{ST} = A(z) . \quad \text{Eq. 2.12}$$

Through the surge tank there are energetic losses, since the flow is subject to cross section changes, it is also common to have a diaphragm at the inlet of the surge tank to increase the damping of water level oscillations. The head losses related to the presence of the diaphragm and to the change in cross section can be calculated as

$$H_d = \frac{K_d}{2gA_{ref}^2} * Q_c^2 . \quad \text{Eq. 2.13}$$

Where  $K_d$  is the diaphragm head loss coefficient and  $A_{ref}$  is the reference cross section for diaphragm head losses. To this head losses it is possible to associate a hydraulic resistance

$$R_d(Q_c) = \frac{K_d(Q_c)}{2gA_{ref}^2} * |Q_c| . \quad \text{Eq. 2.14}$$

It is possible to also define the head at the T-junction as

$$H_{ST} = h_c + R_d(Q_c) * Q_c . \quad \text{Eq. 2.15}$$

Finally, the equivalent scheme of the surge tank is given by a resistance and a capacitance in series, as represented below.

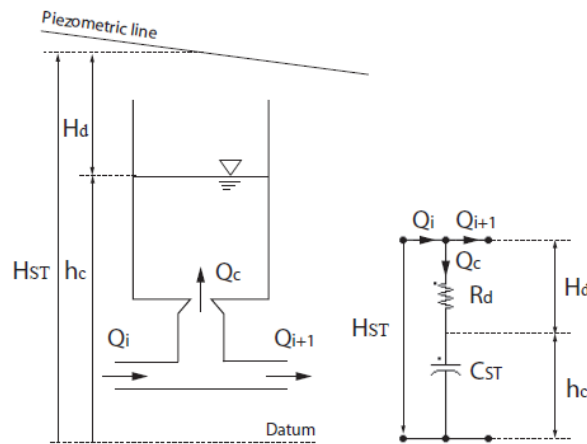


Figure 2.6 Scheme of a surge tank in electrical terms [6]



Where  $Q_c$  is the flow incoming in the surge tank, and it is equal to the difference of the discharges at the T-junction.

### 2.1.4 Surge Shaft

Surge shafts are surge tanks with small cross sections. In the surge tank the effect of the inductance can be neglected since the inductance is inversely proportional to the cross section. In the surge shaft, instead, it is not possible to neglect it since the cross section is smaller. The inductance  $L_{SS}$  (H) related to the water in the surge shaft is given by the integration of the inductance along the elevation axis  $z$  and can be written as

$$L_{SS} = \int_{z_{min}}^{h_c} \frac{dz}{gA(z)} = (h_c - z_{min}) / (g * \bar{A}) . \quad \text{Eq. 2.16}$$

Where  $h_c$  is the piezometric head,  $\bar{A}$  is a mean cross section and  $z_{min}$  is the minimum elevation of the shaft.

The capacitance and the resistance of the surge shaft have the same expression as the ones related to the surge tank, instead the head at the T-junction is given by

$$H_{SS} = h_c + R_d(Q_c) * Q_c + L_{SS} * \frac{dQ_c}{dt} . \quad \text{Eq. 2.17}$$

The resulting equivalent scheme of the shaft is represented in Figure 2.7.

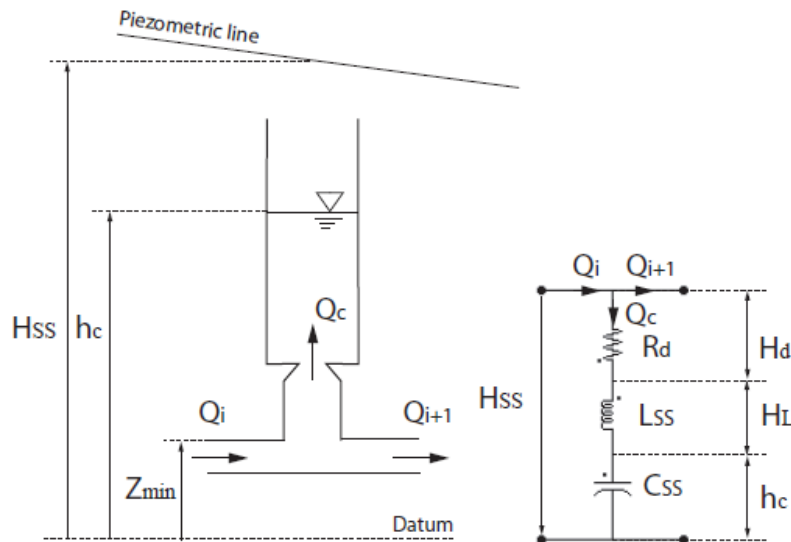


Figure 2.7 Resulting equivalent scheme of the surge shaft [6]

### 2.1.5 Air Vessel

The air vessel is used in hydraulic systems to mitigate pressure fluctuations induced by pumps, vortex shedding, valves opening and closure and other effects. Obviously, the water level  $h_c$  changes in the vessel, the flow discharge  $Q_c$  and the cross section of the vessel can be related as

$$A(z) * \frac{dh_c}{dt} = Q_c . \quad \text{Eq. 2.18}$$

The capacitance can be written as equal to the cross section

$$C_{AV} = A(z) . \quad \text{Eq. 2.19}$$

Inside the vessel there is gas, the gas volume varies for the water level changes, if it is assumed a polytropic transformation of the gas, it is possible to write

$$h_g * V_g^n = const . \quad \text{Eq. 2.20}$$

Where  $h_g$  is the head of the gas and  $V_g$  is the volume of the gas.

Calculating the derivative

$$h_g * n * V_g^{n-1} * dV_g + V_g^n * dh_g = 0 , \quad \text{Eq. 2.21}$$

rearranging and introducing the stored discharge

$$\frac{V_g}{h_g * n} * \frac{dh_g}{dt} = - \frac{dV_g}{dt} = Q_c . \quad \text{Eq. 2.22}$$

From this last equation it is possible to note a non-linear capacitive behaviour of the gas volume, the capacitance can be expressed as

$$C_{AV}(V_g, h_g) = \frac{V_g}{h_g * n} , \quad \text{Eq. 2.23}$$

and the head at the junction is

$$H_{AV} = h_c + h_g . \quad \text{Eq. 2.24}$$

It is possible to conclude that the equivalent scheme of the air vessel is made of 2 capacitances in series, as it can be seen from the following figure.

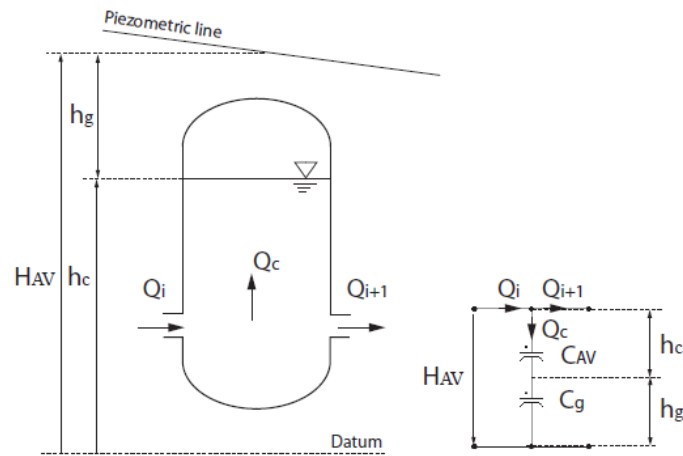


Figure 2.8 Electrical representation of the air vessel [6]

### 2.1.6 Cavitating flow

It is known that cavitation is a source of instability for a hydraulic system, the stability of the system can be studied using a one-dimensional approach to model the cavitation development with lumped elements. The volume of a cavitation development is given as a function of the head and discharge, therefore the derivative of the volume  $V$  ( $\text{m}^3$ ) can be expressed as

$$\frac{dV}{dt} = \frac{\delta V}{\delta h_{i+1}} * \frac{dh_{i+1}}{dt} + \frac{\delta V}{\delta Q_{i+1}} * \frac{dQ_{i+1}}{dt} . \quad \text{Eq. 2.25}$$

It is possible to define the cavity compliance  $C$  and the mass flow gain factor  $\chi$

$$C = - \frac{\delta V}{\delta h} , \quad \text{Eq. 2.26}$$

$$\chi = \frac{\delta V}{\delta Q_{i+1}} , \quad \text{Eq. 2.27}$$

and so, it is possible to find

$$Q_i - Q_{i+1} = Q_c = C * \frac{dh_{i+1}}{dt} + \chi * \frac{dQ_{i+1}}{dt} . \quad \text{Eq. 2.28}$$

Where  $Q_c$  is the flow going into the element. In addition, no losses or inertia effects are considered, so it is possible to end up at

$$h_i = h_{i+1} . \quad \text{Eq. 2.29}$$

The resulting equivalent scheme of cavitation is formed by 1 capacitance, as it is possible to see in the following figure.

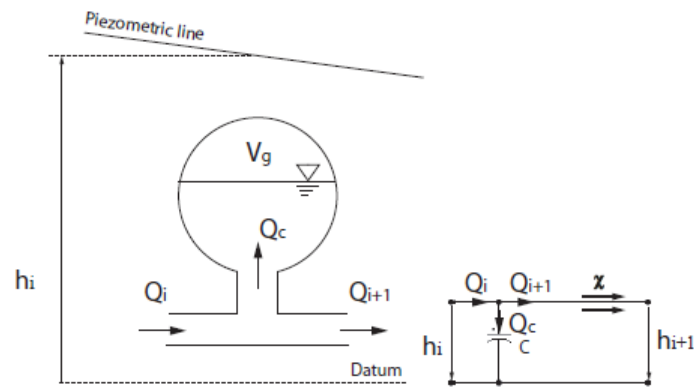


Figure 2.9 Electrical representation of a cavitating flow [6]

### 2.1.7 Reservoir

Another important element of a hydropower plant is the reservoir element, present upstream and downstream the turbine in the case of an open loop system. To study how it is modelled in SIMSEN, Figure 2.10 is taken as a reference.

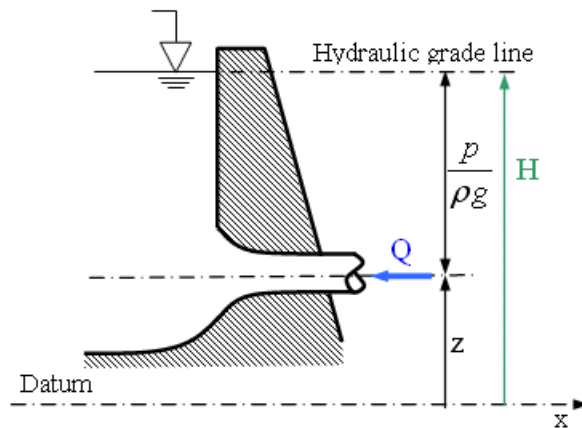


Figure 2.10 Reservoir scheme with main parameters [8]

As usual, the hydraulic head in a generic section can be written as

$$H = z + \frac{p}{\rho g} + \frac{Q^2}{2gA^2} \quad \text{Eq. 2.30}$$

The representation in the software of the reservoir is very simple, it can be seen as a voltage source, in fact it fixes the water level, and so the head, upstream and downstream.

The last element that it is needed to carefully analyse is the turbine.

### 2.1.8 Turbine

In this thesis work a Francis turbine is considered, since it is the one used in the laboratory of NTNU and on which the tests are taken, so here only this kind of turbine will be studied in detail.

To understand how the turbine is modelled, Figure 2.11 is taken as a reference.

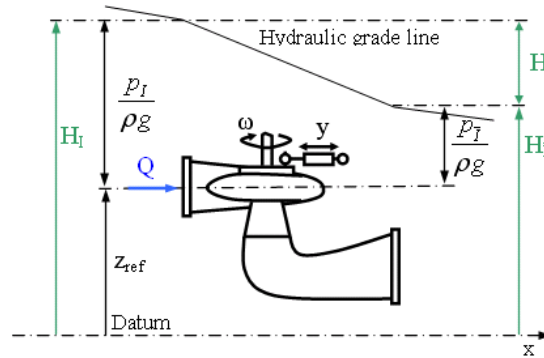


Figure 2.11 Turbine element in SIMSEN [8]

As usual, the hydraulic head can be expressed as the sum of the level  $z$ , the pressure head and the kinetic head. The turbine, as all the other elements, is seen by SIMSEN as a series of RLC electrical components: it is given by a resistance, an inductance, and a pressure source (see Figure 2.12).

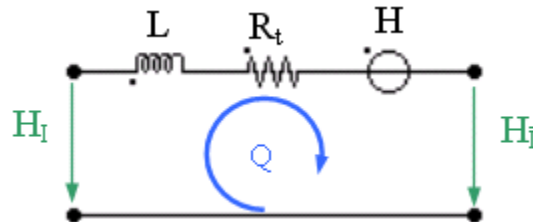


Figure 2.12 Representation of the turbine in the software [8]

Every RLC element is related to one part of the dynamic behaviour of the turbine: the pressure source gives the energy transfer between the fluid and the runner and is driven by the characteristic curves; the resistance is related to the guide vane opening degree; the inductance, instead, corresponds to water inertia effects. More specifically, the inductance term depends on the geometry of the turbine and is given by

$$L = \frac{L_{eq}}{gA_{mean}} \quad . \quad 2.31$$

Where  $L_{eq}$  is the equivalent length of the turbine, considering its geometry, and  $A_{mean}$  is a mean cross section. It is recommended to set appropriate values of these two parameters to consider the water inertia effect properly, due to the presence of the spiral case, the runner, and the draft tube. The values of the equivalent length and of the mean cross section can be chosen according to the following equations suggested by the SIMSEN guide ([8])

$$L_{eq} = (5 \text{ to } 15) * D_{ref} ,$$

$$A_{mean} = \frac{\pi D_{ref}^2}{4} .$$

Where  $D_{ref}$  is generally the outlet diameter of the runner, taken as a reference.

It is also possible to improve the model of the turbine, considering the dynamic behaviour of the spiral case and of the draft tube representing them separated from the machine, with straight pipes. In this way, the compressibility and inertia effects of water are also taken into consideration.

In the software it is assumed that the transition between two operating points corresponds to a succession of steady state points, so the transient behaviour of the machine can be modelled using the characteristics curves. To insert the curves into SIMSEN they must be given in a particular frame of reference, represented by the following expressions

$$n11 = \frac{ND_{ref}}{\sqrt{H}} , \tag{Eq. 2.32}$$

$$Q11 = \frac{Q}{D_{ref}^2 \sqrt{H}} , \tag{Eq. 2.33}$$

$$T11 = \frac{T}{D_{ref}^3 H} . \tag{Eq. 2.34}$$

As already said, for a Francis turbine it is needed to consider the opening degree of the guide vanes, used to regulate the discharge through the hydraulic machine. If there is full closure of the guide vanes there should be no flow rate, this can be achieved in the simulation with a resistance; in particular, the resistance is effective only in case of small discharge, lower than 5% of the rated value.

After the explanation about how the hydraulic elements are implemented into the software, it is also interesting to see how the software finds the initial conditions of a system, before launching the simulation.

## 2.2 Initial conditions determination

For electrical systems, the initial conditions problem is solved by SIMSEN with a load flow calculation using the Newton-Raphson's algorithm; in SIMSEN-hydro instead the initial conditions procedure is performed doing a fast simulation of the transient behaviour, until the steady state is reached. To optimize the procedure an additional damping is introduced, large capacitances are reduced, and the turbine characteristics are bounded, to avoid errors due to the search of an operating point that is outside the hill chart. The additional damping can be introduced setting the viscoelastic resistance of the pipes considering the limit time constants of the system. [6]

When, in the hydraulic circuit, there is a turbine or a pump, there are 2 ways to determine the initial conditions: if the machine is in generating mode (so is acting as a turbine, this is the case studied in this work), it is possible to specify the rotational speed and the torque, while the guide vane opening is calculated. This can be seen in Figure 2.13.

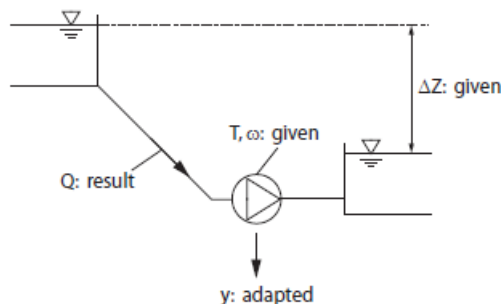


Figure 2.13 Hydraulic load flow procedure for generating mode on the left and for pumping mode on the right [6]

The analysis of the initial conditions' determination ends the overview on how the SIMSEN software works; for further information the various documents reported in the bibliography of this thesis work and cited in this chapter can be used. After this explanation, it is possible to start talking about the model realized: a detailed description on how it was built can be found in Appendix A. The next chapter, instead, will directly focus on the numerical benchmarking of the model, which represents the hydropower plant of the *NTNU WaterPower laboratory*. Before validating the model against experimental results, it is, in fact necessary, to verify if the physic of the phenomena of interest is correct; the interest here is particularly related to pressure oscillations. Basically, the next goal is to verify the effects described in Chapter 1.





# Chapter 3

## Numerical benchmarking: pressure oscillations

The steps done for the implementation of the model in SIMSEN can be read in Appendix A of this thesis work, there a full description of every component inserted and of the parameters chosen is reported. The main focus of this project is related to the validation of a detailed and dynamic model of the hydropower plant object of the studies, but before validating it with experimental results it is needed to verify if it is able to represent known dynamic phenomena. This will be the aim of the current chapter, and already represents a first validation that allows to understand the correctness of what was implemented. This is part of digital twins' development perspective, as known, in fact, in Europe there is the ambitious goal of arriving at least at 64% of electricity production from renewable resources by 2050. This requires an increase in the ability of providing ancillary services by hydropower plants, since it is almost the only renewable resource that is fully controllable. However, the higher flexibility requested has consequences, such as the increase of load variations, start/stop sequences and in general increase the amount of transient with which the plant must deal. In the paper [9] there is a good explanation and example on how SIMSEN can be really used for the digitalization of hydropower plants; specifically, the use of a digital twin can help to monitor in real time the pressure variations induced by transients in the conduits, in order to prevent stresses and help in the managing of a plant.

In chapter 1 the propagation of pressure waves in pipes was explained, and how this can affect the whole hydropower plant, the interest here is related to dynamic simulations and so the first thing to do is to verify that the digital model of the plant is able to represent these effects in the proper way; here the theory should be applied to the model and a comparison should be made. It is also wanted to verify that the pressure waves generated by a disturbance can propagate through the turbine element, see [10] for studying the phenomenon.

### 3.1 Propagation of pressure waves

As already said, it is wanted to verify the presence of water hammer pressure waves and U-tube oscillations when there is fast closure of a valve in a generic point of the plant, the theory about

this was explained in the first chapter of this thesis work. The goal of the next simulation will also be to verify the propagation of a pressure wave through the turbine element of SIMSEN; the document [10] gives a good reference for understanding this phenomenon, it is based on a study about a centrifugal pump, but the theory can be extended to hydraulic turbines.

The importance of analysing water hammer pressure waves is related to the fact that the mechanical loadings given by this effect can lead up to the rupture of the piping system, so such loads must be considered in the design process of a plant. As explained in [10], water hammer can be caused by rapid closure of a valve, this gives rise to a pressure wave that will travel at the velocity of sound into the pipes; the amplitude of the wave can be calculated with the *Joukowsky* equation

$$\Delta p = \rho a \Delta v . \quad \text{Eq. 3.1}$$

Where  $v$  is the velocity of the fluid into the pipe,  $\rho$  is the density and  $a$  is the speed of sound.

After a pressure wave is generated, it will travel towards the first free water surface before the closed valve, then it will be reflected and travel back to the valve; this process is repeated until the energy is dissipated thanks to friction and fluid-structure interaction. It must be said also that, the presence of a surge tank in a hydropower plant allows to dampen out water hammer waves, so it is expected to see only the U-tube oscillations left after the tank; water hammer waves are present only between the closed valve and the first free water surface upstream. [10]

In [10], another interesting point is explained, regarding the possibility for a water hammer pressure wave to pass through a centrifugal pump, this can be extended to a hydraulic turbine. In theory there can be three possibilities: or the pump reacts as a hydraulic open pipe, or like a closed boundary condition, or finally like an open boundary condition. In [10] is explained that, putting a pressure sensor at both suction and pressure side of a centrifugal pump, it was found that the pump let almost all the wave to pass. So, it can be concluded that the pump operates as it is hydraulic open and reacts almost as a pipe; the idea is now to extend this concept on hydraulic turbines and demonstrate that also in the model it is possible to see the same propagation of pressure waves.

### ***3.1.1 Verification in the model***

First it is needed to report here the model realized in the software (see Appendix A for more detail).

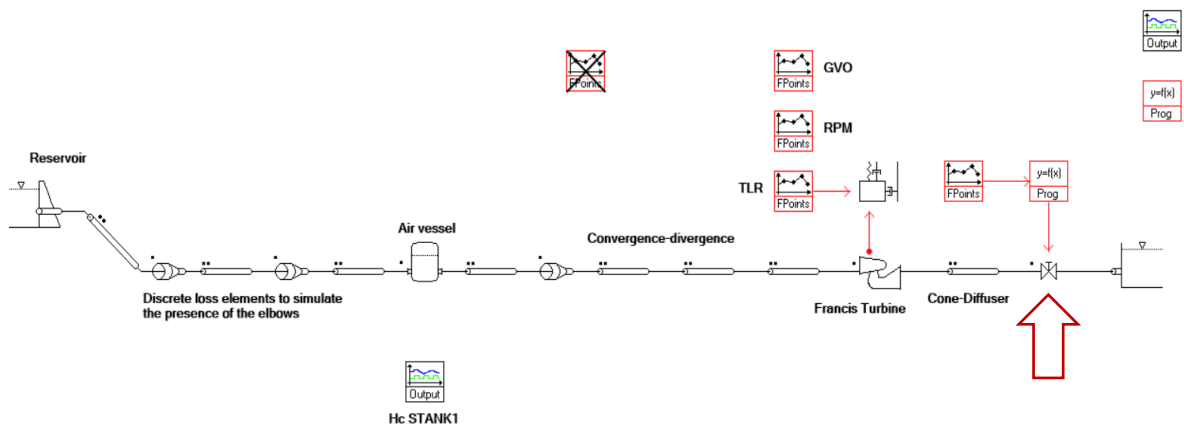


Figure 3.1 Model realized in SIMSEN with the addition of a valve to simulate water hammer pressure waves propagation

To verify what explained before it is possible to insert a valve just before the lower reservoir, after the draft tube, and set the closing of the valve during the simulation period.

The state of the valve is controlled by an “FPoint” element and a “Prog” element, after 20s of simulation and in 0.1s the state of the valve moves from 1 (completely open) to 0 (completely closed). It is possible to say that the closing is almost instantaneous and can represent a water hammer effect in the plant.

With the visual program of SIMSEN it is possible to print the graphs related to the various parameters of the elements, the interest here is on the pressure behaviour, so first it is possible to open the draft tube element and study the pressure at his exit, just before the valve (see Figure 3.2).

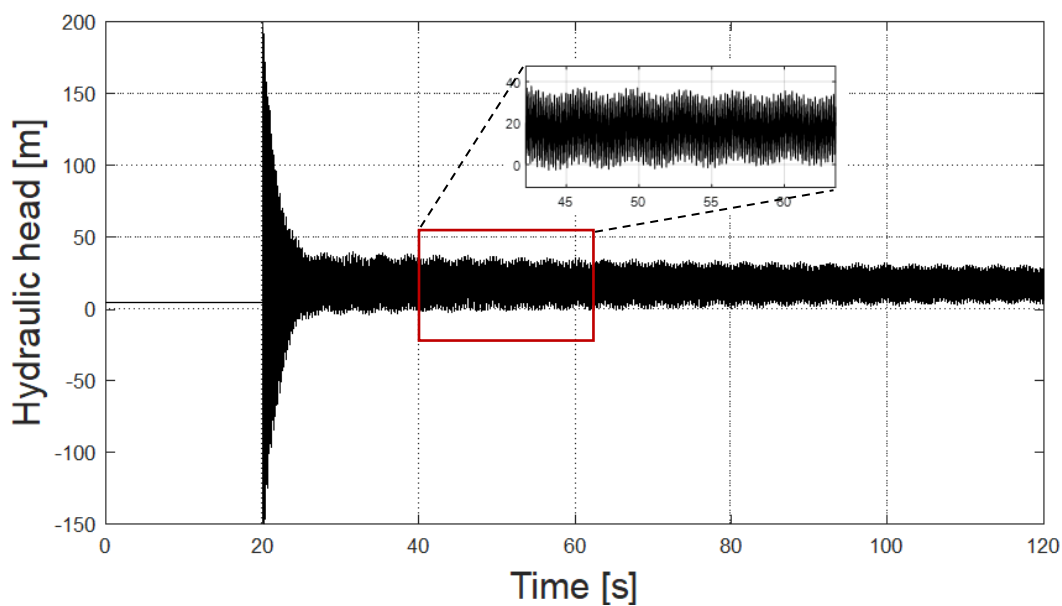


Figure 3.2 Pressure behaviour at the outlet of the pipe before the valve

As expected, after 20s of simulation there is a big jump in pressure before the valve, due to the closure of the latter, then a pressure wave propagates between the valve and the nearest free water surface upstream. This phenomenon creates a pressure oscillation between positive and negative values with very high frequency; looking at the zoom it can be clearly seen that the overall oscillation is given by the composition of a signal at high frequency (water hammer wave), and a signal with lower frequency (U-tube oscillations). The fluctuations are dampened out over the time thanks to the presence of the air vessel.

Now it is interesting to see also the pressure behaviour in the pipe before the turbine, to see if the model can take into consideration the propagation of pressure waves through the turbine element (see Figure 3.3).

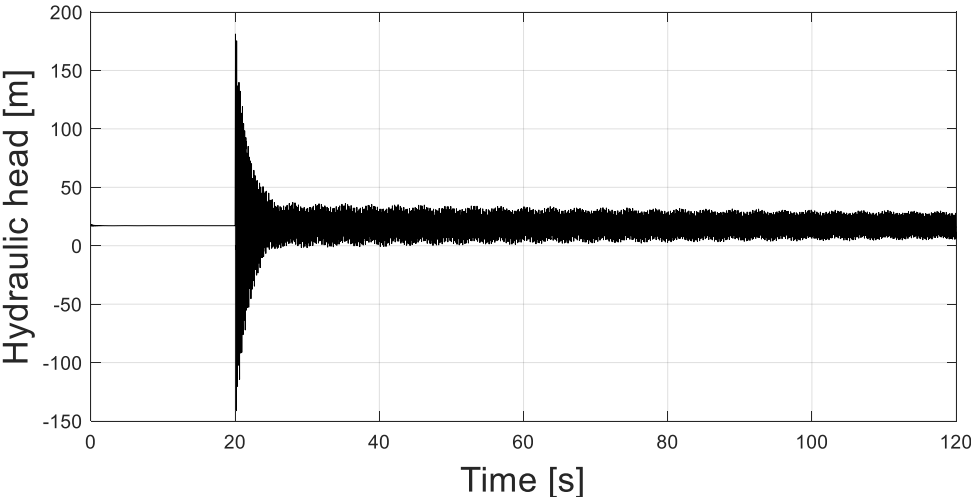


Figure 3.3 Pressure behaviour at the inlet of the turbine after water hammer simulation

The behaviour is the same of the draft tube, so it is possible to confirm that the pressure waves can propagate through the turbine element, as expected from the physic of the phenomena and in real tests (see studies obtained in [10]).

It is also interesting to study the effect of the surge tank before the turbine. This element is present in every hydropower plant and allows to decrease the length of the path between the turbine and the first free water surface upstream; in this way when there are pressure oscillations with high frequency, they are absorbed and dampen out by the tank, as explained in [2]. The effect is that, between the upper reservoir and the surge tank, only U-tube oscillations should be present, given by the change in the water level in the tank (see Figure 3.4).

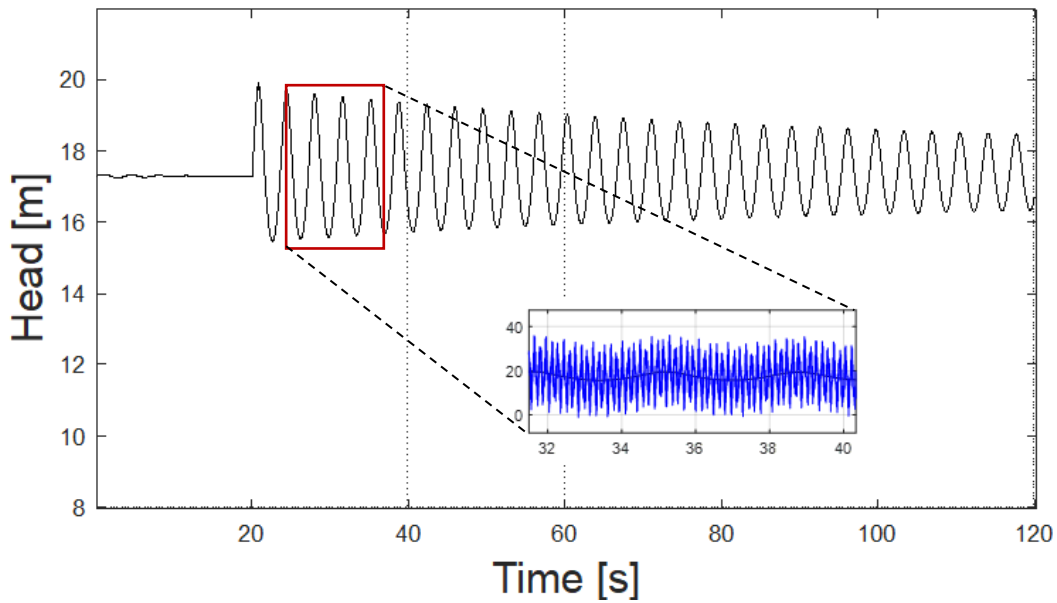


Figure 3.4 Pressure oscillations at the exit of the pipe upstream the tank and zoom with a comparison in the oscillation frequency of the U-tube oscillations for the pipes before the tank and before the turbine, where there are also water hammer waves

From this last figure it is possible to see that, upstream the tank, only the low frequency oscillations are present, called U-tube oscillations. In the graph they are compared with the hydraulic head behaviour before the turbine, it can be noted that the frequency of the low-frequency oscillations is the same for both pipes. Also, it can be confirmed that the air vessel is able to stop the water hammer waves, so the pipes before it, are not affected by the high frequency pressure waves. Finally, it is possible to print the variation of the water level in the vessel, to check the consistency with the previous graph.

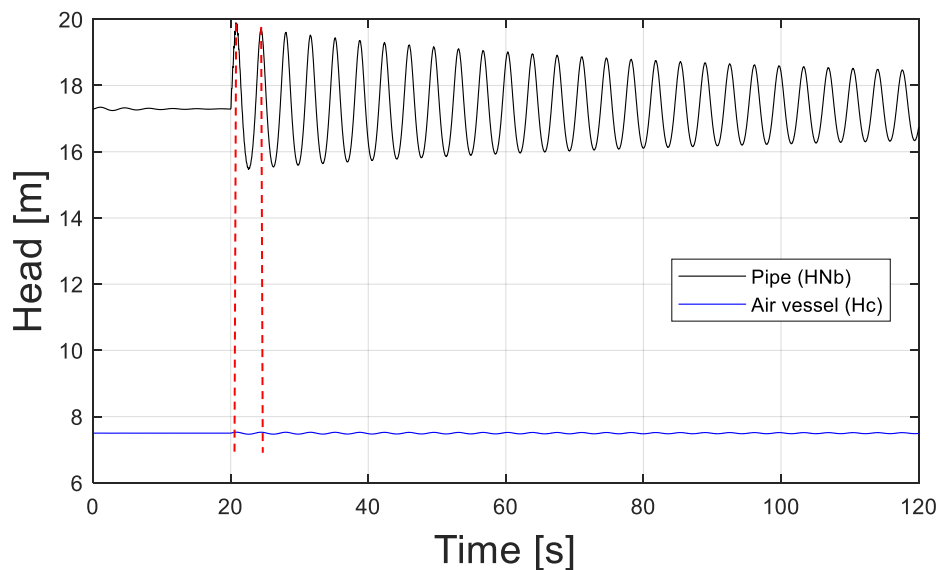


Figure 3.5 Oscillation of the water level in the air vessel

Figure 3.5 shows that the water level oscillations are consistent with the pressure oscillations in the pipe before the tank; in fact, the frequency is the same, as it is possible to note from the two vertical lines traced for highlighting this.

Another interesting thing to verify is the calculation of the wave speed through the pipes, and of the travel time of the pressure waves. This to see if the wave speed results coherent with the value that was chosen at the beginning, with the discretization procedure on the pipes (see Appendix A for the description). To do this, it is possible to calculate the wave speed as

$$a = \frac{4L}{T} = 4 * \frac{21.79}{0.145} = 601 \frac{m}{s}. \quad \text{Eq. 3.2}$$

Where  $L$  is the length of the pipes between the upstream surge tank and the point in the plant where the water hammer is generated;  $T$  is the period of the oscillation, calculated from the graphs looking at the distance between two peaks. The results obtained can be considered acceptable, it is coherent with the adjusted wave speeds inserted in every pipe element.

After this first numerical validation, considering the pressure propagation along the piping system, it is possible to move to the complete validation of the model, using the experimental results available from tests taken in the laboratory, during the spring semester 2022, on the Francis99 rig.

# Chapter 4

## Numerical validation of the model

After completing the construction of the model from the hydraulic point of view and verifying that it can represent known physical phenomena (like water hammer pressure waves), it is necessary to validate it against experimental results; the model will allow a higher digitalization at the *WaterPower Laboratory* of NTNU, helping in the analysis of transients and in the optimization. As a first validation two sets of measures were used, one related to the steady state operation and the other related to a load reduction simulation. The first case is used to verify the correctness of the calculated losses in the piping system; then it is important to see the behaviour also during transients. In the next paragraphs these two cases will be studied to see if the model was realized correctly, and to understand if some modifications are needed.

After the completion of the numerical validation of the model with the available experimental data, a further development will be the introduction of the governor of the turbine in the model; during the semester the governor has been developed and tests have been carried out. The goal is to also add this component in the simulation and then validate the model again, against the new experimental results with the governor implemented. But first let's focus on the analysis realized without considering the presence of the governor and PID control, so controlling manually the guide vane opening of the Francis turbine during transient operation.

### 4.1 Steady state comparison

The measures taken in the laboratory in steady state conditions were used to set the proper loss coefficients in the model; in particular, it is needed to compare the head across the turbine in the simulation with the differential head measured; this value depends on the losses in the whole hydropower plant.

Before going into details on the experimental values, it is therefore necessary to calculate properly the loss coefficients for the pipes and elbows inserted in the model, according to a theoretical procedure. To do this an excel file was created, here it is reported only the table with the main results (for a detailed description see Appendix B, [11]).

Table 1 Summary of the main pipe parameters with loss coefficients

	L [m]	D [m]	Re	lambda	Nb	a [m/s]
<b>PENSTOCK</b>	8.80	0.600	443511.8	0.015367	11	800.0
<b>PIPEZ1</b>	3.20	0.600	443511.8	0.015367	4	800.0
<b>PIPEZ2</b>	2.69	0.600	443511.8	0.015367	3	896.7
<b>PIPEZ3</b>	2.00	0.600	443511.8	0.015367	3	666.7
<b>PIPECONV</b>	2.96	0.387	687082.5	0.015685	4	740.0
<b>PIPEDIV</b>	1.72	0.296	899618.2	0.016153	2	860.0
<b>PIPEZ4</b>	7.72	0.350	760305.9	0.015838	10	772.0
<b>DTUBE</b>	7.39	0.577	461190.8	0.015372	9	820.8

In the table, from the left to the right, it is possible to see the length of each pipe  $L$ , the diameter  $D$ , the calculated Reynolds number  $Re$ , the local loss coefficient  $lambda$ , the number of elements in which the pipe is divided  $Nb$ , and finally the corrected wave speed  $a$ .

Regarding the elbows instead, in Appendix B is reported the procedure used for the evaluation of the loss coefficients  $K$ ; here only the table is resumed, to have clear the starting data.

Table 2 Summary of the local loss coefficients for the elbows

ELBOWS		K
1	smooth with vanes 90°	0.500
2	smooth 90°	0.230
3	smooth 35°	0.052

In the next figure the scheme of the model in SIMSEN is reported, with all the names of the pipes, to have a reference for Table 1.

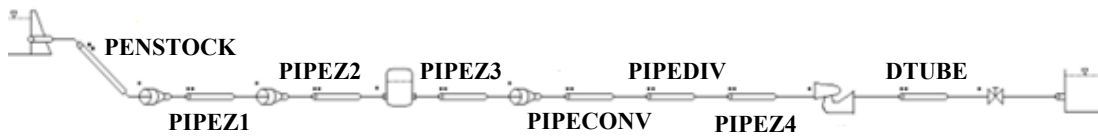


Figure 4.1 Scheme of the plant with pipe's names as in the previous table

After the theoretical evaluation of the loss coefficients, a first simulation can be launched starting from 17.3m of head at the upper reservoir and setting 4.7m of head at the lower reservoir, these values are taken according to the following schematic (see Figure 4.2).



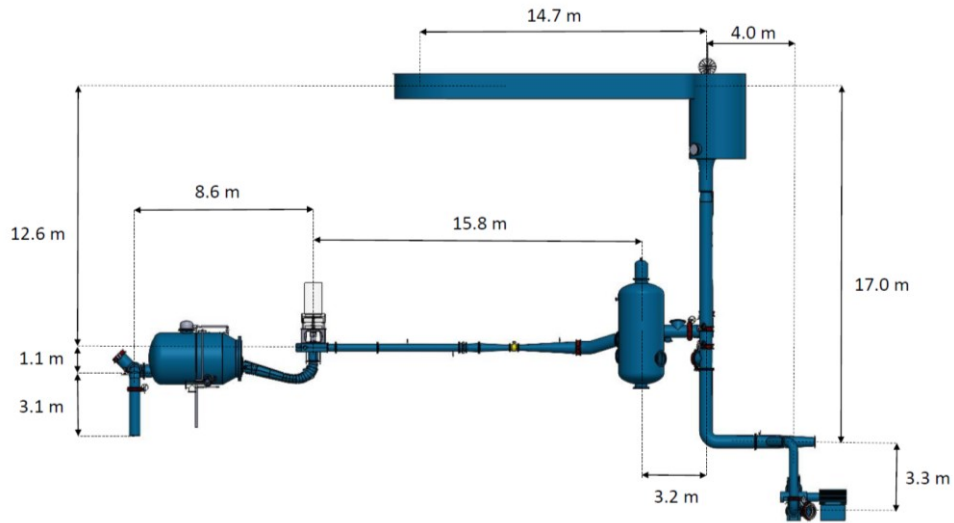


Figure 4.2 CAD of the plant present at NTNU with various lengths

From the figure it is possible to see that the level in the lower reservoir can be seen as the elevation of the vessel (3.1m) plus the elevation of the spiral case (1.1m) plus another amount to consider that the water level in the vessel is higher than the elevation of the spiral case. Regarding the head at the upper reservoir instead, the chosen value is around 17.3m, looking at Figure 4.2 the elevation of the water there is given by  $12.6 + 1.1 + 3.1 = 16.8m$  in respect to the pool; but looking at the measures in steady state condition the head across the turbine is around 12.45m. Considering this value and the losses in was necessary to increase a bit the level in the upper reservoir, in order to match the results and to have the proper differential head between inlet and outlet of the turbine; this can be explained considering that the draft of the plant is not very precise and there can be small changes in the water level changing the position of the overflow present in the reservoir.

In Figure 4.3 the model realized in the software is reported, to have a reference for the simulation.

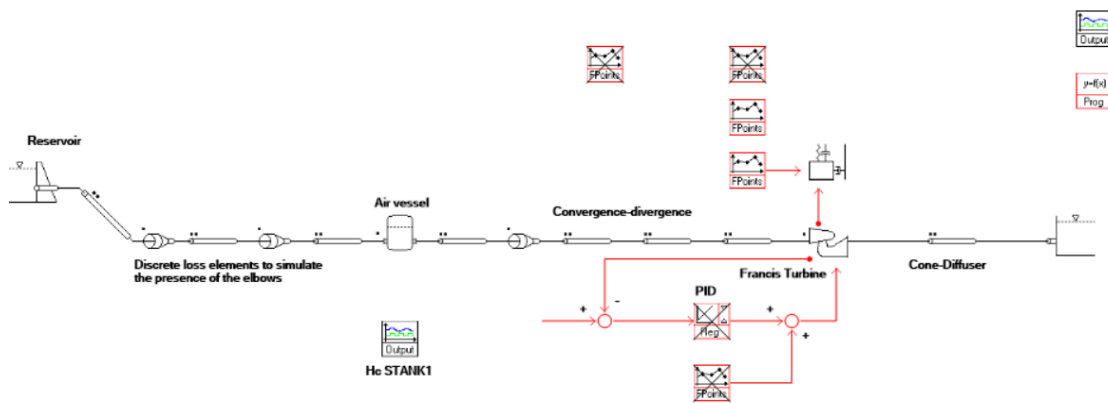


Figure 4.3 Model of the plant realized in SIMSEN

To perform the steady state simulation, it is also needed to set the rotational speed and the torque at which we want that the turbine operates. To do this two “*FPoint*” elements were used: the rotational speed is fixed at  $342rpm$ , according to the experimental setup, instead the external torque applied to the generator is fixed at  $659Nm$ , taking an average of the measured values running the test rig at the best efficiency point. Before performing the real simulation, the “*InHydro*” procedure must be used, to find the initial conditions: the software calculates the guide vane opening needed to guarantee the torque and rotational speed wanted.

Launching the simulation in steady state, so without introducing any disturbance over the time, the matching with the experimental results was reached; also confirming the correctness of the values calculated for the loss coefficients of the pipes through the theoretical procedure described in the appendix, applying some small adjustments.

Here a table is reported, with a summary of the comparison between the results of the simulation and average values of the experimental data.

*Table 3 Comparison between SIMSEN results and experimental data in steady state conditions*

<b>Parameter</b>	<b>Results SIMSEN</b>	<b>Measured value</b>	<b>Error [%]</b>
Q [m <sup>3</sup> /s]	0.209	0.209	0.002
H [m]	12.43	12.46	0.240
P <sub>m</sub> [kW]	23.60	23.67	0.300
y [-]	0.717	0.719	0.320
T [Nm]	659.0	659.0	0.002
n11 [ $\sqrt{m} * rpm$ ]	33.85	33.81	0.120
T11 [N/m <sup>3</sup> ]	1247	1248	0.110
Q11 [ $\sqrt{m/s}$ ]	0.487	0.487	0.020

Looking at Table 3 it is possible to see that the results of the SIMSEN simulation are very close to the experimental given data, so it is possible to confirm the correctness of the model in steady state operation. In Appendix A there is a full description on how the model in the software was realized, considering a faithful representation of the real plant as it is physically in the laboratory; but then, this must be modified to represent the real effects given by the experimental setup (substitution of the downstream part of the plant with a reservoir element).

Now that the steady state operation has been verified, as the losses in the piping system, it is possible to move to the transient operation, to study the response of the model also when disturbances are introduced.

## 4.2 Load Reduction simulation

To study the dynamic response of the simulation in comparison with the real dynamic of the plant, a test in load reduction conditions was taken by some colleagues in the laboratory. After starting the test rig operation, the closing of the guide vanes was applied, from nearly 10° of opening to 6.7°; the closure happened in few seconds, to get a fast transient.

It is useful to report here the representation of the plant in SIMSEN, to highlight the added components for this simulation (see Figure 4.4).

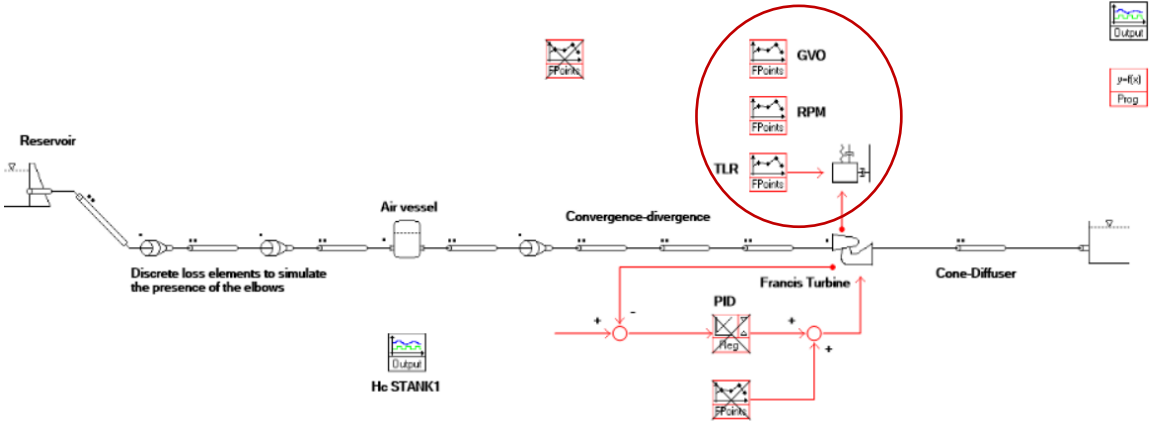


Figure 4.4 Scheme of the plant in SIMSEN for the load reduction simulation

The model is the same used for the steady state analysis, the only differences are the “*FPoint*” elements used to fix some parameters of the simulation. In this case it is needed to fix the rotational speed at 342rpm, it is wanted to keep it fixed during the transient; then another “*FPoint*” is used to set the guide vane opening, changed manually during the tests; finally, also the external torque applied to the generator has to be fixed according to the measured values. All the other parameters in every component of the model are the same. Since it was decided to run the simulation through MatLab, first it is needed to run SIMSEN with the “*InHydro*” procedure, to get the correct initial conditions, setting the wanted torque and rotational speed at the beginning. Then, the simulation can be launched, and an analysis of the graphs can be done (see Figure 4.5, Figure 4.6, and Figure 4.7).

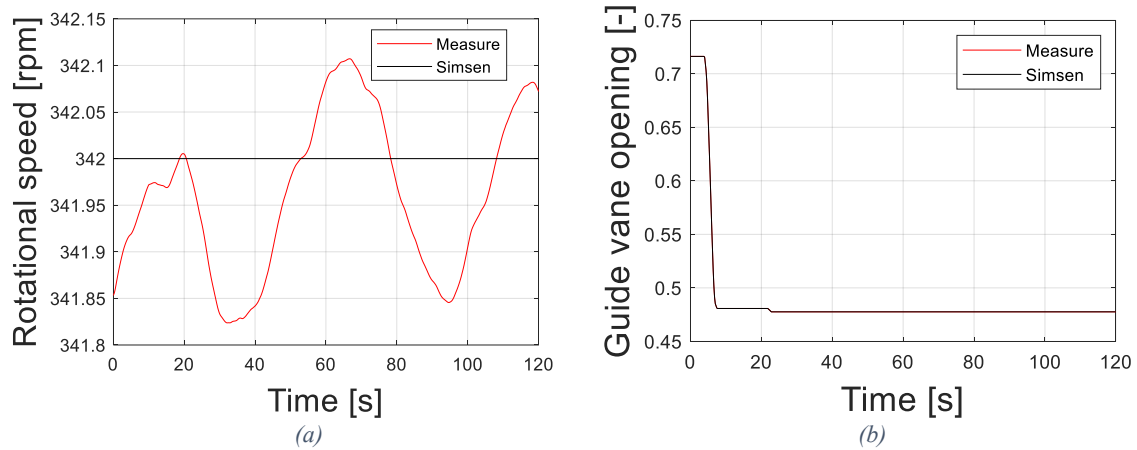


Figure 4.5 Comparison with experimental results for the generator speed and the guide vane opening

Regarding the rotational speed and the guide vane opening the match is obviously perfect, since they are fixed in the model considering the imposed value during the tests. In the real operation of the plant the rotational speed is not perfectly constant, but also the variation around the nominal value is small.

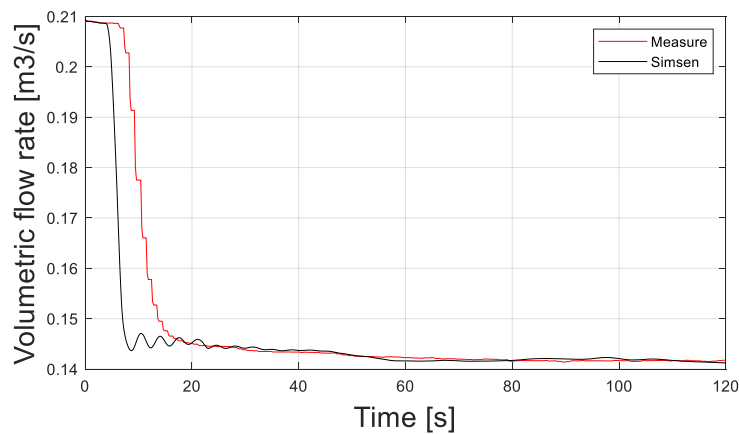


Figure 4.6 Comparison between the model and the experimental results for the discharge through the turbine

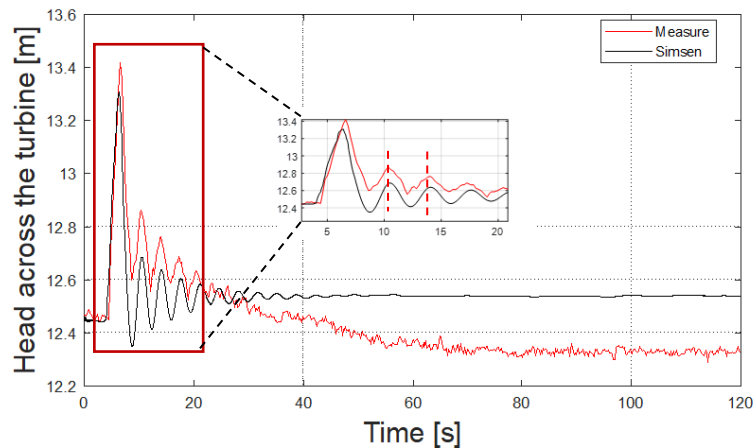


Figure 4.7 Comparison between the model and the experimental results for the head across the turbine

A higher interest is on the results reported in Figure 4.6 and 4.7; where it is possible to analyse the variation of flow rate and head across the turbine. Starting from the discharge, when the guide vanes close there is a fast decrease in the volumetric flow rate of the SIMSEN simulation, instead the decrease in the measured values happens with a certain delay. This can be explained considering that the flow meter, used to detect the flow rate, does not have a fast response; so, basically, this mismatch is due to the ability of the instrument in detecting a change in the discharge through the turbine. However, before the disturbance and after it is possible to see that the simulation is arriving at the same steady state flow of the experimental measures.

Moving to the graph related to the head instead, there are more things that must be pointed out: first it is possible to see that at the beginning the matching with the steady state before the disturbance is correct, there is almost no difference between the simulation results and the real data. Starting from the transient, some differences can be seen. First, the peak of head when there is the closing of the guide vanes it is not perfect, in the simulation a lower peak is detected but the difference is not so relevant; second, after the transient the model is arriving at a steady state head that is slightly higher in respect to the measured one (the difference is around 0.2m, a value that is not negligible). However, it must be noted that the oscillation frequency during the transient is matching almost perfectly with the experimental data, this result was reached working on the initial volume of gas in the air vessel. This parameter affects a lot the frequency of dynamic phenomena in the plant, so it must be chosen properly before running the simulations; from the acquiring program of the laboratory, it is possible to get the pressure inside the tank (see Figure 4.8 for the interface), from this value the evaluation of the volume is possible.

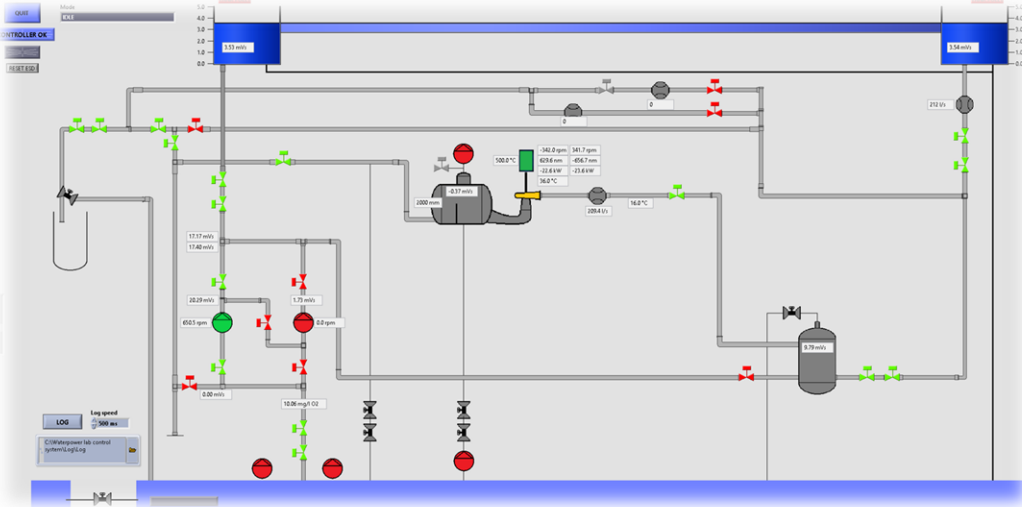


Figure 4.8 User interface of the acquiring program in the lab with pressure values

As it is possible to see, in the tank is reported the value of pressure in terms of meter per water column, but there is no measure of the water level  $H_C$ , so some trials had to be done to arrive at a matching of the oscillation frequency.

The main issue related to the previous graphs is that, after the transient, the simulation and the real data are not arriving exactly at the same steady state operating point, in terms of head; there are around  $0.2m$  of difference. It is needed to go more deeply inside this problem to understand from where the mismatch is coming from. The head in a generic section of the plant can be expressed as

$$H = z + \frac{p}{\rho g} + \frac{Q^2}{2gA^2} . \quad \text{Eq. 4.1}$$

Where  $z$  represents the elevation of the point considered,  $p$  is the static pressure,  $Q$  is the volumetric flow rate and  $A$  is the cross section. Analysing in detail the available data and the results of the simulation the term of head that depends on the flow rate is matching, this is a consequence of the fact that the flow rate itself was behaving well; the level  $z$  cannot be the problem, since it is a fixed parameter; so it is possible to conclude that the error comes from the pressure head. In particular, from the value of the pressure measured at the outlet of the draft tube: this value is remaining almost constant in the simulation; this is due to the fact that after the draft tube there is a reservoir with infinite volume and almost constant water level. Since the level cannot change a lot, the pressure head at the outlet of the draft tube is also remaining almost constant. Instead, looking at the measures, the static pressure at the outlet of the draft tube is increasing (see Figure 4.9).

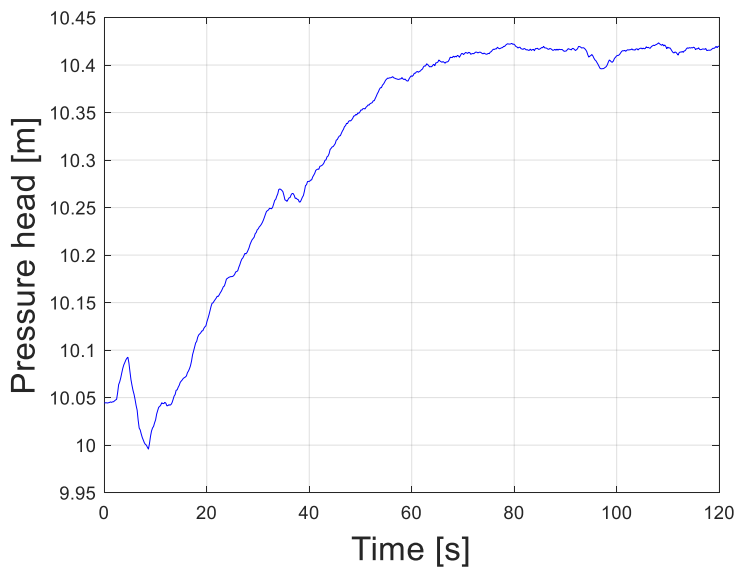


Figure 4.9 Pressure head at the outlet of the draft tube in the real plant

This discrepancy brings to the difference between the steady state operation reached after the transient of load reduction. The problem that must be solved is the understanding of the phenomena that brings the pressure to increase after the transient at the outlet of the draft tube; from a physical analysis the opposite is, in fact, expected. When there is closing of the guide vanes, the pressure increases fast at the inlet of the turbine, because of the retardation of water masses in the pipes; the flow rate discharged through the turbine instead decreases, but for the water inertia effect, there should be a higher flow rate going out from the second tank of the plant (the one after the draft tube). This should bring the pressure head to decrease, since the water level in the tank will decrease as well, as said in [2]. But in the plant is happening exactly the opposite, as shown in Figure 4.9 the pressure head at the outlet of the draft tube is, in fact, increasing.

What happens after the draft tube is not considered into the model, for the presence of an open valve at the exit of the tank the closest representation is given by the introduction of a reservoir with infinite volume; but still the behaviour of the static pressure cannot be explained with the actual knowledge about the plant. For sure a further work into the laboratory will be related to the analysis of this parameter, thanks to the model it was possible to highlight this pressure behaviour that, otherwise, probably would not have been noticed. Once the physical phenomenon will be discovered it will also be possible to eventually modify the model, to have a better representation of the plant.

For the moment the results are considered satisfactory, having also in mind that the way with which the test rig is operated is very specific and it is not what happens generally in a real power plant, where after the turbine there is a direct connection with a big reservoir. The purpose of this thesis work is, in fact, to study how a digital twin of a power plant can be realized with the software SIMSEN, there are already many references that demonstrate the capability of the software on reproducing the real behaviour of a power plant connected to the grid, like the paper [9]. The interest on solving this mismatch and understanding the physical phenomenon happening in the plant, is only related to the possibility of using the SIMSEN model at the *WaterPower Laboratory* of NTNU, but to do this a higher knowledge and further studies are needed. Still, it is possible to say that the model allowed to point out this question mark and, apart for the head mismatch, it allows to prevent dynamic effects and pressure variations happening during transients.

The only way to solve the discrepancy, at the moment, and have a head in the SIMSEN simulation that matches with the experimental data in the steady states before and after the transient, is to change the water level in the lower reservoir of the model, trying to reproduce

the effect happening in the plant. An “*FPoint*” element can be used, setting an increase in the water level after the transient, this allows to arrive at the following graph.

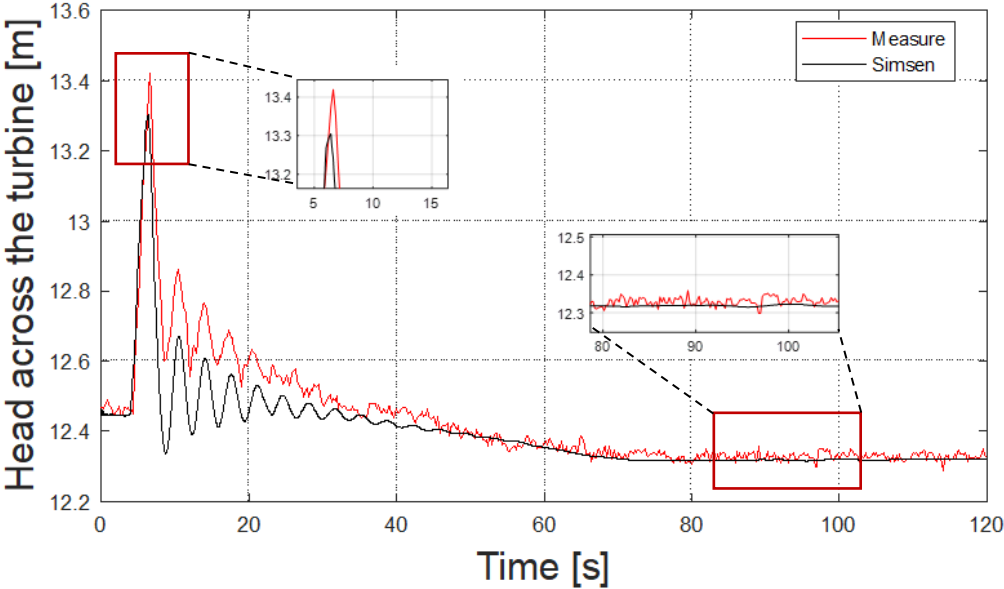


Figure 4.10 New head behaviour considering a change in the water level of the lower reservoir in the simulation

As it is possible to see from Figure 4.10 the steady state before and after the transient is the same, between the model and the real data, the peak in head just after the closing of the guide vanes is lower in the model, but the results are acceptable, having also the same oscillation frequency.

There is not the possibility in the software of introducing a different surge tank after the draft tube, to better model the laboratory set up, and consider an automatic change of the water level. This because the software is designed for simulating real power plants for the production of electricity; the plant in the laboratory of NTNU, used for research purposes, has a too specific arrangement: with a tank that is not an air vessel, since it is not fully closed, but it is neither behaving as a reservoir with infinite volume, in which the water level cannot change significantly.

The last figures reported are related to the torque and power comparison (see Figure 4.11)



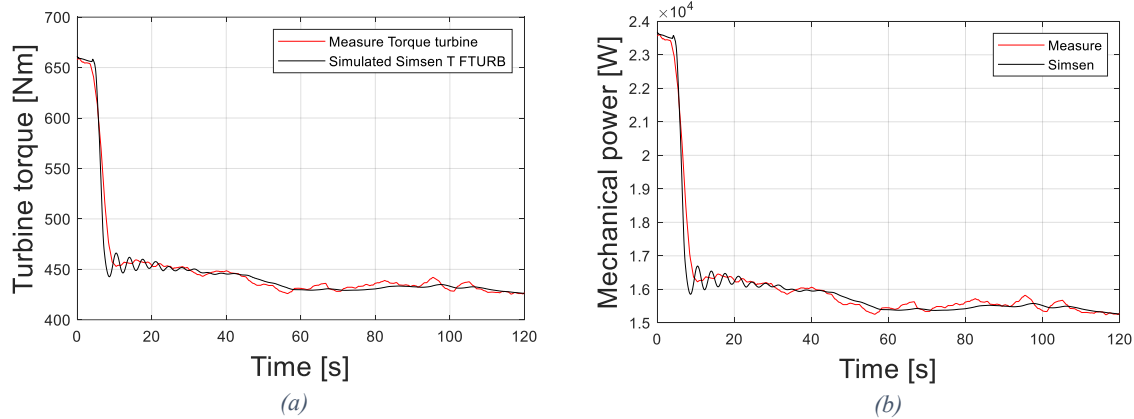


Figure 4.11 Comparison with experimental results for torque and power

In Figure 4.11 it is possible to see the turbine torque and the mechanical power produced, the first one is matching perfectly since it is a fixed parameter of the model, but as can be seen, also the turbine power is almost perfect in comparison with the experimental results, it depends in fact on the torque.

After these evaluations, the correctness of the model has been verified for most of the parameters, the differences that are still present can only be commented, until the physical effect after the draft tube is not explained it is not possible to improve the model; this will be a further work in the laboratory, using more available data from future tests.

The next chapter will be focused on the governor implementation and on a further validation of the model considering the possibility to have an automatic adjustment of the guide vane opening degree, thanks to a PI control system.



# Chapter 5

## Governor implementation

Until now the hydraulic part of the plant has been verified, the model has been validated considering the losses present in the piping system and considering the behaviour during a transient of load reduction. During the semester other researchers were working on the implementation of the speed governor for the Francis rig present in the laboratory, in this way instead of changing the opening of the guide vanes manually (as done previously) there will be an automatic system of control. This work was related to an experimental campaign that, as a goal, had the use of the power plant of the laboratory in isolated grid conditions, connected to the smart grid laboratory of NTNU; it was wanted to verify the possibility of doing primary frequency regulation, keeping the rotational speed of the turbine stable and at the nominal value. This possibility is given by the fact that, at NTNU, they can operate both in grid connected conditions, but also in islanding, simulating with the power plant a frequency regulation, in case a change in the connected load happens. Obviously, the governor must be tested after its implementation in the laboratory system, and the SIMSEN simulation can be of help for understanding and studying the behaviour of the rig. For this reason, it is interesting to introduce the governor in the simulation and then compare the new model with the experimental tests carried out for different transient operations.

### 5.1 Implementation in SIMSEN

Before moving to SIMSEN, the block diagram and the logic of the governor must be studied. The idea is based on an example of the IEC standard, reported in Figure 5.1.

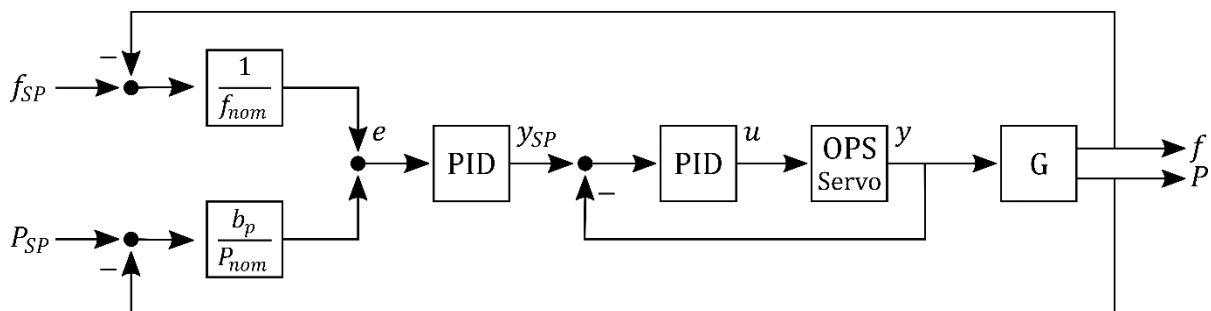


Figure 5.1 Example of governor logic block diagram from the IEC standard [12]

According to this logic the inputs of the governor system are two, it is needed to detect both the frequency and the power at the outlet of the generator, to calculate the input error for the PID control. However, often in Norway it is preferred to use another logic, which uses as input only the frequency coming from the generator; in this way there is no need to also detect the power. Another advantage is that the presence of the power at the inlet (as in the previous logic) creates more instability in the system. Following what is generally done in Norway, another block diagram was followed for the implementation of the governor system into the laboratory, this new logic is reported in Figure 5.2.

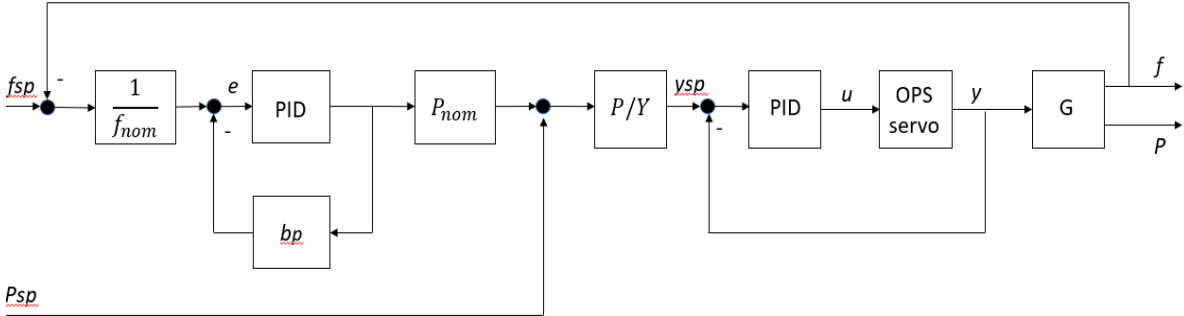


Figure 5.2 Block diagram used for the implementation of the governor in the laboratory

The regulator gives the guide vane opening degree to be applied to the turbine, there is no need to consider the servomotor in the model. Basically, the system takes as inputs the measured frequency at the outlet of the generator, then calculates the error in respect to a reference value; it is better to work in per unit so, for the frequency it is needed to divide by the nominal one, for the power instead also the permanent droop coefficient  $b_p$  must be inserted. To understand the meaning of this coefficient the following expression of it is reported

$$b_p = \frac{\frac{\Delta f}{f_n}}{\frac{\Delta P}{P_n}} \tag{Eq. 5.1}$$

Basically,  $b_p$  represents the relative variation of frequency given by a unitary relative variation of power, is the slope of the frequency-power curve characteristic of the generator.

Moving into the software, it is needed to translate the logic using the blocks present in SIMSEN, the implementation is reported in Figure 5.3.

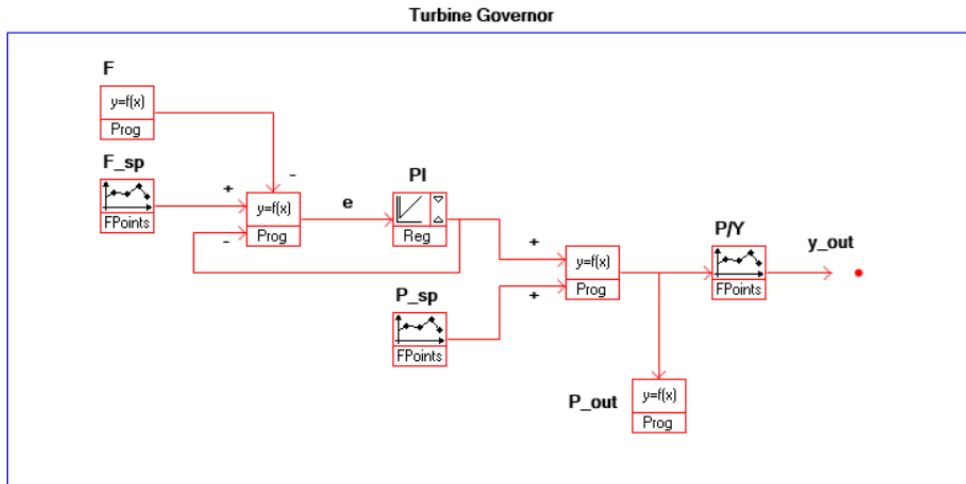


Figure 5.3 SIMSEN implementation of the governor

The frequency must be detected and gives the input to the control system; in SIMSEN a “Prog” element was used (named “F”) to detect the rotational speed of the turbine, then this value is subtracted to the set point rotational speed (fixed by the  $F\_SP$  block) to get the frequency error. All the system is done in per unit, dividing by the nominal values, in this way is easier to change the parameters if needed; so, the set point frequency can be inserted using an “FPoint” element with output fixed at 1. Before entering in the PI regulator, another “Prog” element is inserted, this allows to introduce the retroaction, taking the output of the regulator and subtracting it to the frequency error; this is necessary to stabilize the system. In particular, the retroaction is needed to calculate the input of the PI-regulator as

$$e = \frac{\Delta f}{f_{nom}} - b_p * \frac{\Delta P}{P_{nom}} . \quad \text{Eq. 5.2}$$

Where  $\Delta f$  is the frequency error,  $\Delta P/P_{nom}$  is the output of the regulator and  $b_p$  is the permanent power droop.

As a difference with the previous regulator logic, here the output of the PI block is in terms of power, it is not directly the guide vane opening of the turbine; so, before giving the command to the turbine element, it is needed to insert a curve that gives the relationship between the power and the guide vane opening, necessary to have that power. Since the system is implemented in per unit, before entering in the P-Y curve, it is needed to sum a value between 0 and 1 to the relative variation of power coming from the regulator, the value depends on the chosen power set point; then it is needed to multiply by the nominal power (that is  $30kW$ ), this can be done with a “Prog” element. Specifically, the “Prog” element allows to insert any kind of function and saves it in the output  $y$ .

To insert the P-Y function, an “*FPoint*” element can be used; the function is, in fact, known per points and was created by other colleagues as a *Sigmoid function*. This is a “S”-shaped curve that gives a good approximation of the relationship between the power and the opening degree of the turbine guide vanes.

In the beginning the curve implemented in the system was the one reported in Figure 5.4; however, taking the tests, the colleagues working on the governor noticed that this curve was not behaving as wanted and an improvement could have been introduced. So, a second curve was then realized, and it is reported in Figure 5.5.

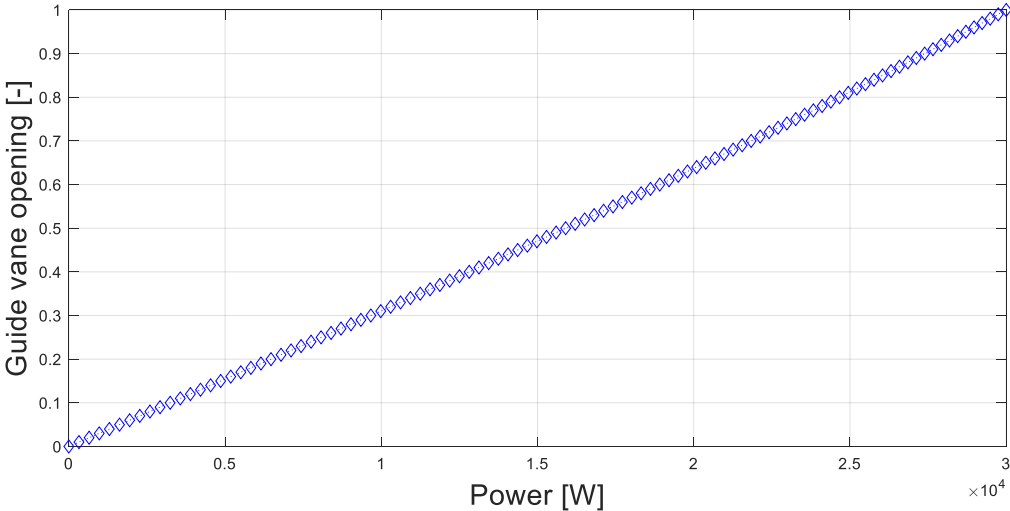


Figure 5.4 Old function that gives the relation between the power and the guide vane opening

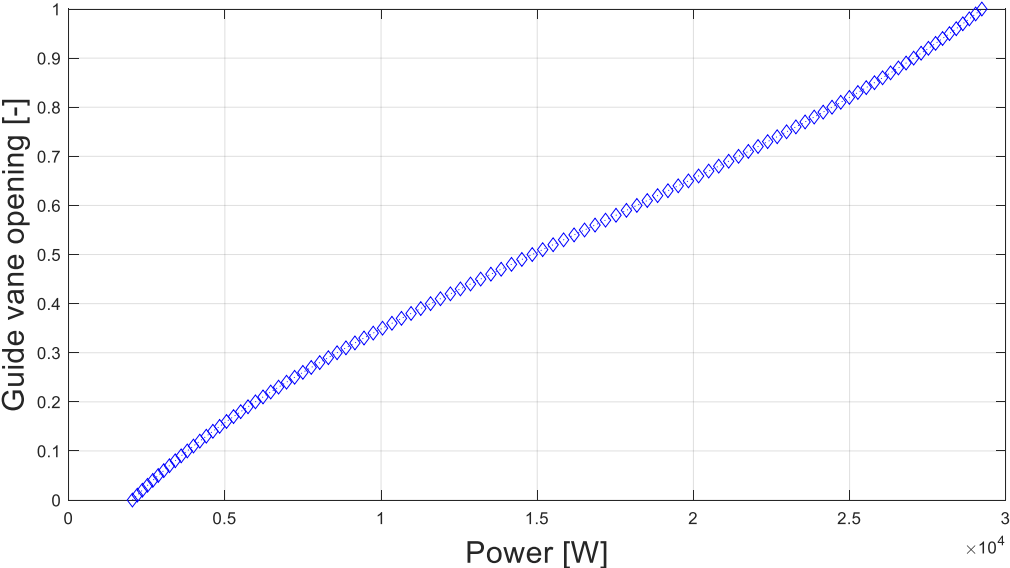


Figure 5.5 Sigmoid function that gives the new relation between the power and the guide vane opening

However, the simulations with SIMSEN were carried out considering the first curve, not the updated one, since the tests in the laboratory were not taken again after changing the curve.

The most important element of the control system is the PI regulator, in Figure 5.6 the user interface is reported, to explain which are the parameters that must be inserted, and which are the characteristics of this element.

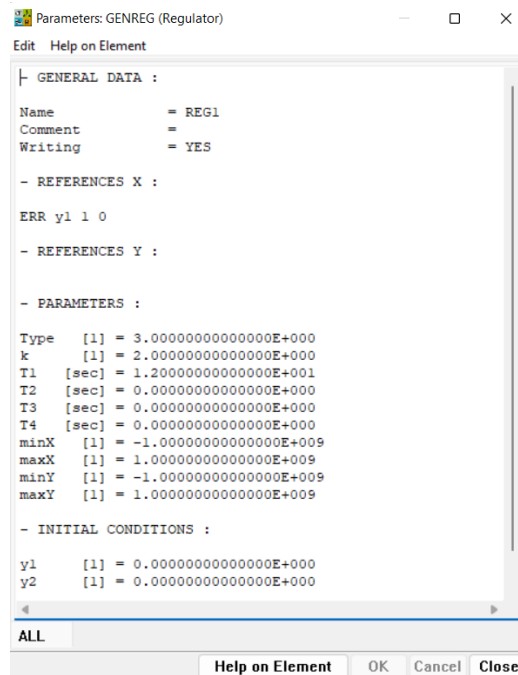


Figure 5.6 User interface for the regulator element

In the section “REFERENCE X” the input error is introduced, then in the section “PARAMETERS” it is needed to specify the characteristics of the regulator: in this case a PI regulator is considered (Type 3 in SIMSEN). The transfer function, after using the Laplace transformation, can be expressed as

$$G(s) = k * \frac{1 + sT_1}{sT_1} . \quad \text{Eq. 5.3}$$

Where  $k$  is the gain that gives the proportional term, while  $T_1$  is the integral time constant. [8]

According to the studies made in the laboratory by the other colleagues a gain of 2 and an integral time constant of 12s were inserted. In this thesis work it will not be explained how this parameters were evaluated, since it was part of the work of another colleague of the laboratory; but a useful reference for understanding how these values can be determined and how a control system works in more details, is given by the paper [13]. There are different methods for calculating the characteristic parameters of a control system, one of the most used is the Ziegler-

Nichols method; the paper [13] explains and compares this method with others, also giving an overview on how to insert a control system in the SIMSEN software.

Looking at the big picture, the interest on doing simulations with a governor logic implemented is also related to understand the capability on primary frequency control of a hydraulic power plant, studying the ancillary service that the power plant can give. This is also the goal at the *WaterPower Laboratory* of NTNU, being able to use the power plant in isolated grid condition, providing power regulation and control of the rotational speed; the simulations are useful for digitalizing the analysis and as an added tool for making evaluations, and for understanding the correctness of the chosen PI parameters. [13]

After describing the implementation of the governor system, the next step is the comparison with the tests results, to understand if the control logic inserted in the model corresponds to the one implemented by the other colleagues in the laboratory, and if the model is behaving as expected.

### 5.2 Verification of the P-Y function

A first validation has to be done on the P-Y curve implemented in the last portion of the governor system, to verify the matching of the model results in respect to the tests when a change in the power set point is applied. From the modification of the power set-point, the system has to find the corresponding guide vane opening in the P-Y function in order to have a power production of the turbine exactly equal to the one wanted. No disturbances are introduced in this case, the rotational speed of the turbine remains the same all along the simulation, only a change in the power set point is applied using an “*FPoint*” element, as can be seen in Figure 5.7.

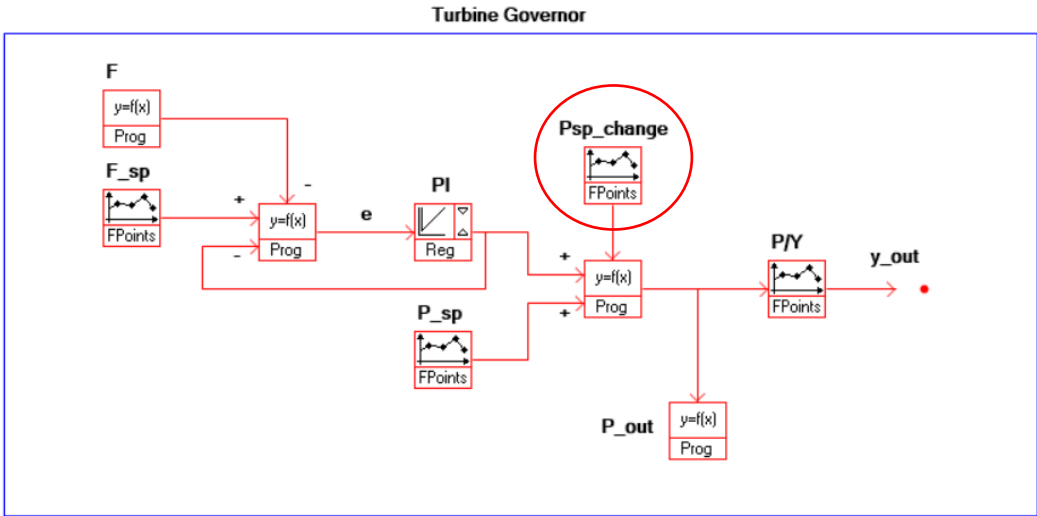


Figure 5.7 Governor modification to add the Power Set Point change



It is better to launch the simulation using MatLab, in this way the variation of the power set point can be directly created into a MatLab code, having a curve that reflects better the reality, and having also the possibility to print figures with a direct comparison between the simulation results and the measurements available. All the graphs related to this first simulation are reported below, then comments should be made to verify the applicability of the model.

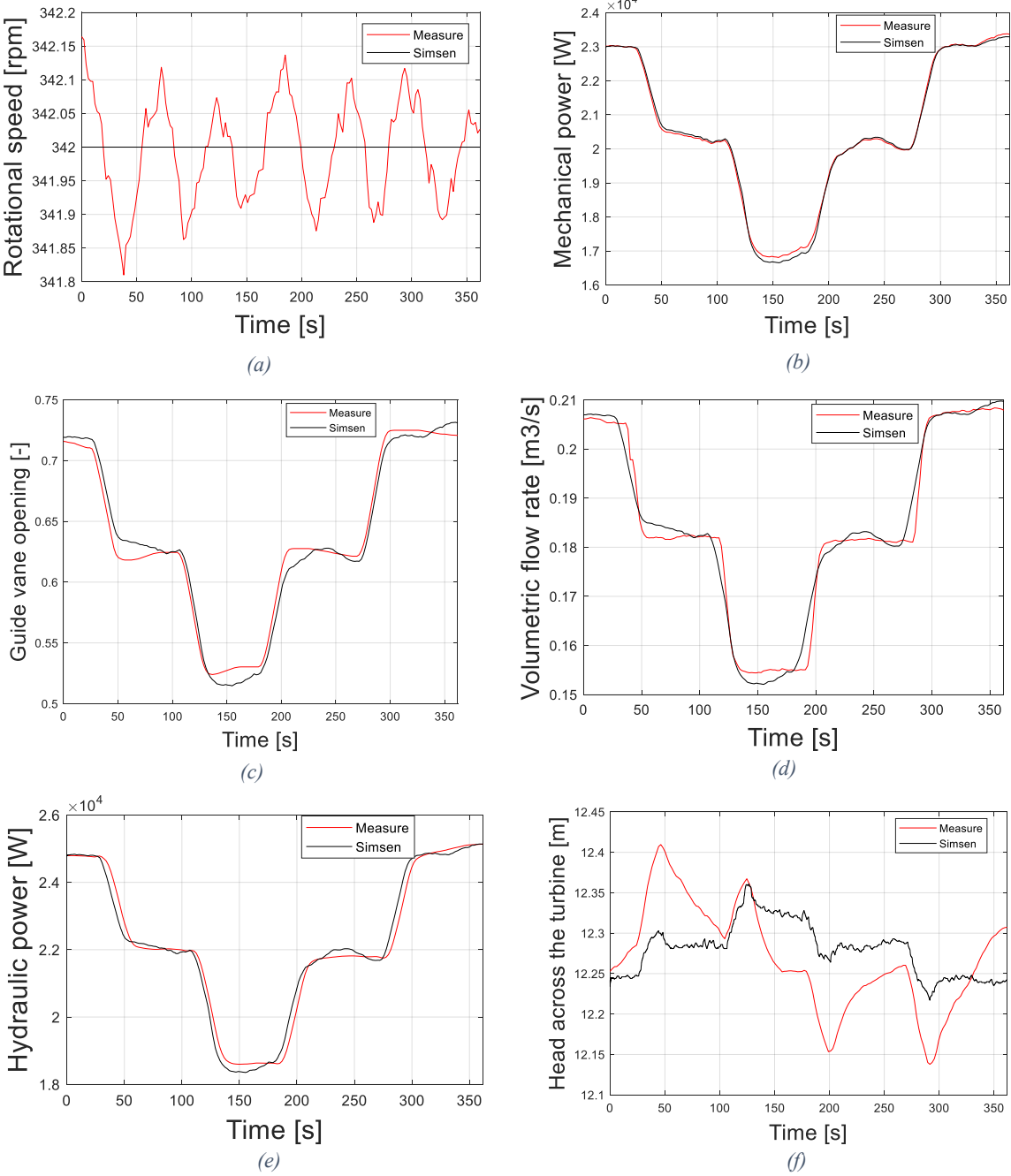


Figure 5.8 Comparison between experimental results and SIMSEN simulation for change in Power Set Point

First, the trend is the same for every parameter, this gives an idea of the fact that the implemented control system is going in the right direction in respect to the real one. Starting from the top, in this kind of simulation the governor is not really acting, for the whole simulation

period the rotational speed of the turbine is constant, and no frequency error is inserted; so, the PI-regulator is not giving any increase or decrease of power that should be applied. At constant rotational speed a change in the power set point is introduced, therefore there is a variation in the guide vane opening according to the P-Y function, a variation of the discharge and of the power production. Looking at the behaviour of the guide vane opening and of the flow rate, it is possible to say that the reached match is satisfying, there is a small delay in the measures of the volumetric flow rate, but this is due to the response of the flow meter present in the plant. The only parameter that is showing a big and clear difference in respect to the experimental data is the head, a deeper discussion can be made on this parameter.

In respect to all the other parameters, the head value results quite different in the simulation in respect to the experimental results, as was happening also with the load reduction analysis made without the governor. The behaviour is still coherent with what is happening, when there is a closing of the guide vanes the head increases rapidly, there is a peak in pressure just before the turbine. On the opposite case, when the guide vanes are opening, the head decreases. Also if the values are not perfectly matching, it is still possible to say that the simulation represents well the real behaviour of the plant, and what is expected from the theory of these phenomena. Also considering that, since the arrangement of the plant at NTNU is very specific, it is impossible to represent in a very precise way the tank after the draft tube with the actual knowledge, as already said. The decision of considering a reservoir with infinite volume is both related to what generally is present in hydropower plants connected to the grid and used for large production, but also to the fact that is still the closest situation to the plant of the laboratory; at least until other measurements will be available in the future.

### **5.3 Frequency drop**

This second comparison regarding the governor system is related to a frequency drop test in grid connected configuration. This test was carried out to see the response of the governor system in the case of a drop in frequency happening in the grid, this means to simulate an increase of the load request that brings the external torque to increase. As a consequence, the rotors of the generators connected to the grid tend to decelerate and, at that point, the governor must act in order to increase the power production and bring back the system to a balance between the generator torque and the external torque. The same can be realized with the SIMSEN model, it is only needed to delete from the model the mechanical mass, which represents the inertia of the generator and runner system. This because it is considered to have the power plant connected to the grid, the grid has a very high inertia and basically fixes the frequency, and so the rotational speed of the generator. It is therefore needed to insert an

“FPoint” element that changes the rotational speed of the turbine as done in the laboratory, in the next figure the drop inserted is reported.

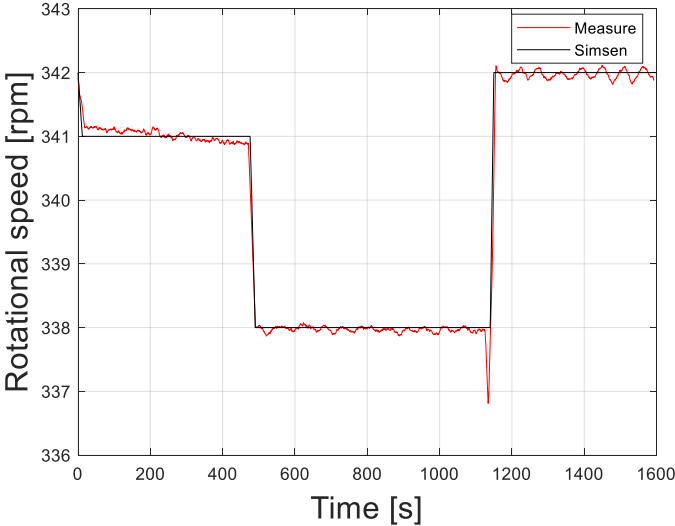


Figure 5.9 Speed drop applied to the generator to study the response of the governor

As it is possible to see from Figure 5.9, the speed starts from the nominal value (342rpm, corresponds to the nominal frequency of 50Hz) and then decreases by steps to 341rpm and then to 338rpm over 1600s; the black line represents the rotational speed applied to the model, the red line instead is the one coming from the experiments. The power droop for this test is considered at 6%.

At 342rpm at the best efficiency point, a power production of around 24kW is present, with the inserted speed drop an increase of around 5kW of power production is expected; in the next figures the graphs with the comparison between the experimental results and the simulation are reported, this test is interesting specially to verify the response of the PI-parameters.

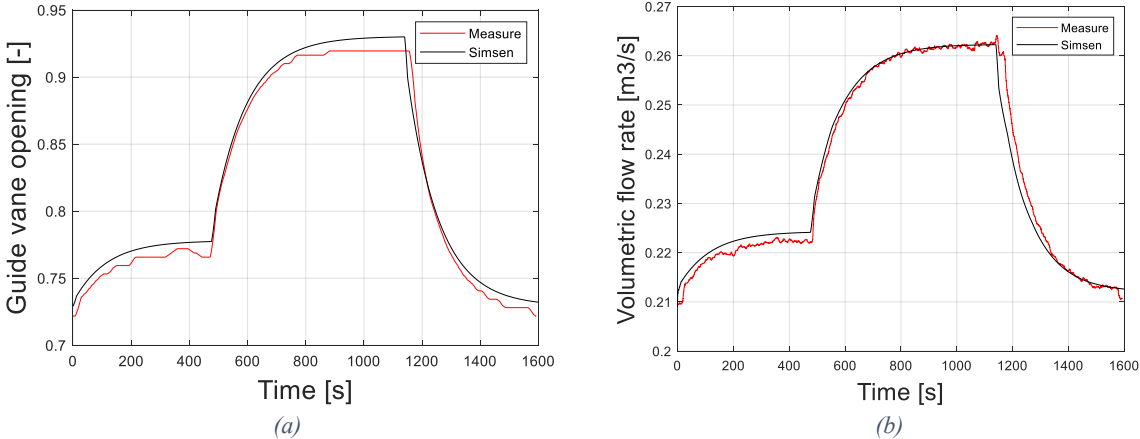


Figure 5.10 Guide Vane Opening applied to the turbine and discharge during the speed drop simulation

As usual the red line represents the experimental results from the test rig, the black line instead represents the results of the simulation. It is possible to see that in both cases, when the rotational speed decreases, the system reacts opening the guide vanes and this brings, obviously, the discharge through the turbine to increase. In Figure 5.11, instead, the variation in power production is reported.

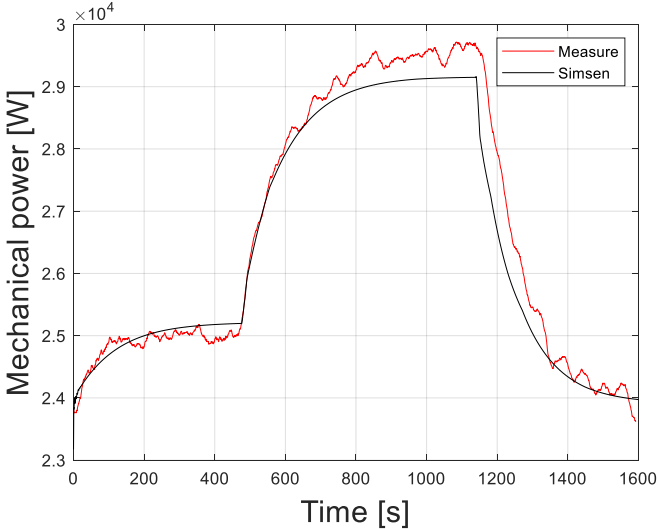


Figure 5.11 Increase in power production due to the frequency drop

As seen from the previous figure, the power increases in both the experimental results and simulation from a value of 24kW to more than 29kW, as expected. From Figure 5.10 and Figure 5.11, it is possible to confirm that the governor is behaving as wanted, changing the power production to react at the frequency error.

Now let’s look also at the head behaviour, that in the other simulations was always the most critical parameter.

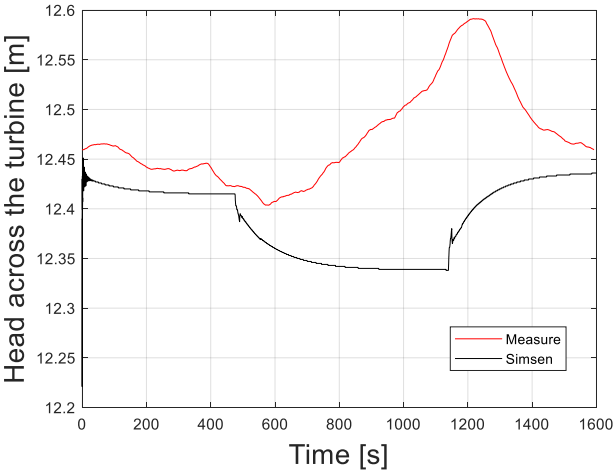


Figure 5.12 Comparison for the head across the turbine

Looking at the last graph a clear mismatch can be seen. Analysing the pressure head before and after the turbine for both the simulation and the experimental data, it was found that the problem is always the same: at the outlet of the draft tube the behaviour of the pressure measured in the plant is the following.

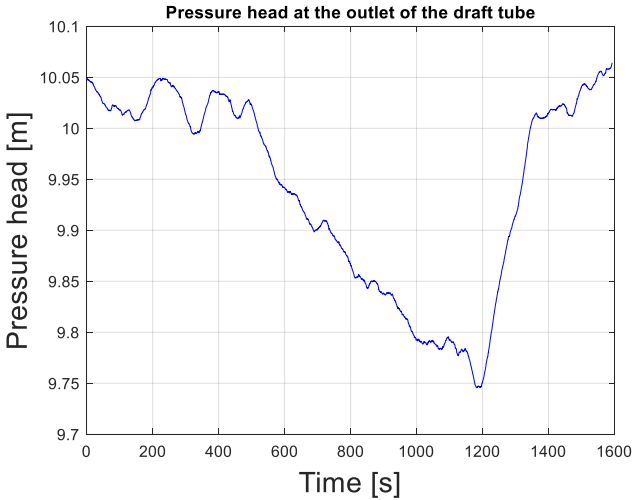


Figure 5.13 Pressure head at the outlet of the draft tube in the plant

There is a decrease in the pressure head after the draft tube, when the disturbance is introduced in the system. This decrease cannot be present in the SIMSEN simulation since, as said before, the part of the plant after the turbine is modelled considering only a reservoir with almost fixed water level. The interesting thing to be noticed is that, comparing the pressure head at the inlet of the turbine with the pressure head at the outlet of the draft tube, in the plant they are almost decreasing of the same amount. In Figure 5.14 also the pressure head at the inlet is reported to clearly see what is exposed.

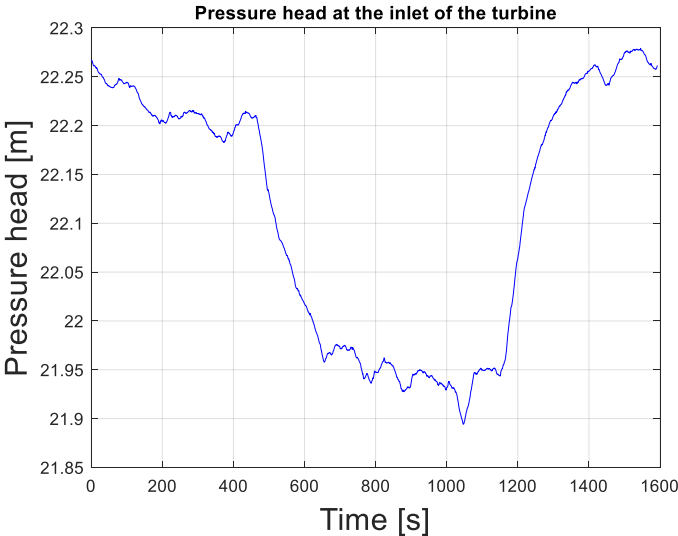


Figure 5.14 Pressure head at the inlet of the turbine in the plant

Since the head across the turbine is given by the difference between inlet and outlet, basically the pressure head is not influencing the change in the overall value. That is why in the measures the head is increasing, the behaviour is following the one of the kinetic head, the volumetric flow rate is increasing because the guide vanes are opening during the transient, and this brings the kinetic head to increase.

In the simulation instead, the pressure head is decreasing before the turbine, as logic since the guide vanes are opening, but at the same time there is not a significant decrease in pressure after the draft tube, so the head behaviour is following the one of the inlet pressure.

In the next chapter a further evolution of the SIMSEN model will be presented, regarding the introduction of a mechanical slack in the governor system. This was done since, while doing the tests, it was noticed the presence of a backlash into the mechanical control of the guide vane opening; this effect was not giving problems in case of grid connected tests, however, it did not allow to prove the good response of the PI parameters in islanding conditions, which was the next goal.

# Chapter 6

## Final SIMSEN model

As said in the previous chapter, while doing the tests for studying the response of the governor implemented in the laboratory for the Francis turbine rig, it was noticed the presence of a backlash in the mechanical system that controls the guide vane opening degree of the turbine itself. This is obviously a problem that must be solved in the nearby future, in order to be able to prove the ability of the new governor system to control the plant, to provide primary frequency regulation, keeping an almost constant rotational speed of the turbine during the connection with the smart grid laboratory of NTNU.

For the modelling purposes it can be interesting to study how to introduce the mechanical backlash into the SIMSEN model, to demonstrate the capability of the software on representing something as close as possible to the reality, and to understand how much the results can be affected by this defect. For a description about how a mechanical backlash works see appendix C.

In the next sub-chapters, first a simulation without the slack will be presented, then the same simulation will be performed with its introduction, in order to see how much it can affect the operation of the governor system.

### 6.1 Isolated grid operation of the SIMSEN model

The main purpose of the development of a governor system for the Francis rig of the *Waterpower Laboratory* is to demonstrate the possibility to operate in isolated grid conditions, with the plant connected at the smart grid laboratory of NTNU. In this way the idea is to have a plant that can provide frequency regulation, in case of a change in load, and so in case there is a deviation of the rotational speed from the nominal value. Specifically, it must be proven that the transient speed deviation does not exceed the limit of 0.65Hz/%kW and that the speed converges to a steady state with nominal speed and without oscillations, evaluating in this way the response of the PI parameters chosen when a change in load is applied.

The idea, during the semester, was to take tests in isolated grid conditions, setting different changes in the power load and evaluating the response of the system. This was not possible for the presence of the mechanical slack into the control of the guide vane opening of the turbine.

In the previous tests taken in grid connected configuration, the slack was not affecting the governor operation. In that case, the rotational speed was externally fixed, the changes were slower, and the feedback used in the control was the angle, not the stroke position. Basically, the mechanical slack acts giving a space delay between the stroke position and the opening angle of the guide vanes; in grid connected configuration, using the angle as feedback, the governor was able to handle the slack, which explains why the effect was not seen in the previous frequency drop test.

When, instead, the tests in isolated grid condition started, it was realized that the governor was not able to handle the backlash problem with the PI parameters chosen, therefore it was not possible to demonstrate the capability of the system to provide frequency regulation and to keep the rotational speed at the nominal value during operation. Probably changing the PI parameters or working on the inertia, an improvement could have been possible, but there was not the time and the knowledge to work on that. Still, the introduction of this mechanical backlash into the SIMSEN model, can be interesting, to compare (from only a simulation point of view) the behaviour in isolated grid conditions without and with the slack.

After some analyses it was found that the slack has an amplitude around  $0.65^\circ$  over a full opening of the guide vanes of  $14^\circ$ . In figure 6.1 some graphs are reported for a better understanding of the slack effect, comparing the angle position with the stroke position.



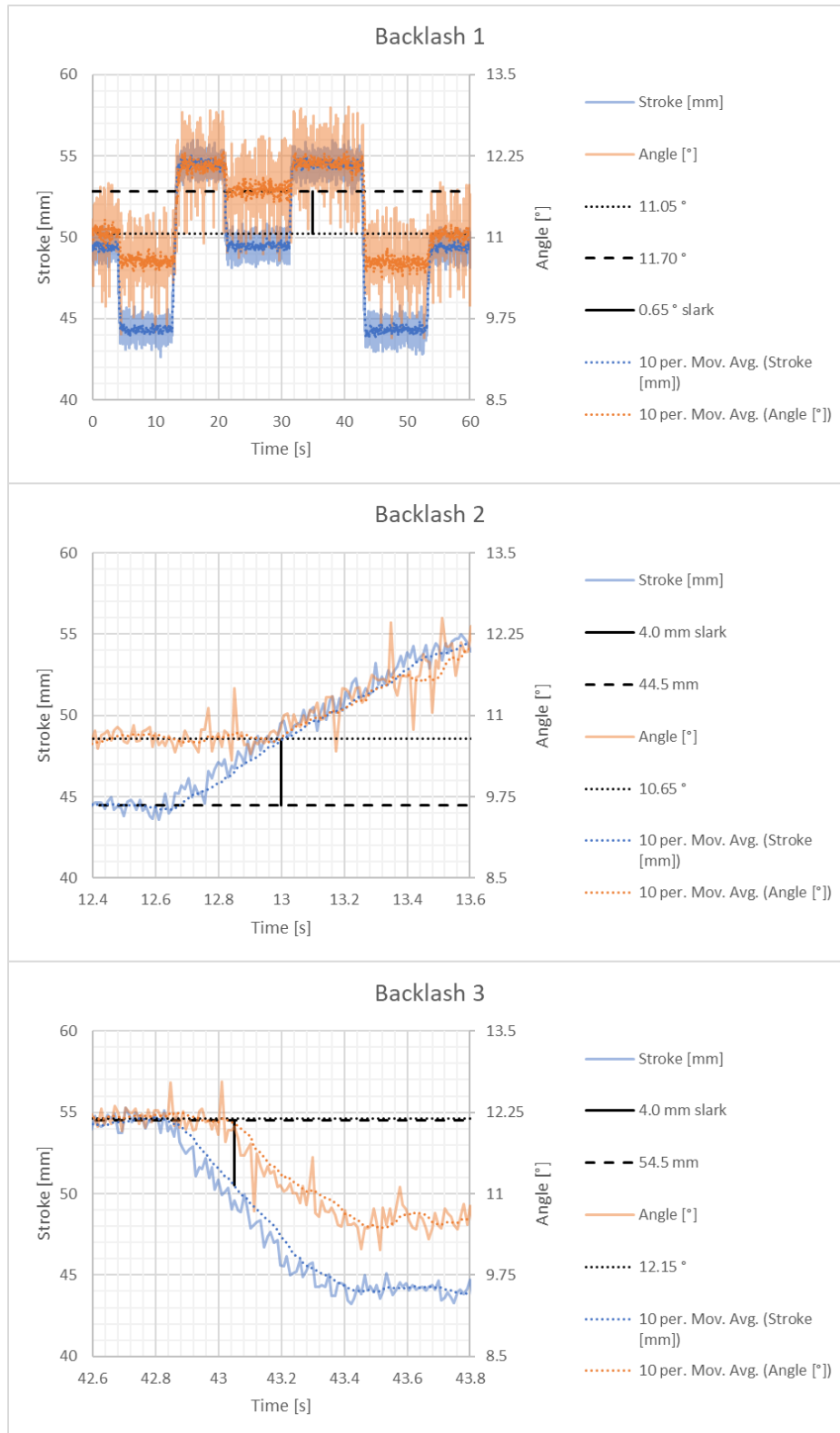


Figure 6.1 Effect of the mechanical slack on the difference between the stroke and the real opening degree of the guide vanes

As can be seen, the signal given by the governor that controls the stroke position, cannot be transferred to the guide vanes of the turbine, due to the space delay present in the system. When

the stroke position moves up or down, in fact, there is a delay before the angle starts also to follow the movement of the stroke.

Thanks to the SIMSEN model of the hydro plant, it is still possible to verify the response of the chosen PI parameters in isolated grid conditions, giving an idea on how the real system will work once the mechanical problem will be solved. To do this, the same model tested in the previous chapters will be used, the only needed modification is related to the re-introduction of the mechanical mass connected to the turbine, which plays a fundamental role when working in islanding conditions. The value of the inertia was set according to the laboratory setup ( $J = 1400 \text{ kgm}^2$ ); in reality, this parameter can be changed freely since it is “simulated”. The motor drive is much more powerful than the turbine, so it can be used to set whatever speed is wanted and to change the speed arbitrarily fast; this enables to simulate the inertia that is preferred; the starting value used in the laboratory was  $1400 \text{ kgm}^2$ , so it was decided to start with this value also in the simulation. Then, the external torque applied to the generator has to be fixed with an “*FPoint*” element, to simulate the wanted change in the load request.

It was decided to do a first trial with a  $1\text{kW}$  reduction of power load, from  $82.7\%$  of the nominal power, with a droop of  $2\%$ . The results are the following.

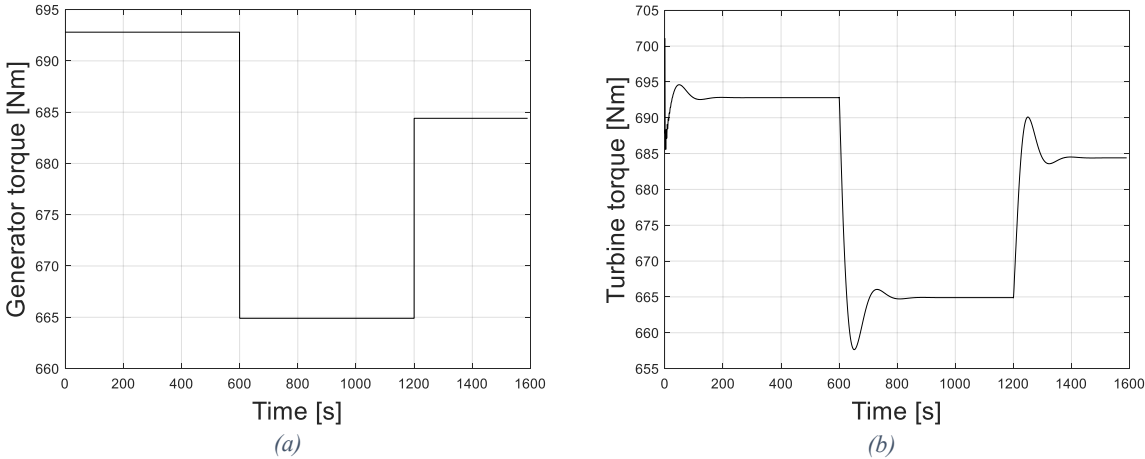


Figure 6.2 Reduction on power load inserted and torque plot for governor and turbine

The simulation is done for  $1600\text{s}$ , to have a good response of the integral time constant of the PI speed regulator. As it is possible to see after  $600\text{s}$  a decrease in power is introduced, that is translated into a decrease in the external torque applied to the generator, the power goes from  $24.8\text{kW}$  to  $23.8\text{kW}$ . After  $1200\text{s}$ , instead, the power increases again to  $24.5\text{kW}$ . When a decrease of power is applied it is expected that the turbine tends to accelerate, since the external torque will be lower than the torque applied by the turbine. At this point the governor must act, closing the guide vanes of the turbine, to decrease the discharge and so decrease the power

production, arriving again at a torque balance and keeping the rotation speed at the nominal value of 342rpm. It is needed to verify that the system can regulate, without having speed oscillations after the transients, and with a frequency deviation that must be at maximum 0.65%Hz/%kW. In the next figure the governor action can be seen.

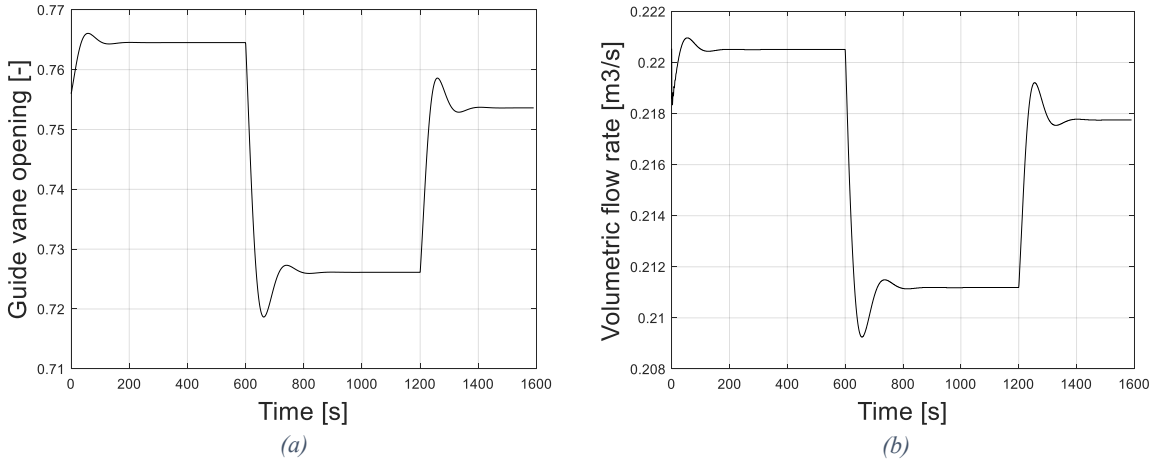


Figure 6.3 Guide vane opening and flow rate through the turbine with load reduction

From Figure 6.3, when the load decreases, the governor acts giving the command to close the opening degree of the guide vanes, to decrease the flow rate that passes through the turbine, and so decrease the power production. When instead the load increases, here at 1200s of simulation, the guide vane opening degree must increase, to let more water to pass and increase again the power production.

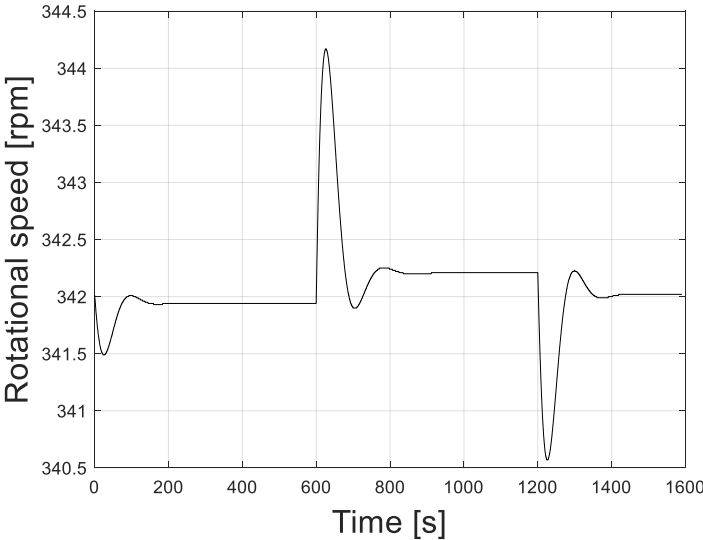


Figure 6.4 Rotational speed behaviour during the simulation

Looking at the last graph, it is possible to see that at the beginning of the simulation, and every time a disturbance is introduced (decrease or increase in the power load), the rotational speed

has a peak, positive or negative. The maximum deviation from the nominal rotational speed is around  $2.27rpm$ , or  $0.0378 Hz$  of difference; this value is less than the maximum acceptable deviation, which is around  $0.325Hz$  every  $kW$  of power. So, this can confirm the correctness of the chosen PI parameters, and the ability of the governor to provide frequency control in islanding conditions.

After the first power drop, it is possible to note that the steady state reached presents a rotational speed a bit higher than  $342rpm$ , the difference is not big, and it is due to the droop characteristic. The droop is described by the following formula (as already presented previously)

$$b_p = \frac{\left(\frac{\Delta f}{f_n}\right)}{\frac{\Delta P}{P_n}} . \quad \text{Eq. 6.1}$$

Where  $f_n$  and  $P_n$  are the nominal frequency and the nominal power, while  $b_p$  is the droop and was chosen at 2%. With a  $\Delta P$  of  $1kW$  and a droop of 2%, the speed deviation according to the formula would be

$$\Delta N = \frac{\Delta P}{P_n} * 342 * 0.02 = 0.228rpm .$$

This value is coherent with the deviation that can be seen from the graph.

Now the same simulation can be performed introducing the mechanical slack into the SIMSEN model and analysing the differences in the behaviour of the system.

## 6.2 Isolated grid operation with backlash implementation

In the next figure the new governor model is reported, to understand the modifications done for implementing the backlash problem.

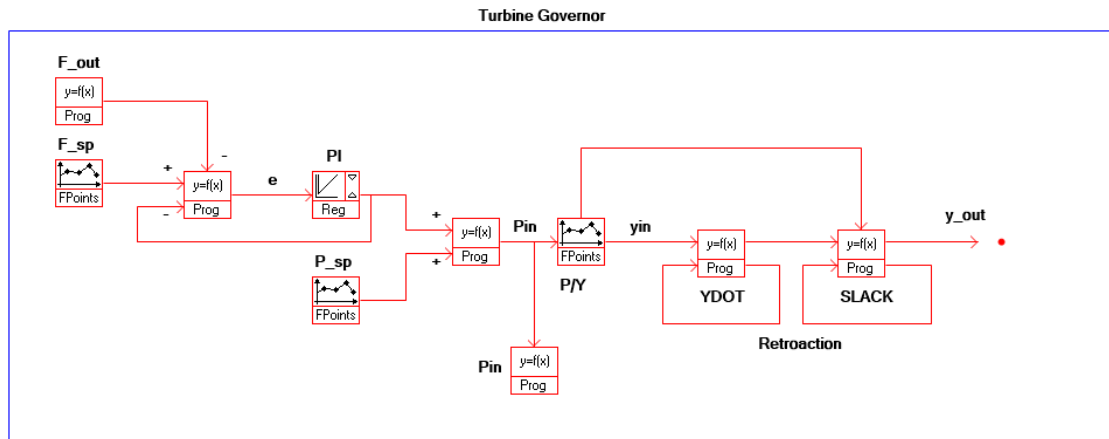


Figure 6.5 New governor model with implementation of the mechanical backlash

As it is possible to see, the guide vane opening at the outlet of the P-Y function does not go directly to the turbine, it enters into two “Prog” elements, that are used to simulate the backlash effect; two retroactions are needed, to understand if there is a ramp up or down, and to control if the value coming from the governor minus the value that should be applied to the turbine is lower or higher than the slack amplitude, and higher or lower than zero (see Appendix C for more details regarding the logic implemented). First, in Figure 6.6 is reported the graph that represents the comparison between the signal given by the governor and the signal really applied to the turbine element, due to the presence of the slack, doing the same kind of simulation done in the previous paragraph (1kW of power load decrease with 2% droop).

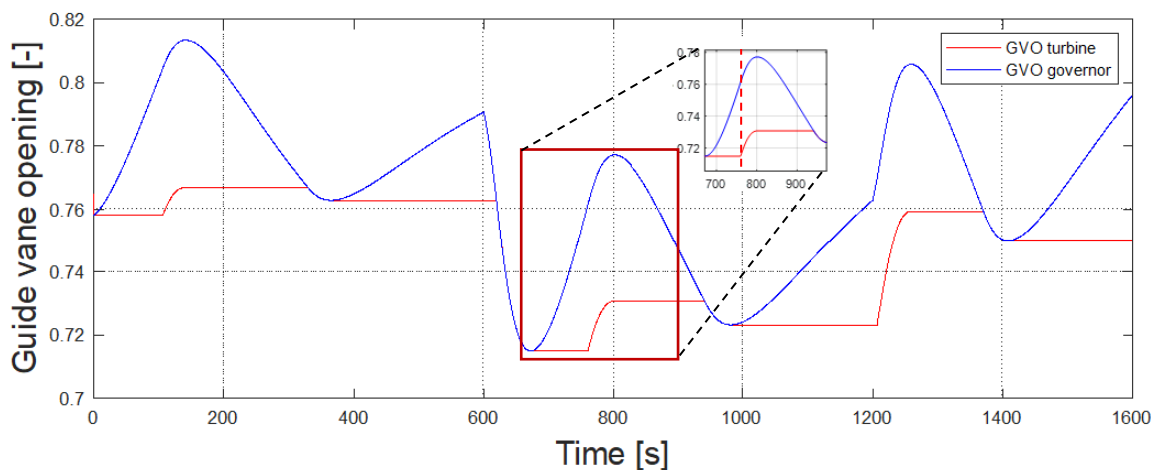


Figure 6.6 Comparison between the governor signal and the guide vane opening degree really applied to the turbine

As it is possible to see from the figure, the opening of the vanes is not able to follow properly the signal given by the PI-regulator; when the opening degree should increase, there is a delay, and the system starts to move after a certain dead band. The same happens when the signal

starts to go in the opposite direction. This brings to a rotational speed of the turbine that, along the simulation, varies as in Figure 6.7.

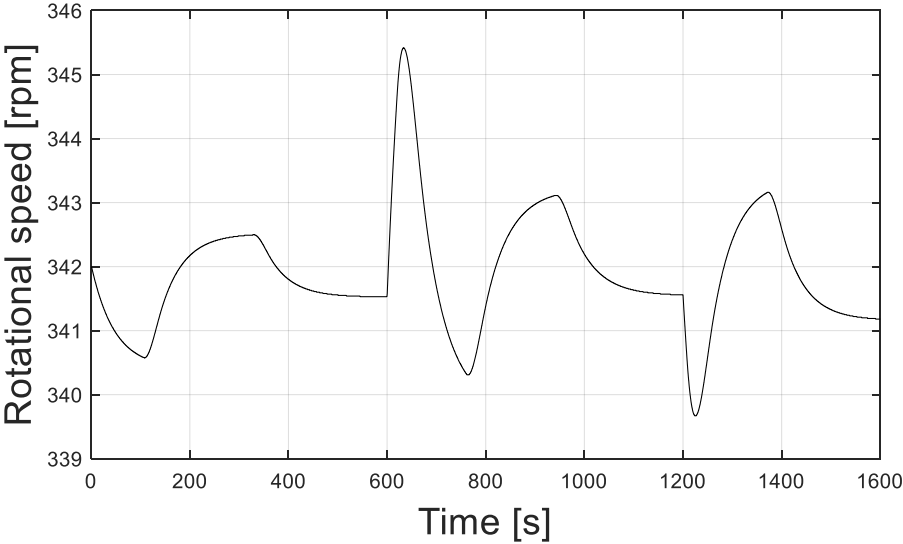


Figure 6.7 Rotational speed behaviour along the simulation

Comparing this speed behaviour with the one analysed without the slack, it is possible to see that the system is not able to keep constant the speed, and to bring the speed back to the nominal value after a transient. This gives an idea of the problem, and how this problem affects the results in islanding operation. The same effect was noticed while running the rig, and that stopped the series of tests that the other colleagues were supposed to take to prove the ability of the system to provide primary frequency control.

For giving more confirmation about the slack effect, another simulation can be done, and a comparison between the results without the slack and with the slack can be made again. In this case a 15% increase of power load, from 80% of nominal power will be done, with a droop always at 2%; so, the power starts at 24kW and goes to 27.6kW, this corresponds to an increase in the torque applied to the generator from 670Nm to 771Nm. Here it is reported directly the graph related to the rotational speed, which is the one of interest (see Figure 6.8).

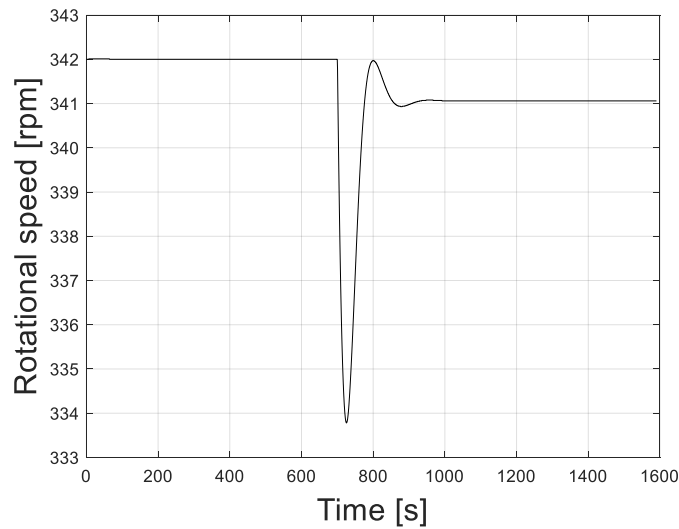


Figure 6.8 Rotational speed behaviour with an increase in power load

After 700s of simulation, an increase in the power requested by the load is applied, this means that the external torque starts to increase, and the turbine decelerates; the frequency error is detected by the governor system that acts opening the guide vanes at the inlet of the turbine to bring the speed back to the nominal value. This is exactly what happens looking at Figure 6.8: the speed tends to decrease when the disturbance is introduced, then the governor acts correcting the frequency error and the speed increases, going back to a stable value.

Now let's see, instead, what happens with the backlash effect (see Figure 6.9).

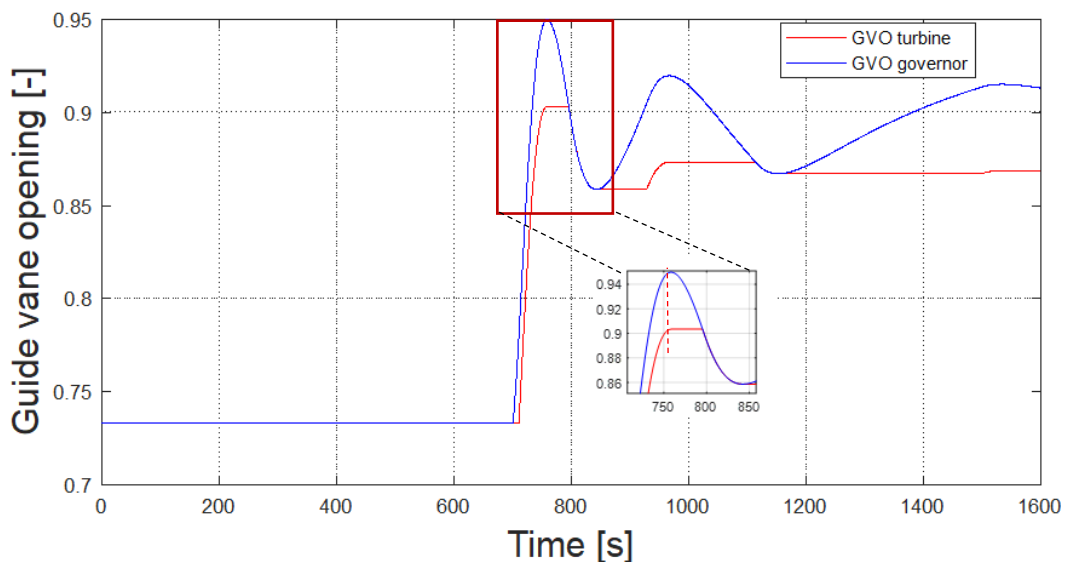


Figure 6.9 Comparison between the signal given by the governor and real guide vane opening applied to the turbine

Before the increase in power is introduced, the system works in steady state with a nominal rotational speed of 342rpm as wanted (as in Figure 6.10); then the power increases, so the

governor gives the signal to open the guide vanes of the turbine. However, the red curve (that represents what goes to the turbine element), does not follow the blue one (governor signal), this is due to the backlash present in the system. To understand the effect on the speed, in Figure 6.10 also the rotational speed is reported.

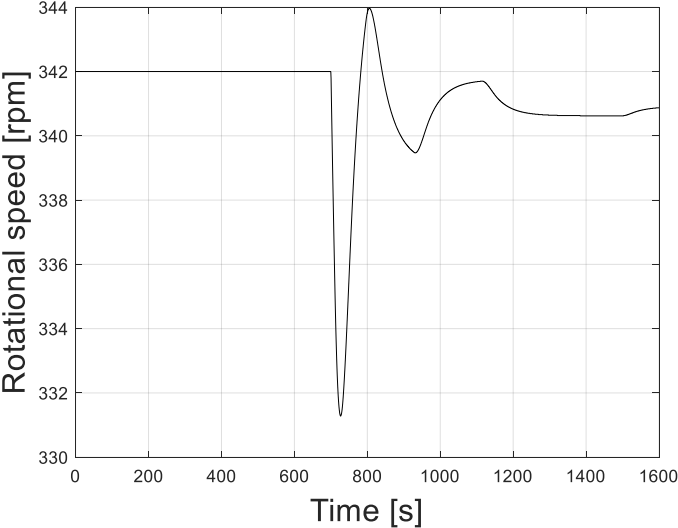


Figure 6.10 Rotational speed behaviour during the simulation

After the transient the governor should bring the speed back to the nominal value, but in the beginning, it sets a too high opening of the guide vanes, so the speed goes back up but too much; as a consequence then the guide vanes should close in respect to the first peak. This happens following the blue curve of Figure 6.9. But then, the speed decrease too much, so the guide vane opening degree should go up again. For the backlash presence the red curve does not follow the blue one, and in fact the speed remains unstable after the disturbance and does not go back to a value enough close to the nominal one.

With these evaluations it is possible to conclude that the slack is something that must be solved, to be able to prove the ability of the new governor system to provide primary frequency regulation in islanding conditions. The stability of the system depends on different variables, it is also possible to work on the PI parameters and on the inertia of the generator-runner system; these are things that can affect the governor action, giving and higher or lower impact of the mechanical slack. The space delay that the slack creates does not allow a stable governing with the current chosen parameters (inertia and PI values), and the speed cannot be kept at the nominal value without oscillations after a transient. Therefore, a further analysis can be made working on the inertia applied to the system, to see if the results can be improved.



To study the effect of the inertia another simulation was carried out, changing only this parameter, from  $1400\text{kgm}^2$  to  $140\text{kgm}^2$ , this in accordance with a trial made in the laboratory by the colleagues. The simulation implemented in SIMSEN is exactly as the first one presented in this work for the islanding operation, to give a more direct comparison. First, in Figure 6.11 the comparison between the signal given by the governor and the guide vane opening applied to the turbine is reported.

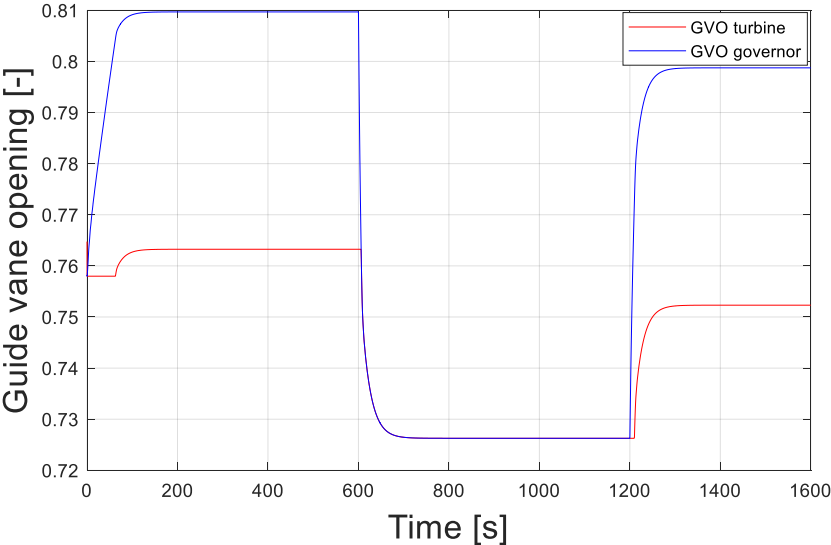


Figure 6.11 Comparison between the signal given by the governor and the guide vane opening applied to the turbine

The first thing that is noticed is that, in this case, the signal is stable, the inertia is giving an important effect on the behaviour and stability of the system. The confirmation is also given by the rotational speed graph, reported in Figure 6.12.

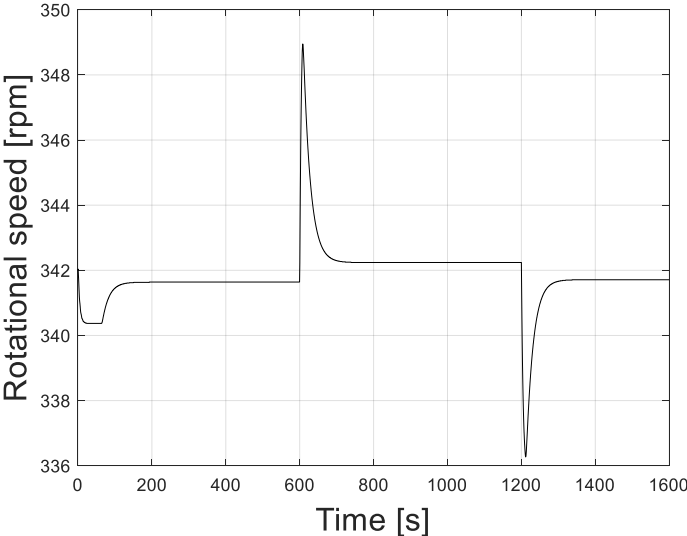


Figure 6.12 Rotational speed during the simulation

The change in the inertia value allows to have a stable governing also in the presence of the mechanical backlash into the system, setting a lower inertia gives the possibility to bring the rotational speed at a constant value after a transient of load change. This is an interesting conclusion for understanding what can be done in the laboratory to improve the response of the system, before solving completely the mechanical problem. This is allowed by the fact that the inertia can be changed using the motor drive (frequency converter), as explained previously.

This ends the implementation of the model of the hydropower plant present at the *WaterPower Laboratory* of NTNU. The results can be considered satisfactorily, taking into account the actual knowledge about the plant and the measurements available. As already said, a further development will be needed to solve the discrepancies still present and to be able to use the plant providing frequency regulation.

# Conclusions

The report starts with the explanation of the most important dynamic effects that can happen during hydropower operation. These effects are related to high load variations, especially in load reduction cases, and to the action of the governor system. Today it is more and more important to have flexible hydropower plants, which can provide frequency regulation and various ancillary services; this for the increase in the penetration of renewable energies, considering that hydropower is almost the only RES fully controllable. However, the flexibility required, increases the presence of dynamic problems and the risk of water hammer; so, it is also important to develop strategies for monitoring the plant, for helping the decision making and for studying possible improvements. With this in mind, digital twins are the perfect tool for studying the behaviour of a plant, simulating transients that can happen in reality and looking on the reaction of the system. Therefore, the second part of this report is focused on the development of a digital model of the hydropower plant present at the *WaterPower Laboratory* of NTNU (Trondheim), using the software SIMSEN. This is a quite new tool that allows the representation of both the hydraulic and electrical part of a power plant, giving the possibility to study transients and the interaction with the grid. No CFD simulations were realized, and no experimental tests were carried out personally, but the results of the tests coming from the laboratory were used to validate the model, demonstrating that it can represent the behaviour of the real plant, both in steady state and transient operation. Also, the governor system was considered, giving the possibility to simulate the connection with the grid and the action of the plant in case of primary frequency control. The model is still not perfect, and further work is needed to understand some dynamic effects happening at the outlet of the draft tube in the plant: the model in fact shows a mismatch in the head values, for all the simulations, which is due to the pressure behaviour in that part of the plant.

The set up with which the laboratory works is quite specific, keeping an open valve after the downstream air vessel, consequently this vessel does not behave as a closed one but neither as a reservoir with infinite volume (used in the SIMSEN model). With the actual knowledge, the use of a reservoir element to model the downstream part of the plant, is still the solution that allows to better represent the reality; but in the nearly future a more detailed analysis on the behaviour of the pressure after the draft tube will be needed, first to understand the phenomenon, second to allow an improvement of the model.

The model is still capable of giving a good representation of the transient behaviour, and of the pressure oscillations, and so represents a useful tool for studying the plant. The model itself allowed also to identify the strange effect in the draft tube that otherwise would not have been noticed.

Regarding the last part of this work, the implementation of the governor was verified, but the most interesting results are related to the final model with the presence of a mechanical backlash in the system. The simulations clearly showed the difference in behaviour between a perfect system and a system where a space delay between the mechanical parts is present.

It can be concluded that the implementation of the model in SIMSEN is satisfactorily, considering the data available from the laboratory and the actual knowledge of the power plant. The objectives set initially have been achieved almost completely, and it was also possible to adapt the model when new things were noticed.

# Bibliography

- [1] C. Trivedi, M. J. Cervantes and O. G. Dahlhaug, “Experimental and Numerical Studies of a High-Head Francis Turbine: A Review of the Francis-99 Test Case,” *Energies*, 2016, 9, 74.
- [2] T. K. NIELSEN, *Dynamic Dimensioning of Hydropower Plants*, Trondheim, Norway: NTNU.
- [3] E. B. WYLIE and V. L. STREETER, *Fluid transients*, United States of America: McGraw-Hill International Book Company, 2004.
- [4] P.-T. Storli and T. K. Nielsen, “Simulation and Discussion of Models for Hydraulic Francis Turbine Simulations,” *ELSEVIER*, pp. 109-114, 2018.
- [5] C. NICOLET, P. F. AVELLAN, P. ALLENBACH, D. A. SAPIN, P. J.-J. SIMOND and D. J.-J. HEROU, “TRANSIENT PHENOMENA IN FRANCIS TURBINE POWER PLANTS: INTERACTION WITH THE POWER NETWORK,” *11th International Meeting of the Work Group on THE BEHAVIOUR OF HYDRAULIC MACHINERY UNDER STEADY OSCILLATORY CONDITIONS*, p. 11, 2003.
- [6] C. NICOLET, “Hydroacoustic modelling and numerical simulation of unsteady operation of hydroelectric systems,” EPFL, Lausanne, 2007.
- [7] C. Nicolet, J.-E. Prenat, F. Avellan, A. Sapin and J.-J. Simond, ““A NEW TOOL FOR THE SIMULATION OF DYNAMIC BEHAVIOUR OF HYDROELECTRIC POWER PLANTS”,” in *10th International Meeting of the Work Group on the Behaviour of Hydraulic machinery under steady Oscillatory Conditions*, Trondheim, Norway, 2001.
- [8] Power Vision Engineering, “Quick User Guide,” Power Vision Engineering, Lausanne, 2021.
- [9] M. Dreyer, C. Nicolet, A. Gaspoz, N. Gonçalves, S. Rey-Mermet and B. Boulicaut, “Monitoring 4.0 of penstocks: digital twin for fatigue assessment,” in *30th IAHR Symposium on Hydraulic Machinery and Systems*, Lausanne, Switzerland, 2021.

- [10] A. Ismaier and E. Schlücker, “Fluid dynamic interaction between water hammer and centrifugal pumps,” *Elsevier*, p. 4, 2009.
- [11] F. Avellan, *Hydraulic Machine Formulary*, Lausanne: EPFL, 2010.
- [12] Various, *CEI IEC 61362 - Guide to specification of hydraulic turbine control systems*, Geneva, Switzerland, 1998.
- [13] C. Landry, C. Nicolet, J. Gomes and F. Avellan, “Methodology to determine the parameters of the hydraulic turbine governor for primary control,” *Proc. of HYDRO 2019 Conference*, p. 20, 2019.
- [14] Y. A. Cengel and J. M. Cimbala, *Fluid Mechanics: Fundamentals and Applications*, Singapore: McGraw-Hill Education, 2014.
- [15] M. Nordin and P.-O. Gutman, “Controlling Mechanical Systems with Backlash,” *Elsevier*, vol. 38, p. 33, 2002.

# APPENDIX A : Detailed construction of the SIMSEN model

In this first appendix the detailed description about how the SIMSEN model was built is reported, starting from the measurements of the pipes in the laboratory until the full implementation of every component. First, it was necessary to visit the laboratory in order to see the plant, to understand which are the components and which is the path of water from the reservoir to the Francis turbine. Then it is needed to translate the system into the software, choosing the number of pipes to be inserted, the surge tanks and the elbow elements for the concentrated losses.

It is useful to report here a representation of the plant present in the laboratory (see Figure A.1), before introducing the model realized in the software. In the figure the main elements are marked with a number for a clearer description.

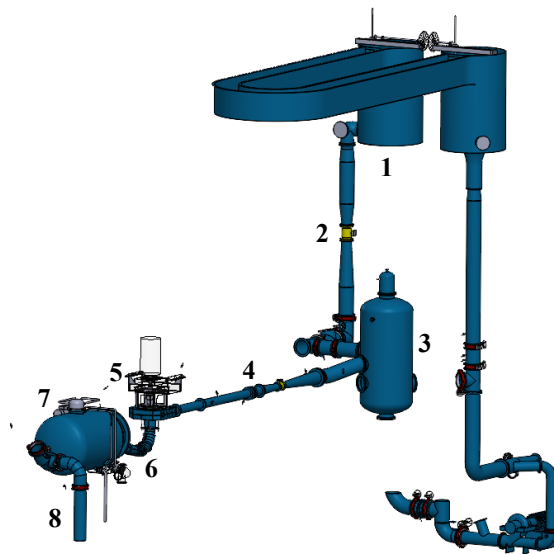


Figure A. 1 Hydropower plant present at the WaterPower laboratory of NTNU

From the figure it is possible to see the whole open-loop power plant of the *WaterPower Laboratory* at NTNU. The hydraulic system can give a head up to 14m for the open loop case and 100m for the closed loop. In this thesis work only the open-loop operation is analysed; in this case the water is pumped with constant flow rate to the overhead tank, and from there can flow down to the turbine. The water level is kept constant in the tank with an overflow piping

system. According to tests previously taken, at best efficiency point operation, the head was around 12m and the discharge around  $0.2m^3/s$ . [1]

In Figure A.2 is also reported a representation of the Francis99 turbine, used for the tests.

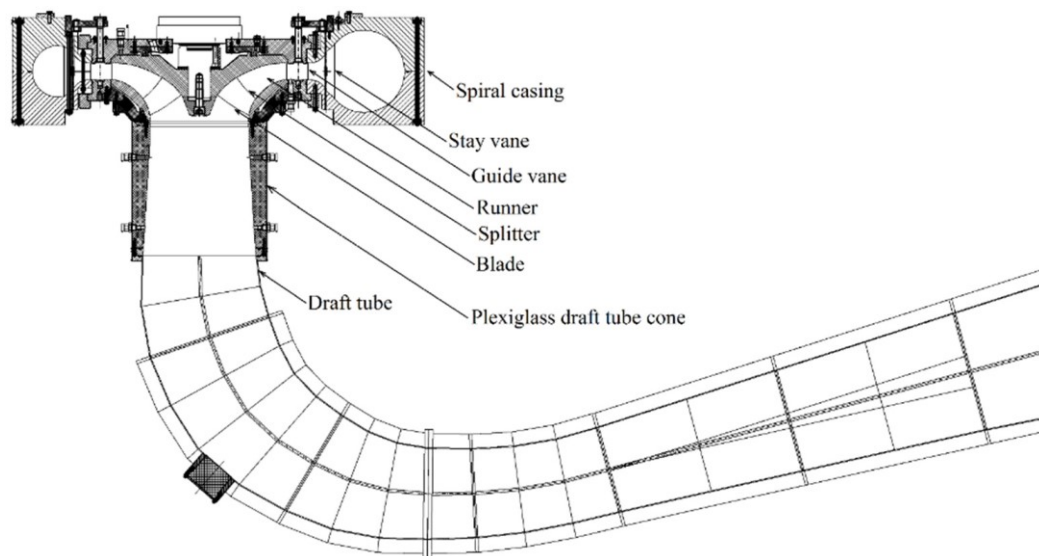


Figure A. 2 2D view of the Francis turbine model [1]

The turbine presents a spiral casing, a distributor with 14 stay vanes and 28 guide vanes, the runner with 15 blades and 15 splitters and an elbow-type draft tube. In particular, this turbine is a reduced scale model that refers to the prototype that operates at the *Tokke Power Plant* in Norway, see [1] for more information.

Looking at the path of water in Figure A.1, down to the reservoir there is the vertical conduit (penstock), here there is a decrease in cross section in the middle for the presence of a flow meter; but this will not be considered in the model since it does not affect the behaviour of the plant and the pressure oscillations. After two elbows and two pipes, the surge tank is inserted and then the fluid goes to the Francis99 turbine; after that there is the tailrace surge tank and finally the water goes to the pool (or lower reservoir).

Since the SIMSEN software is a 1D simulation software, in order to take into account the presence of elbows, it is possible to insert “*Discrete Loss*” elements, that allows to introduce concentrated losses. Another problem is the presence of part of the pipes with variable section, in SIMSEN there is not the possibility to have a pipe with variable diameter; it is possible to use a normal pipe element with constant diameter but calculating an equivalent diameter considering different sections of the conduit, in order to have the same inertia effect. Finally, to model the two surge tanks, one just after the vertical conduit and the other after the turbine,



the air vessel was chosen; this to not consider losses due to an inlet diaphragm, that in the real plant is not present.

According to all these evaluations a first model was created and shows up as in Figure A.3.

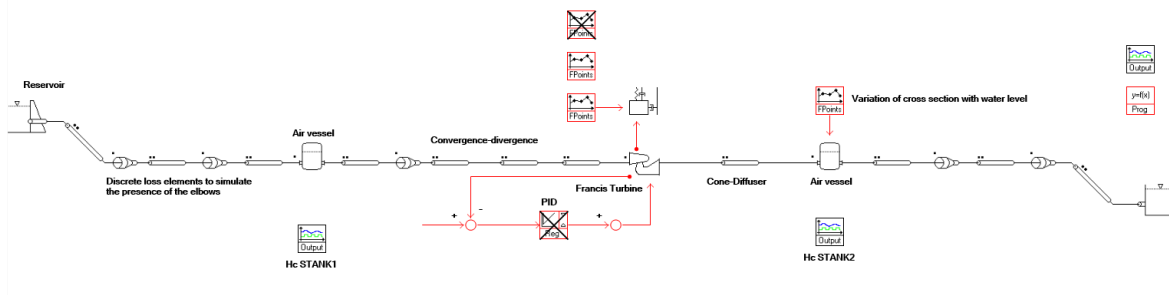


Figure A. 3 SIMSEN model of the power plant present at NTNU

As it is possible to see the 3D path is modelled in a 1D simulation, adding the “Discrete Loss” element to simulate the presence of the elbows, so introducing a concentrated loss. Then there are the two air vessels, before and after the turbine. In the air vessel the gas capacitance term can be expressed considering perfect gas behaviour and a polytropic transformation of the gas.

Between the first air vessel and the turbine there is a pipe of around 15m in total (element 4 in Figure A.1), but in the middle of this pipe a flow meter is inserted. Before that instrument the diameter of the pipe decreases, instead after increases again. It is needed to consider this in the model so a first pipe is inserted, then there is an elbow with a deviation angle of around 35°, then a first “PipeZ” element is inserted in order to model the convergent conduit and after it, there is a second “PipeZ” to model the divergent conduit.

After the turbine there are pipes that bring the water to the lower reservoir, it is necessary to consider the presence of the elbows and the real arrangement of these pipes to get a model as faithful as possible to the reality.

From the figure of the model, it is possible to note also the presence of a PID controller (Proportional Integral Derivative regulator), but for the first simulations realized, and used to validate the model, this regulator is not taken into consideration. Subsequently the governor of the turbine will be better implemented, to introduce the possibility to automatically control the guide vane opening in transient operation. Then there is also an “FPoints” block, related to the mechanical mass connected to the turbine, to introduce the possibility to control the external torque and in this way simulate some disturbances, like load rejection.

To have the proper lengths of the pipes to be inserted it was necessary to measure them with a laser meter; this because in the draft of the plant there were the dimensions of the whole pipes, but because of the presence of elbows or changes in cross section it was necessary to divide the whole pipes in smaller elements, to be able to model them in the software.

Now it is needed to analyse the plant element by element, to understand how the implementation was carried out.

## Reservoir (1)

The element used in the software, called “*Dam*”, models a reservoir with infinite volume; the discharge is considered positive when it flows in. In the SIMSEN’s logic this component corresponds to a voltage source, considering the electrical analogy with which the software works.

After the introduction of the element in the software it is necessary to open the user interface of it and set the main parameters; in this case it is needed to choose the piezometric head, the density of the fluid (water) and the gravity acceleration. If the values are wanted in per unit, it is also necessary to set the rated piezometric head and the rated discharge.

For a better understanding the user interface of the component is reported (see Figure A.4).

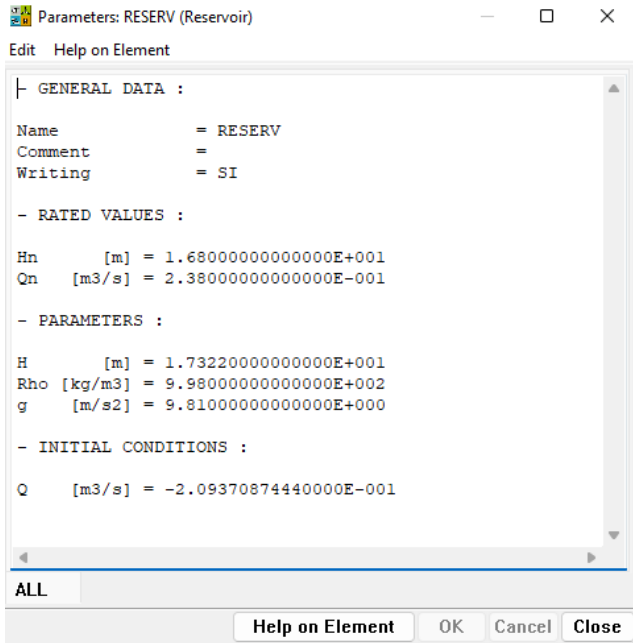


Figure A. 4 User interface for the reservoir element

The quantities for reading are the time, the piezometric head and the discharge.

The head was chosen considering the elevation of the upstream reservoir in respect to the level zero, given by the downstream pool.

Now it is possible to move to the second element of the model, which is the vertical conduit.

## Penstock (2)

The vertical conduit of the plant is modelled with the “PipeZ” element, which allows also to set the level of the inlet and of the outlet of the pipe. This is a circular cross section pipe with constant diameter  $D$ , wave speed  $a$ , length  $L$  and loss coefficient  $\lambda$ ; the discharge  $Q$  is considered positive when it enters on both sides of the pipe.

In each section the hydraulic head is defined as

$$H_i = z_i + \frac{p_i}{\rho g} + \frac{Q_i^2}{2gA_i^2} . \tag{Eq. A.1}$$

The first two members represent the piezometric head, the second is the pressure head and the last one is the kinetic head.

To understand better which are the parameters that it is needed to set up it is possible to report here the user interface of the component.

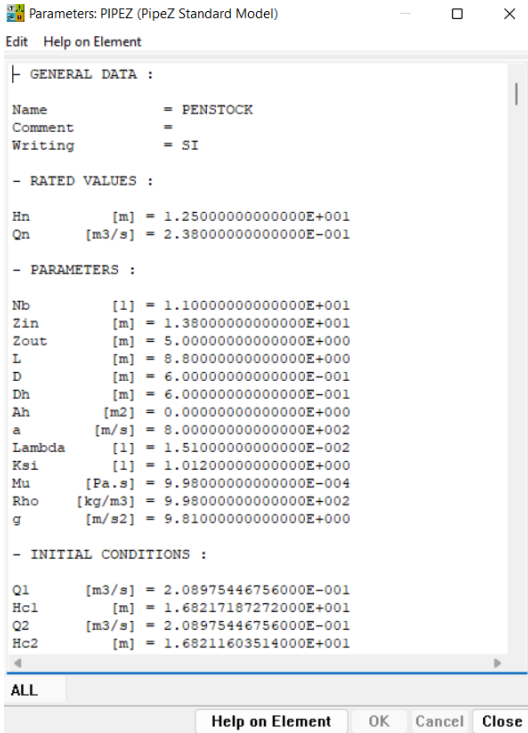


Figure A. 5 User interface of the Penstock element

As already explained in previous chapters, the pipe is divided in  $Nb$  parts of length  $dx$ . To ensure integration stability it is important that the hydraulic quantities are transferred between pipes at the same time; for this it is necessary to use a proper discretization of the pipes and to set an adapted wave speed. Since the ratio between the length of the pipe and wave speed never gives the same propagation time, it is necessary to adapt the wave speed from the value  $a$  to  $a'$ . The process to discretize a pipe can be described by the following passages:

- First it is needed to compute the wave speed  $a$  in the pipe, it was decided to start from  $800 \text{ m/s}$  that can be considered as a coherent value for the size of the plant considered.
- Then it is needed to select a time basis  $dT$ , in case of a small plant as the one present at NTNU a value of  $0.001\text{s}$  is used.
- Now it is possible to calculate the spatial discretization,  $dx = dT * a$ .
- Then compute the number of elements in which it is needed to divide the pipe,  

$$Nb = \frac{L}{dx}.$$
- Since  $Nb$  must be an integer, it is necessary to calculate the new wave speed  $a'$  according to the following equation:  $Nb = \frac{L}{a' * dT}$ .

This procedure is done for every pipe inserted in the simulation, in order to find the number of elements in which the pipe has to be divided. [8]

It is then needed to set other characteristic parameters of the pipe, as the level at inlet and outlet, the diameter, the length, the local loss coefficient  $\lambda$ , the inertia coefficient  $\xi$ , the viscosity of the fluid, the density, and the gravity acceleration. The initial conditions are instead calculated once the simulation is launched for the first time. Regarding the calculation of the loss coefficient in Appendix B is reported the full description of the procedure.

## Elbow element

To model the presence of elbows a “*Discrete Loss*” element is used, it allows to introduce a concentrated loss setting the  $K$  coefficient. The user interface of this element shows up as reported in Figure A.6.

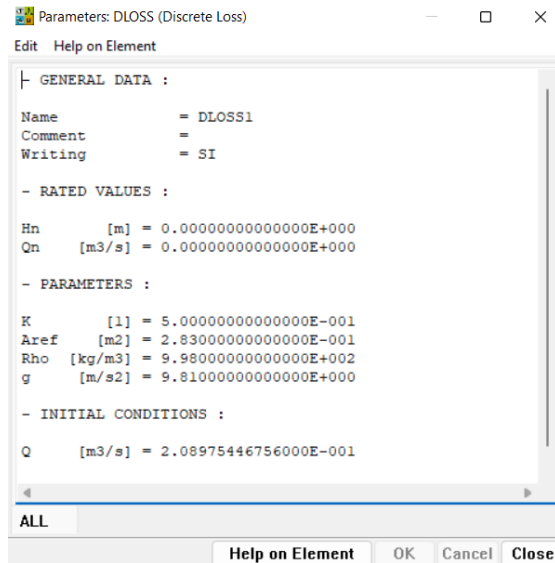


Figure A. 6 User interface for the DLOSS element

As it is possible to see from the figure it is needed to set the  $K$  loss coefficient, the reference area, the density of water and the gravity acceleration. As reference area the cross section of the pipe before the elbow was chosen; to set instead the value of  $K$ , a research in the literature was necessary. This first elbow in particular is a smooth elbow with vanes inside, in order to guide the fluid and decrease the turbulence, and characterized by an angle of  $90^\circ$ . The corresponding value of  $K$  chosen is 0.5 (see Appendix B for a description on how the loss coefficient were calculated).

All the other elbows present in the plant create a deviation of  $90^\circ$ , except for the one just after the first air vessel, and are all without vanes. For smooth elbows with  $90^\circ$  deviation a  $K$  value of 0.23 is used; for the elbow after the vessel  $K$  was chosen as 0.052, considering  $35^\circ$  deviation. Finally, there is also a sharp elbow of  $90^\circ$  deviation just after the second air vessel, for which a  $K$  value of 1.13 was inserted. For all the “DLOSS” elements present in the model the user interface is exactly the same, only  $K$  and  $A_{ref}$  are different, depending on the type of elbow; so, it is not necessary to report here all the related figures.

Now it is possible to move to the description of the path before the first air vessel.

## First pipe

The element used is a “PipeZ” element, as for all the pipes with constant diameter present in the plant, from now on it will be reported only the user interface of the considered pipe to show the characteristic parameters inserted: the length, cross section, number of elements, wave speed exc.

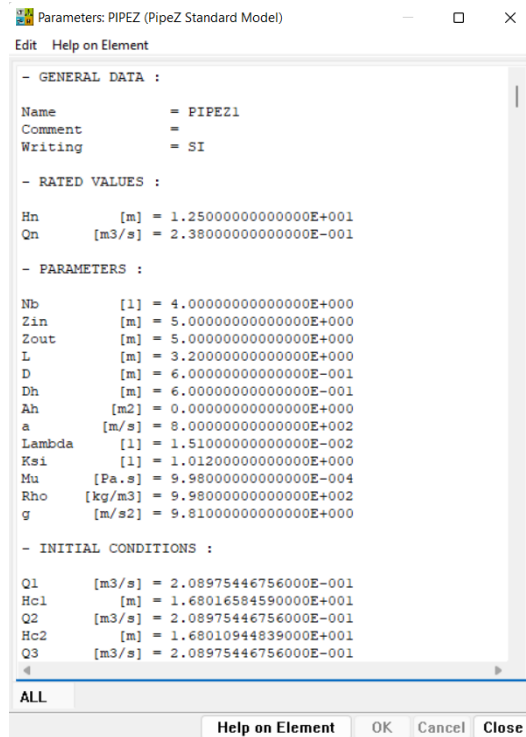


Figure A. 7 User interface for the first horizontal pipe of the model

The procedure for the discretization of the pipe is always the same.

## Second pipe

Again, only the user interface is reported (see Figure A.8).

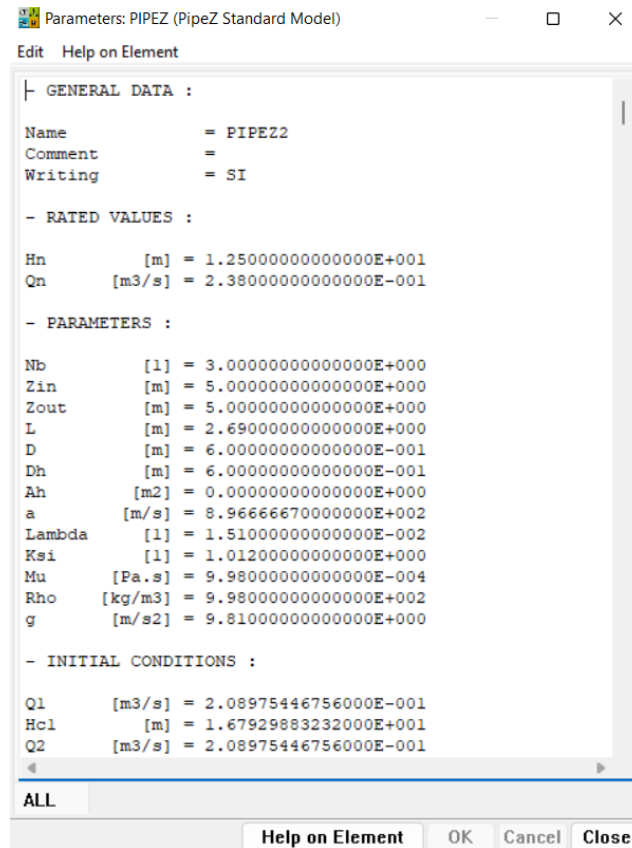


Figure A. 8 User interface for the second pipe of the model, the one just before the first air vessel

### Air vessel (3)

To model the surge tank present before the turbine an “*Air Vessel*” element was chosen, the tank in fact is closed with air inside, so this can be considered as the proper element for this component. The air vessel allows to not consider losses due to an inlet diaphragm, which is instead inserted in other elements like the open “*Surge shaft*” or the “*Surge vessel*”, for this reason they are not considered for this model.

In the plant, the first surge tank is basically a vertical cylinder, with variable amount of air inside, this can be used to set the pressure level in that point of the plant. The cross section is not constant, as in a perfect cylinder, but on the top part varies (cross section decreases). It was decided to take the element as a perfect cylinder to simplify the model, when the comparison with the experimental results will be made it will be evaluated if there is the necessity to have a more detailed description.

To see which are the inserted characteristic parameters, in Figure A.9 the user interface of this element is reported.

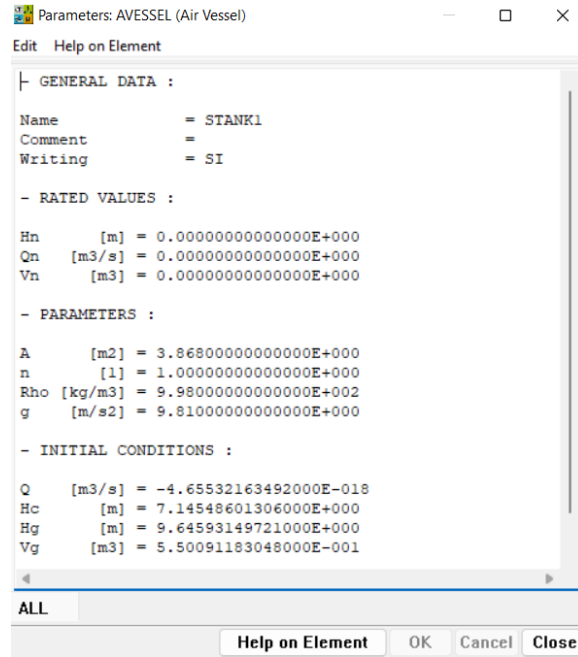


Figure A. 9 User interface for the Air Vessel element that model the first surge tank of the plant

In the section “PARAMETERS” the needed values are inserted:  $A$  is the vessel cross section, after measuring the diameter of the cylinder the area was calculated as equal to  $3.868 \text{ m}^2$ ;  $n$  is the polytropic exponent (related to the polytropic transformation of the gas inside the vessel), the value was set as equal to 1, and then as usual there are the fluid density and the gravity acceleration.

For the simulation to run in the proper way it is also necessary to set at the beginning the volume of gas  $V_g$  and the head  $H_g$ , in the section “INITIAL CONDITIONS”; this to initialize the level of pressure and the amount of air present inside. To do this a specific procedure has to be carried out:

- First it is needed to run a simulation removing the 2 air vessels present in the model and leaving all the other components. This was done simply saving the model again in another file, removing the 2 elements, keeping all the rest equal. From this simulation the pressure at the exit of the pipe that is supposed to be the one just before the air vessel can be taken, reading the head  $H$  at the exit.
- Then it is needed to choose a specific value of the water level in the tank ( $H_C$ ), that depends on the conditions at which the experimental tests are carried out.
- Having the measure of the height of the vessel it is possible to calculate the volume of air  $V_g$  as  $V_g = \Delta z * A$ , where  $\Delta z$  is the difference between the height of the tank and the level of water  $H_C$ , instead  $A$  is the vessel cross section.



- Now with the value of the pressure at the inlet of the surge tank, taken in the previous simulation, it is possible to find the head of the gas as:

$$H_g = H - H_c ,$$

where  $H$  gives the pressure at the inlet of the tank.

At the end of this procedure the values of  $H_g$  and  $V_g$  are found and it is possible to insert them in the main file of the model, to give the initialization of the two air vessels.

Now let's proceed to the other components of the model, it was decided to not report the user interfaces of the other pipes since the parameters to be inserted are always the same, and also a better evaluation of them is carried out in Appendix B, where there is the full description on how the losses for the pipes can be evaluated.

## Convergent-divergent portion (4)

Before the turbine there is a long pipe around 15m long, this pipe is divided into different portions in the model; the first part is given by a normal “PipeZ” elements, then there is a convergent conduit and a divergent conduit just after. To model this, it was decided to use two “PipeZ” elements, calculating an equivalent diameter for the 2 sections, which allows to simulate the same inertia effects of variable cross section pipes. The equivalent diameter must be evaluated following the procedure described below.

It is needed to calculate an equivalent inductance, expressed as

$$L = \sum \frac{L_i}{gA_i} . \quad \text{Eq. A.2}$$

Where  $A_i$  is the cross section and  $L_i$  is the length of the pipe portion in which it is considered to have that section. In the case of these two pipes, it is enough to consider which is the diameter at the inlet and at the outlet and then take 3 or 4 sections, discretizing in this way the pipe.

Having the inductance, it is possible to calculate an equivalent diameter using the following expression

$$L_{pipe} = L * g * \frac{\pi D_{eq}^2}{4} . \quad \text{Eq. A.3}$$

Where  $L_{pipe}$  is the real length of the pipe,  $L$  is the inductance previously calculated and  $D_{eq}$  is the diameter to be inserted in the pipe element.

## Turbine (5)

The turbine is modelled with the proper element taken from the library of the SIMSEN software; in this case a Francis turbine is considered in the model since it is the kind of turbine present in the laboratory and on which the tests will be carried out. In order to understand which are the parameters that have to be inserted, first the user interface of the element is reported (Figure A.10).

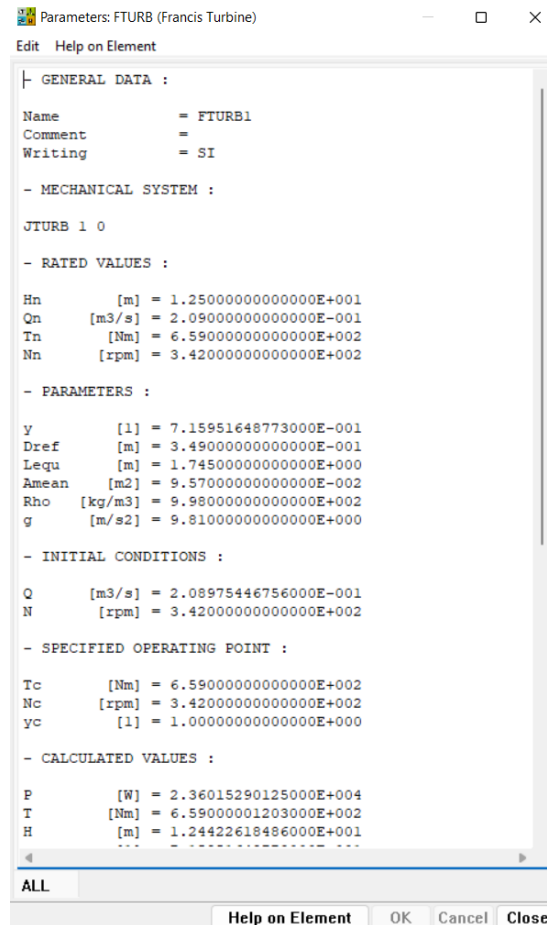


Figure A.10 User interface of the turbine element

Starting from the top, in the section “*MECHANICAL SYSTEM*” it is needed to insert the name of the mechanical mass connected to the turbine, that model the rotor and its inertia. Then, the main parameters of the turbine are: the guide vane opening  $y$  (for this it is enough to choose a random value between 0 and 1, then when the simulation is launched the software calculates the value and automatically substitute it), the reference diameter, the mean cross section and the equivalent length, then the fluid density and the gravity acceleration. Regarding the mean cross section and the equivalent length, these two parameters can be used to consider turbine water inertia effects, correlated with the spiral case, the runner, and the draft tube. In this case

it was chosen to consider only the spiral case and add after the turbine two pipes to model the cone and the diffuser (in which the draft tube is divided). If no specific information are given, in the SIMSEN user guide [8] it is suggested to set

$$L_{equ} = (5 \text{ to } 15) * D_{ref} , \quad \text{Eq. A.4}$$

$$A_{mean} = \pi * \frac{D_{ref}^2}{4} . \quad \text{Eq. A.5}$$

Where  $L_{equ}$  is the equivalent length,  $A_{mean}$  is the mean cross section and  $D_{ref}$  is the reference diameter. In this case, since it was decided to model only the spiral case in the turbine element, it was chosen to set the equivalent length as 5 times the reference diameter. This diameter is taken as the outlet diameter of the runner (0.349m).

From Figure A.10 it can be seen that it is also necessary to set a specified operating point, for a first trial it was chosen to use the best efficiency point. Inserting the rated torque and the rated rotational speed, and then launching the “*InHydro*” procedure to find the initial conditions, the value of the corresponding guide vane opening is calculated; this is the value that allows to have that torque and that rotational speed.

At the end of the user interface of the turbine element, there is also a section “*DATA*” where it is needed to insert the .txt file with the characteristic curves of the considered turbine, in order to let the software reads the curves.

Now it is possible to move to the part of the plant downstream the turbine.

## Draft Tube (6)

In this first model the draft tube is inserted introducing a “*PipeZ*” element. In order to set the proper lengths and diameters a specific procedure was carried out, since in reality the draft tube has not a constant diameter and also it is not straight.

First of all, it was necessary to go in the laboratory in order to get the measures of a certain number of sections of the draft tube, in particular to take: the diameter at the inlet and at the outlet of the cone and two diameters in the middle of the portion of draft tube that creates the deviation from the vertical cone. Then also the lengths of every part must be measured. In this way it is possible to discretize the element considering that the diameter increases by steps.

Having these measures, it is needed to calculate an equivalent inductance, expressed as

$$L = \sum \frac{L_i}{gA_i} . \quad \text{Eq. A.6}$$

Where  $A_i$  is the measured cross section and  $L_i$  is the length of the portion in which it is considered to have that section. In the case of the cone there are 2 cross sections available and also the total length of the cone was measured, as a first approximation it was decided to consider the cone as formed by two cylinders of length equal to half the length of the cone. The first one with a diameter equal to the inlet diameter and the second one with a diameter equal to the outlet one.

*Table 4 Length and cross section of the 2 portions of the cone*

$L_i$ [m]	$A_i$ [m <sup>2</sup> ]
0.215	0.0707
0.215	0.0962

Considering this, it is possible to find the equivalent inductance related to the cone as the sum of 2 terms.

Regarding the diffuser there are 3 cross sections available, so using the same logic used for the cone, the diffuser is approximated as three cylinders, with the following values of cross section and length.

*Table 5 Length and cross section of the 3 portions of the diffuser*

$L_i$ [m]	$A_i$ [m <sup>2</sup> ]
1.23	0.0962
1.2	0.136
1.45	0.274

From the values in the two tables the equivalent inductances are

$$L_{cone} = 0.538 \text{ s}^2/\text{m}^2 ,$$

$$L_{diffuser} = 2.742 \text{ s}^2/\text{m}^2 .$$

Having the inductances, it is possible to calculate an equivalent length for the cone and for the diffuser, which should be used as the length of the pipe inserted in the model. For the cone the result is

$$L_{eq,cone} = L_{cone} * g * \frac{\pi D_{ref}^2}{4} = 0.438m . \quad \text{Eq. A.7}$$

Where  $D_{ref}$  is the reference diameter and for the cone is chosen as 0.325m, average between the inlet and outlet sections.

For the diffuser the result of the equivalent length is instead

$$L_{eq,diff} = L_{diffuser} * g * \frac{\pi D_{ref}^2}{4} = 7.02m . \quad Eq. A.8$$

Where  $D_{ref}$  in this case is equal to  $0.576m$ , that is the diameter in the middle section of the diffuser, calculated knowing the area in the middle section ( $0.261m^2$ ).

To have a more precise estimation of the equivalent length for the cone it is possible to perform an integration procedure, instead of discretizing the elements with two cylinders. This is possible since the shape is conical. First it is needed to find a function that expresses the area of the circle circumscribed to the cone in respect to the height  $z$ ; for the cone considered this is

$$A(z) = \pi * (-0.116 * z + 0.35)^2 . \quad Eq. A.9$$

Then it is needed to integrate this function between  $z$  equal zero (base of the cone) and  $z$  equal to  $0.43m$  (length of the cone measured). Finally, having the equivalent inductance by integration it is possible to find the length as before; with this procedure the final value is

$$L_{eq,cone} = 0.116m .$$

After these passages are done, it is possible to carry out the discretization procedure to get the number of elements in which the pipe should be divided. Doing this it was noticed that, since the cone has a very small length, the value of the corrected wave speed was too low and not comparable with the wave speeds of the other pipes. For this reason, it was decided to combine cone and diffuser in a single pipe element; to do this it is simply necessary to sum the two equivalent inductances and then calculate the length for the whole draft tube element, that results equal to  $7.387m$ , considering the reference diameter of the diffuser as the diameter to apply the formula for the length. This ends the discussion about this element.

Now it is possible to move to the next element present in the SIMSEN model.

## Tailrace Surge Tank (7)

The element is exactly the same used for the first surge tank, the “*Air Vessel*” is used. The main difference in respect to the previous surge tank is that this vessel is horizontal, so the cross section is not constant and cannot be fixed in the user interface of the element, as before. Also if it is not a perfect cylinder (in correspondence to the inlet and to the outlet the section decreases), it is treated as it is for simplicity.

As usual, in Figure A.11, the user interface of the element is reported.

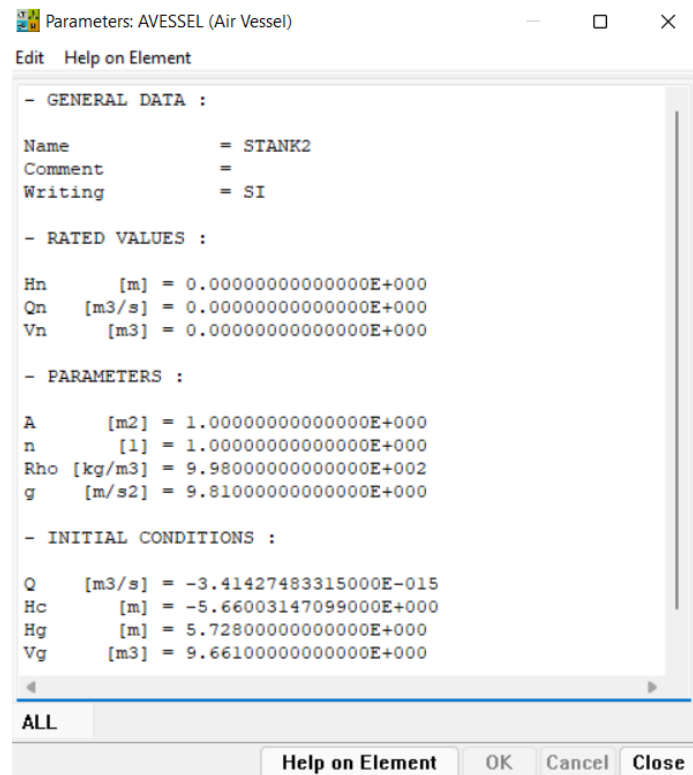


Figure A. 11 User interface for the second surge tank

As it is possible to see the value of the cross section is fixed randomly, then an “*FPoint*” element is added to the model to set the variation of the cross section with the heigh. This because the vessel is horizontal, so the cross section is basically a rectangle that varies with the level  $z$ . In the next figure the user interface of the “*FPoint*” element is reported.

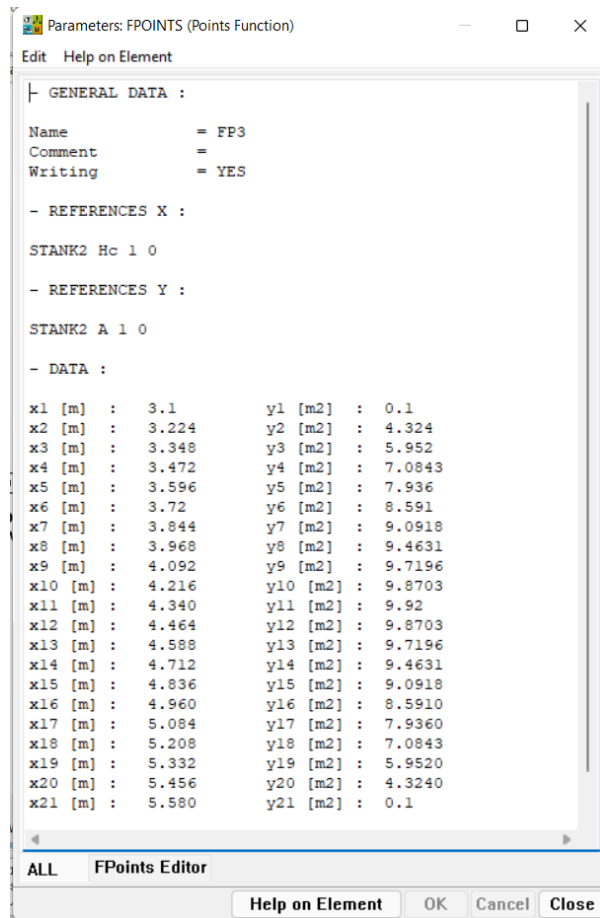


Figure A.12 User interface for the FPoint element that sets the cross section of the horizontal surge tank

To get the function per points implemented in the figure above (Figure A.12) an easy MatLab code was used, the equation for the area can be expressed as

$$A(z) = 2 * \sqrt{2zr - z^2} * L . \quad \text{Eq. A.10}$$

Where  $r$  (m) is the radius of the cylindrical vessel,  $L$  is the length and  $z$  the height. It was decided to vary  $z$  between  $3.1m$ , that indicates the lower level of the vessel, and  $5.58m$ , that is the lower level plus the diameter of the vessel, with a step of  $0.124m$ . For every value of the level  $z$  the area  $A$  was calculated according to the previous formula.

Then for both the 2 vessels, before starting a simulation, it is needed to set the volume of gas in the tank and the pressure of the gas (in terms of head). The procedure is the same used for the first vessel, the only difference is that, after setting the level of water inside, since this vessel is horizontal it is needed to perform an integration to get the volume of air. It is needed to integrate the function of the area between the chosen level of water and the upper ending of the tank (done in the same MatLab code used for the point function).

From now, it remains only the tailrace part of the powerplant to analyse, after the surge tank there are the pipes that bring the fluid to the pool; the pool is taken as the zero-reference level in the model.

### Last part of the plant (8)

Basically, it is the path that brings the water from the second surge tank to the pool that ends the hydropower plant present at NTNU, formed by pipes and elbows. The characteristics of these elements were already reported previously, so it is not necessary to go into details; to set length and cross section of these pipes the measures taken in the laboratory with the laser meter were used. It can be only interesting to report the downstream reservoir than ends the open loop power plant.

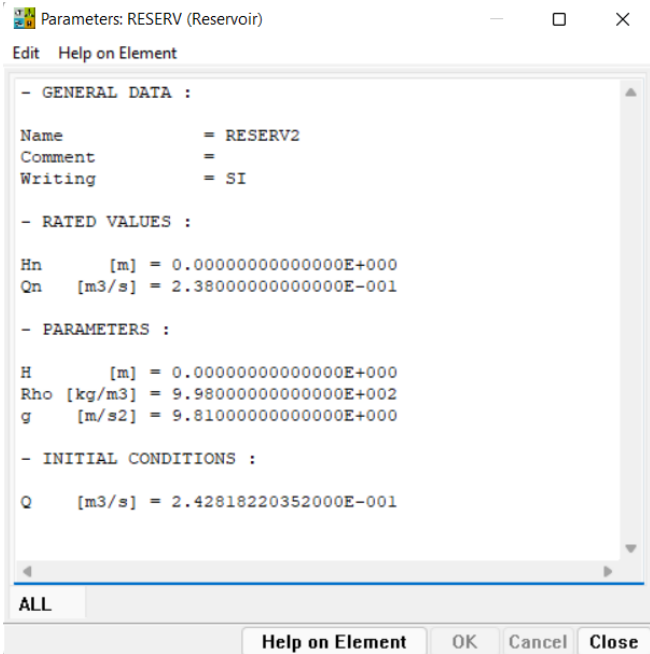


Figure A. 13 User interface for the reservoir that simulates the pool of the powerplant

There are other elements inserted, but it is not necessary to analyse them in detail since they are only needed basically to create the output for the simulations (like the “Output” element and the “Prog” element, used for saving in a single block the characteristic parameters of the turbine).

The described implementation is the one that perfectly follows the plant as it is in the laboratory. Subsequently the laboratory setup, used when running the test rig, was analysed, before performing the simulations and comparing them with the experimental results. In particular, the tests taken during the spring semester 2022, were realized keeping a valve open just after the second air vessel, in the tailrace part of the plant. This decision was taken for having a higher



stability of the system, eliminating around 3m of head across the turbine, between the tailrace vessel and the pool. This changes completely the implementation in the software, because basically the turbine does not see the part of the plant after the draft tube. It was decided to model this configuration considering having directly the reservoir with infinite volume after the draft tube, since the second air vessel is communicating with the atmosphere; this is the configuration that goes closer to the reality.

The new model realized in SIMSEN is reported in Figure A.14, to highlight the modification done.

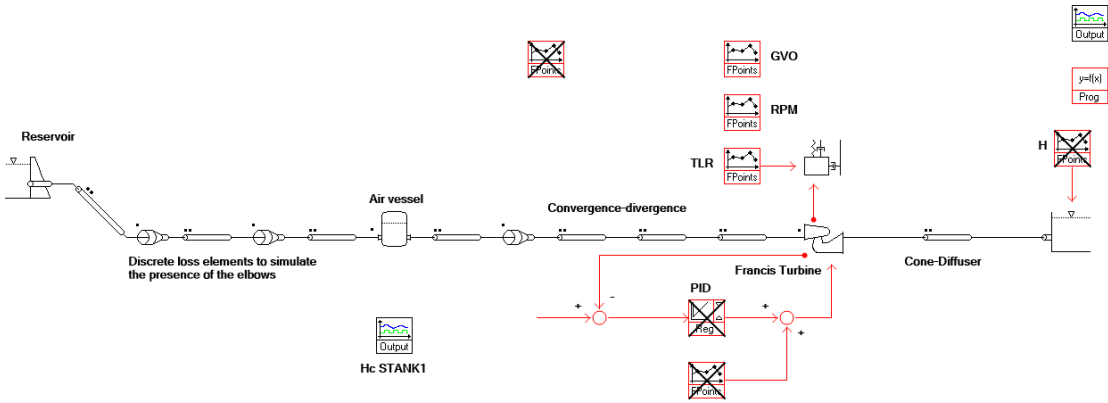


Figure A. 14 New model realized in the software, modifying the tailrace part of the plant

With the comparison between the model and the experimental results, it is then possible to understand if the considerations made were correct and if this representation of the plant is satisfying.



# APPENDIX B : Computation of the plant's head losses

To compute the head losses in the piping system it is necessary to calculate the loss coefficients for every pipe inserted in the model, and for the “*DLoss*” elements used to represent the elbows. To do this an excel file was created, where all the characteristic parameters of the piping system were collected. First, it is needed to set some fixed values, in the following table these values are reported to have an overview of what was chosen.

*Table 6 Parameters that must be fixed for the computation of the losses*

Parameter	Symbol	Value	UoM
Volumetric flow rate	Q	0.209	m <sup>3</sup> /s
Density	$\rho$	998	kg/m <sup>3</sup>
Viscosity	$\mu$	0.000998	Pa*s
Equivalent sand roughness	ks	0.0001	-
Kinematic viscosity	$\nu$	1.00E-06	m <sup>2</sup> /s
Initial wave speed	a	800	m/s
Time interval	dT	0.001	s
Inertia coefficient for the pipes	$\xi$	1.012	-

The volumetric flow rate used for the computation is the one that refers to the tests realized in steady state conditions at the best efficiency point of the turbine. From these values it was possible to get the following table that gives all the parameters related to every pipe of the plant.

*Table 7 Characteristic parameters for the piping system of the SIMSEN model*

	L[m]	D[m]	AREA[m <sup>2</sup> ]	V[m/s]	Re	A	B	lambda
<b>PENSTOCK</b>	8.80	0.600	0.282743	0.739186	443511.8	5.39E+21	6.91E-18	0.015367
<b>PIPEZ1</b>	3.20	0.600	0.282743	0.739186	443511.8	5.39E+21	6.91E-18	0.015367
<b>PIPEZ2</b>	2.69	0.600	0.282743	0.739186	443511.8	5.39E+21	6.91E-18	0.015367
<b>PIPEZ3</b>	2.00	0.600	0.282743	0.739186	443511.8	5.39E+21	6.91E-18	0.015367
<b>PIPECONV</b>	2.96	0.387	0.117811	1.774032	687082.5	4.58E+21	6.28E-21	0.015685
<b>PIPEDIV</b>	1.72	0.296	0.068720	3.041306	899618.2	3.62E+21	8.42E-23	0.016153
<b>PIPEZ4</b>	7.72	0.350	0.096211	2.172303	760305.9	4.24E+21	1.24E-21	0.015838
<b>DTUBE</b>	7.39	0.577	0.261482	0.799291	461190.8	5.38E+21	3.7E-18	0.015372
<b>PIPEZ5</b>	0.70	0.600	0.282743	0.739186	443511.8	5.39E+21	6.91E-18	0.015367
<b>PIPEZ6</b>	1.60	0.500	0.196350	1.064428	532214.1	5.22E+21	3.74E-19	0.015430
<b>PIPEZ7</b>	3.10	0.500	0.196350	1.064428	532214.1	5.22E+21	3.74E-19	0.015430

Now the procedure for the loss's calculation will be explained in more details. The goal is to find the local loss coefficient  $\lambda$  for every pipe, the computation of this parameter comes from the Churchill formula, which can be expressed as

$$\lambda = 8 * \left( \left( \frac{8}{Re} \right)^{12} + \frac{1}{(A + B)^{\frac{3}{2}}} \right)^{\frac{1}{12}} . \quad \text{Eq. B.1}$$

As can be seen from the expression, it is needed the Reynolds number for every pipe and two parameters  $A$  and  $B$ . To compute the Reynolds number, it is first needed the velocity in the pipe, which can be read from the table, then  $A$  and  $B$  are calculated as

$$A = \left( 2.457 * \ln \left( \frac{1}{\left( \frac{7}{Re} \right)^{0.9} + 0.27 * \frac{k_s}{D}} \right) \right)^{16} , \quad \text{Eq. B.2}$$

$$B = \left( \frac{37530}{Re} \right)^{16} . \quad \text{Eq. B.3}$$

In  $A$  it is needed the parameter  $k_s$ , that is the equivalent sand roughness; this parameter was fixed at 0.0001 considering typical values for industrial pipes. [11]

Regarding the elbows instead, in the plant there are basically three types of elbows: one is smooth with vanes to rectify the flow (this is the one just after the penstock), then there is one that is considered as sharp, and all the others are smooth. For a sharp elbow the value of the loss coefficient  $K$  depends only on the angle, for a 90° elbow the value is 1.13. For a smooth elbow instead the loss coefficient can be calculated with the following expression

$$K = \left( 0.131 + 1.847 * \left( \frac{D}{2r} \right)^{3.5} \right) * \frac{\theta}{90} . \quad \text{Eq. B.4}$$

In Figure B.1 a scheme of the two types of elbows is reported.

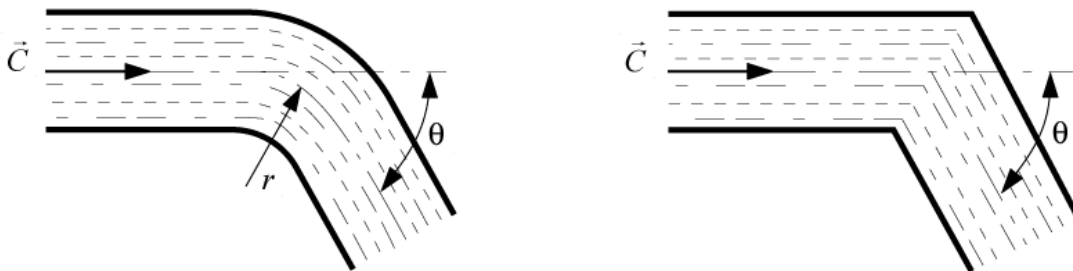


Figure B. 1 Smooth and sharp elbows with related parameters [10]

As a summary of the  $K$  loss coefficients calculated following the literature, a table can be reported (see Table 8), for finding the values the documents [11] and [14] were used as a reference.

*Table 8 Summary of the loss coefficients for the elbow's losses*

<b>ELBOWS</b>		<b>K</b>
<b>1</b>	smooth with vanes 90°	0.500
<b>2</b>	smooth 90°	0.230
<b>3</b>	smooth 35°	0.052
<b>4</b>	sharp 90°	1.130
<b>5</b>	smooth 90°	0.230

In this appendix the calculation of the loss coefficients is explained for all the pipes and elbows present in the first realized model (see beginning of Appendix A); however, as explained in Appendix A, the downstream part of the plant was modified for the set up used while running the test rig. So, in the final model only the first 3 elbows are present and only the pipes until the draft tube.

In respect to the values of the losses calculated here, some small modifications were applied, in order to match better the experimental results in steady state conditions (see Chapter 4 for the comparison). Specifically, the loss coefficient  $\lambda$  of the pipes was set at 0.0151 for all the pipes, except for the draft tube that has a value equal to 0.015188. Regarding the elbows instead the final values used are the one reported in Table 8.



# APPENDIX C : Mechanical backlash

A mechanical backlash can be described by a dead space between adjacent movable parts, as it often happens in a series of gears; it is always present when there is a driving member that is not directly connected with the driven member (load). If a backlash is present the control of the load is difficult, the driving member can lose contact with the load when a change in direction is needed. [15]

When there is no backlash a motor-load system can be represented as two masses connected by a shaft, the shaft is considered mass and inertia free for simplicity; this system is reported in Figure C.1. [15]

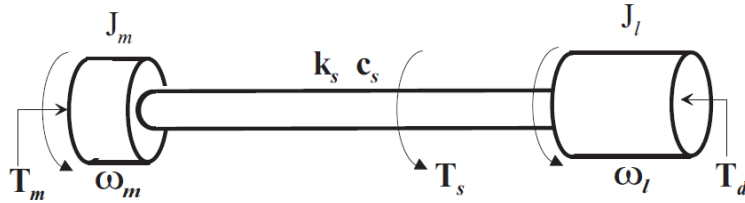


Figure C. 1 Linear two-mass system for connection between a motor and load [15]

The equations that describe the behaviour of this system can be written as

$$J_m \dot{\omega}_m = -c_m \omega_m - T_s + T_m , \quad \text{Eq. C.1}$$

$$J_l \dot{\omega}_l = -c_l \omega_l + T_s - T_d , \quad \text{Eq. C.2}$$

$$\omega_d = \omega_m - \omega_l . \quad \text{Eq. C.3}$$

Where  $J_m$  [kgm<sup>2</sup>] is the motor moment of inertia,  $c_m$  [Nm/(rad\*s)] is the viscous motor friction,  $T_s$  [Nm] is the transmitted shaft torque,  $T_m$  [Nm] is the motor torque,  $J_l$  [kg\*m<sup>2</sup>] is the load moment of inertia,  $c_l$  [Nm/(rad\*s)] is the viscous load friction,  $T_d$  [Nm] is the load torque disturbance. The rotational speeds  $\omega_m$  and  $\omega_l$  [rad/s] are instead the motor angular velocity and the load angular velocity, respectively.

As done in this work for controlling the turbine, for two-mass system the most common controller is the PI-regulator. To add a mechanical backlash into the model, this must be seen as a nonlinearity; considering the previous figure as a reference, the new scheme will be the following (Figure C.2).

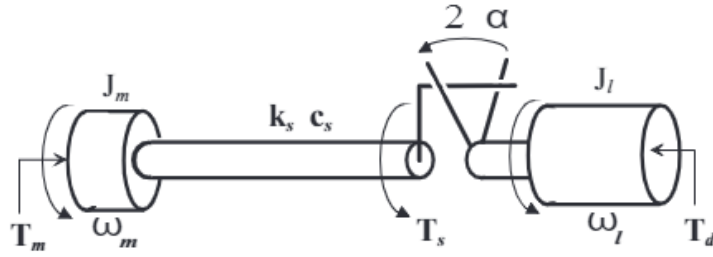


Figure C. 2 Two mass system with backlash [13]

There are different models that can be used to describe the backlash nonlinearity in a mechanical system, here only the *Dead zone model* and the *Hysteresis model* will be briefly presented.

### Dead zone model

This model can be described by a function, called “dead zone function”, that can be expressed as

$$D_a(x) = \begin{cases} x - a & \text{if } x > a \\ 0 & \text{if } |x| < a \\ x + a & \text{if } x < -a \end{cases} \quad \text{Eq. C.4}$$

Where  $x$  represents the movement before the backlash,  $a$  is the amplitude of the backlash and  $D_a$  is the output considering the delay given by the backlash. [15]

### Hysteresis model

The hysteresis model relates the output angle of the backlash  $\theta_l$ , with the input angle  $\theta_m$  considering a stiff shaft. The describing equation is the following

$$\dot{\theta}_l(t) = \begin{cases} \dot{\theta}_m(t) & \text{if } \dot{\theta}_m(t) > 0 \text{ and } \theta_l(t) = \theta_m - a \\ \dot{\theta}_m(t) & \text{if } \dot{\theta}_m(t) < 0 \text{ and } \theta_l(t) = \theta_m + a \\ 0 & \text{otherwise} \end{cases} \quad \text{Eq. C.5}$$

This equation represents the, so called, friction driven hysteresis; it describes that the driven member maintains its position when the gap given by the backlash is not closed.

For more details regarding these two models and the mechanical backlash in general see paper [15].

In this thesis work, this description was taken as a starting point to understand how to implement the backlash into the SIMSEN model. The idea implemented is not exactly equal to one of these



two models, but the paper [15] was useful to understand better the problem and how this nonlinearity works. The implemented logic is represented in the following figure.

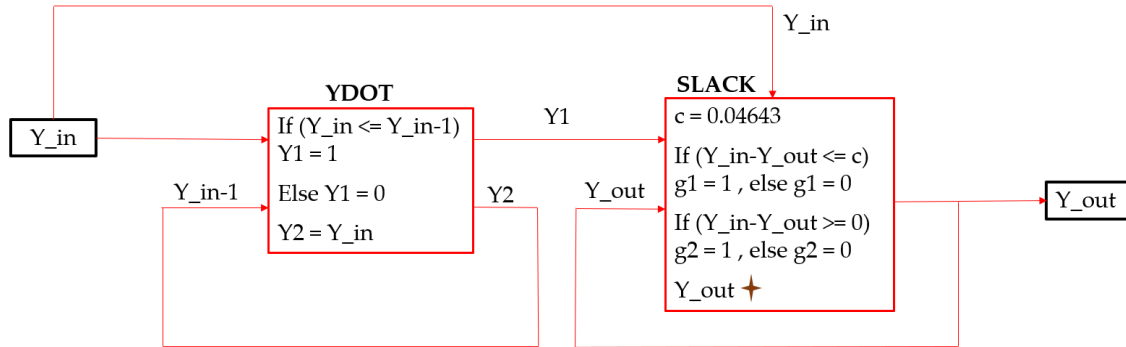


Figure C. 3 Logic of the backlash implemented into the SIMSEN model

The parameter  $Y_{in}$  represents the guide vane opening degree that should be applied, coming from the governor system; this value enters in a first “Prog” element called *YDOT*, where a logic operation is needed. The element *YDOT* takes also a second input, given by a retroaction, in order to be able to compare the value of the guide vane opening degree that should be applied with the one of the previous instant of time ( $Y_{in-1}$ ). This operation is necessary to understand if the guide vane opening degree is increasing or decreasing. Then the two outputs are saved, and the logic result (1 or 0) from the comparison is sent to a second “Prog” element, called *SLACK*. In this last element first, it is needed to define a constant that gives the amplitude of the backlash (this is  $c$ ), then it is needed to compare the signal given by the governor with the output signal, which is the real guide vane opening applied to the turbine considering the presence of the mechanical backlash. This operation is possible thanks to a second retroaction. It is needed to check if the difference between  $Y_{in}$  and  $Y_{out}$  is lower or equal to the slack amplitude, and if it is higher or equal to zero; then the results of these two controls are saved in the variables  $g1$  and  $g2$ .

Finally, the formula to calculate  $Y_{out}$  (guide vane opening really applied to the turbine) can be inserted

$$\star Y_{out} = Y_{out} + (Y_{in} - Y_{out}) * (1 - y1) * (1 - g2) + (Y_{in} - C - Y_{out}) * \quad Eq. C.6 \\ * y1 * (1 - g1) .$$

This last equation allows to calculate the signal affected by the backlash problem, to control then the turbine, simulating the real operation of the power plant present in the laboratory. An example can be reported here to show how the logic implemented works (see Figure C.4).

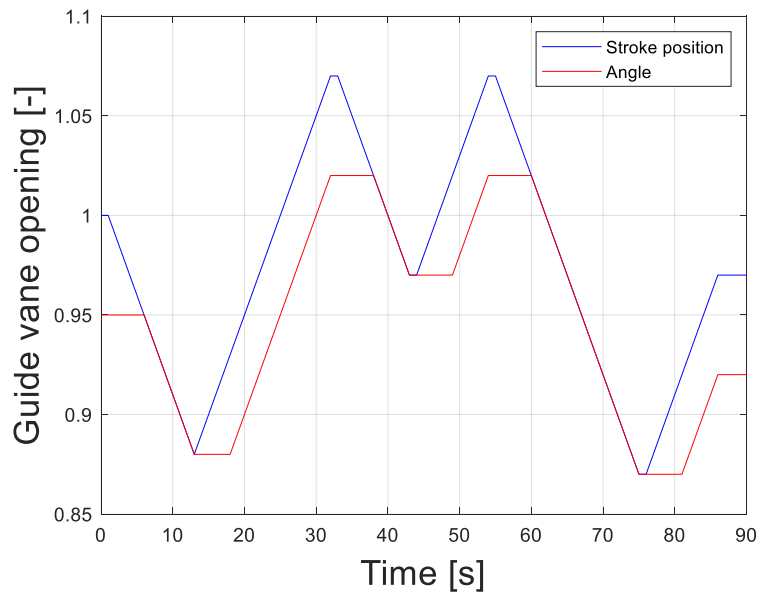


Figure C. 4 Example of the effect of a mechanical backlash

Looking at Figure C.4, the blue line represents the signal given by the governor and that should be applied to the turbine in case of a perfect mechanical system; instead, the orange curve gives the guide vane opening degree with the presence of the slack. When the guide vanes opening should start to decrease, they will not move until the dead space of the slack is covered, then the orange line starts to follow the blue one. When again the direction of the signal changes, before the guide vanes start to move in the opposite direction, the dead space has to be covered, causing a space delay in the signal. Obviously, it must be considered the relative position between the two mechanical elements at the beginning; stroke and angle can start from different values, as in the example, but they can also start from the same value, having the two signals superimposed in the beginning until the direction is changed.

